Doctoral thesis

Advanced Voltage Control of Distribution System with a Large Amount of Photovoltaic Generators

2013

Shinya Sekizaki

Contents

List of Figures

List of Tables

Acknowledgements

First of all, I would like to express my sincere gratitude and appreciation to Professor Hiroyuki Ukai who provided me with his continual support, invaluable guidance, inspirations, challenges and encouragement. This doctoral dissertation could not have been completed without his insightful and invaluable technical advice.

I also would like to thank Associate Professor Mutsumi Aoki, for providing me with the continuous support and encouragement which he provided throughout during my work. His useful and valuable suggestions were essential in improving the dissertation.

I wish to express my sincere thanks to Prof. Naoki Mizuno, Prof. Yukio Mizuno, and Prof. Takaharu Takeshita for invaluable advice.

The research work in this thesis was supported in part by Chubu Electric Power Co.,Inc. Special thanks go to Mr. Takaya Shigetou, Mr. Shunsuke Sasaki, and Mr. Takuma Sakaguchi for their valuable comments and technical support. I also would like to express my sincere to my advisor at the Chubu Electric Power Co.,Inc., Ph.D. candidate of my laboratory Mr. Toru Amau for his many comments and design ideas.

The help of Katsuma Watanabe, Lim Meng Thoung, Ryosuke Hibi, and Shinya Morita of my laboratory in the preparation of this manuscript is gratefully acknowledged.

I am truly indebted to Ms. Mayumi Yahata as a secretary of my laboratory for their endless support, and encouragement.

Finally, I would like to thank all my friends in Nagoya Institute of Technology, who helped me through the course of my studies, discussed ideas about my research, and made my life at NIT enjoyable.

Shinya Sekizaki

Abstract

This Ph.D. thesis documents the research work for obtaining the Ph.D. degree from the Nagoya Institute of Technology.

POWER SYSTEM is one of important infrastructures that contributes to the economic growth and welfare of any country. Recently, smart grid is being focused on all over the world. The term “smart grid” does not yet have a unique agreed definition. However, smart grid is usually defined as a power grid utilizing Renewable Energy Sources (RES) such as wind power, and solar power in a smart manner. In particular, smart grid will be introduced in Japan for energy savings and reduction of greenhouse gas emissions using RES. Since RES is sustainable and inexhaustible, utilizing RES as a new energy source is effective to reduce environmental impacts such as nuclear wastes and global warming. Meanwhile, introducing RES into the conventional power system may cause multiple problems.

A shift towards RES from conventional energy sources such as natural gas, coal, and oil will further stress the power system as these sources are intermittent and thus not reliable. The research initiated with issues about deterioration of power quality caused by increasing RES connected into the electric power system. The content of this thesis is for improving voltage management in the electric power system with a large amount of Photovoltaic generators (PV). Japanese government attempts to introduce RES as mainly PV, roof top type in residences. Since voltage in a distribution system with PVs fluctuates according to weather conditions due to PV, this issue attracts attention nowadays. Conventional voltage management strategy using existing facilities in the power system will not be able to maintain the power quality under this severe condition. These changes emphasize the importance of incorporating new and extending existing infrastructures in a systematic way.

From these viewpoints, in this paper, several novel control methods for voltage on distribution system using the novel and existing facilities are proposed.

Chapter 1
Introduction

1.1 Background

Electric power system consists of various facilities such as generators, transmission lines, substations, and receiving equipment. Generators in power plants generate electric power, transmission lines send the electric power to substations, and distribution systems (DS) distribute the electric power to consumers. DS is closest to the consumers in the electric power system and hence Distribution System Operator (DSO) plays a critical role to keep several power qualities at a proper level. The power qualities include voltage magnitude, harmonics, flicker, voltage sag, and so on [1] [2]. Among them, there is an increasing requirement to properly maintain voltage magnitude with the increase of Distributed Generation (DG) using Renewable Energy Source (RES).

In recent years, renewable and clean energy such as solar power and wind power is being focused on worldwide as next generation energy source due to a concern about the environmental issues such as global warming and exhaustion of fossil fuels such as natural gas, oil, and coal. In Japan, the government attempts to introduce DG; mainly Photovoltaic generator (PV), to reduce greenhouse gas emissions. Figure 1.1 shows goals of the amount of PV introduced to the power system in future set by the Japanese government [3] [4]. The Japanese government has set a goal to introduce 28GW of PV to the power system in Japan by 2020, and 53GW by 2030. Furthermore, at the moment, most of nuclear power plants in Japan have stopped generation for ‘nuclear risk’, which is attributed to the severe accident of the first Fukushima nuclear power plant caused by the Great East Japan Earthquake. This situation causes the lack of electric power supply and also impacts on the reconstruction of the energy best mix in Japan. For this reason, RES is being aggressively introduced to electricity market as alternative energy sources of nuclear energy and fossil fuel energy. As a result, vast number of DGs utilizing RES will be introduced into the power system in near future. In introducing RES into the power system, however, there are various issues of electric network technology in order to manage voltage quality.

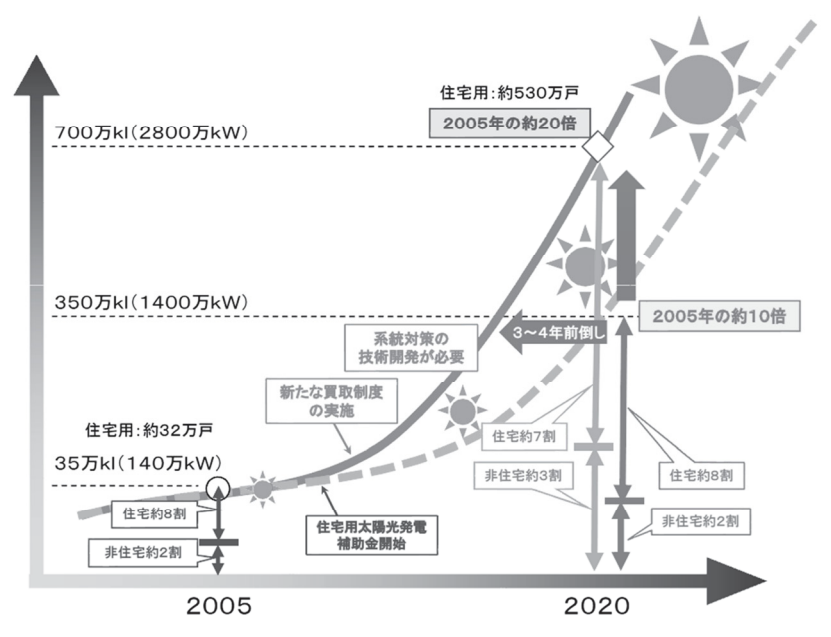

Figure 1.1 Scenario for introduction of PV in Japan [3] [4].

There are two problems when a large amount of DG is connected to DS. One is that the output of DG such as PV and wind generators randomly changes according to the weather condition. The other is the reverse power flow that active power flow streams from consumers to the substation, which causes the 'Ferranti effect'. The Ferranti effect is the voltage rise occurring at the receiving end of a transmission line, to the voltage at the sending end. In these cases, it is more difficult to manage the line voltage in DS compared with the conventional voltage management method, because the voltage uncertainly depends on the output distribution of DGs in the amount as well as in the direction. This paper focuses on these voltage problems in DS caused by PV, and several methods for properly managing voltage in DS are proposed.

1.2 Conventional voltage management in distribution system

In Japan, the allowable voltage range in DS is prescribed by Article 44 of the Enforcement Regulations of the Electricity Business Act. Table 1.1 shows the allowable range at receiving point of consumers in DS.

Table 1.1 Specified voltage at receiving point of consumers.

Voltage level	Allowable range
100V	101±6V
200V	202±20V

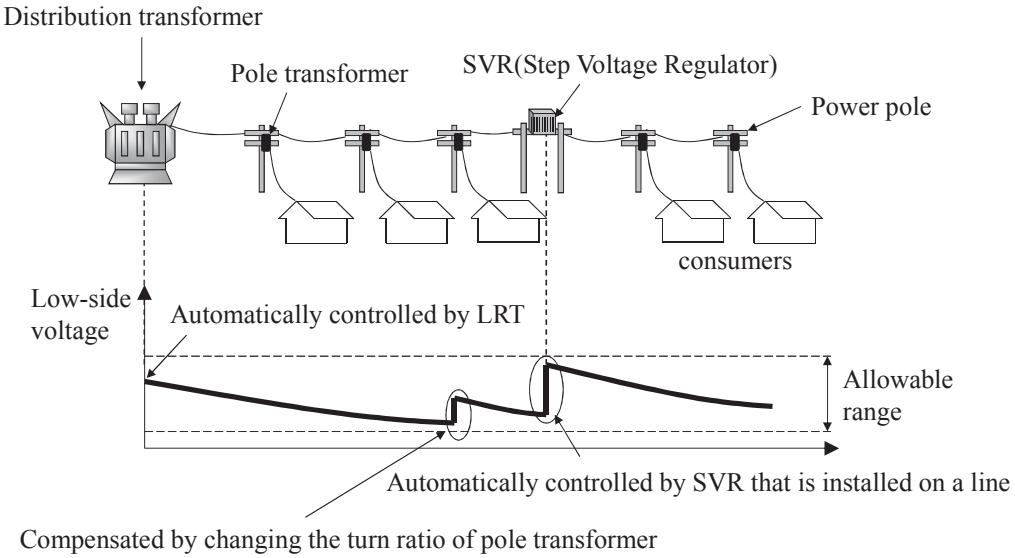

Figure 1.2 Voltage management in DS.

To meet the requirement shown on Table 1.1, voltage in DS is managed using several facilities. Conventional constitution of DS for voltage management is shown in Figure 1.2. In Figure 1.2, a distribution transformer sends electricity power to consumers through distribution line. The secondary voltage of distribution transformer in a distribution substation is maintained to the rated voltage in DS (usually 6600V). Usually the voltage drop through distribution line occurs owing to load distribution, it is necessary to keep voltage within the allowable range. The line voltage is managed by the following control facilities in DSO.

(1) Load Ratio control Transformer

Distribution transformer has the tap changing function to adjust the secondary voltage according to load current flow in DS. The transformer with this function is called Load Ratio control Transformer (LRT). Usually, a LRT in a distribution substation has multiple DSs, hence the control of a LRT makes an impact on voltage in multiple DSs. LRT operates and adjusts the sending voltage of multiple DSs considering voltage profiles in those networks.

(2) Step Voltage Regulator (SVR)

When voltage drop in distribution line is large, it might not be possible to control voltage within the allowable range using only LRT. In that case, Step Voltage Regulator (SVR) installed on distribution lines is employed to compensate for voltage drop. It is usually installed on a long distribution line. The SVR is a transformer similar to LRT which can control its secondary voltage by changing its tap position. A detail structure and control algorithm of SVR are explained in Appendices A1.

(3) Adjustment for a turn ratio of pole transformer

Ordinary residences receive electric power as rated voltage 100V or 200V transformed from high-side voltage (6600V) using a turn ratio of pole transformer on a distribution line. The pole transformers are installed on power poles and electric power on low-side voltage line can be delivered through a lead-in wire. The turn ratio is modified by DSO corresponding to voltage profile to meet requirement shown on Table 1.1. Once the turn ratio is set by DSO, it is very difficult to change the ratio. DSO must adequately determine the ratio considering a load profile and load growing in future.

1.3 Technical issues caused by PV

1.3.1 Issues occurred in distribution system

Japanese government estimates that many residences in DS will introduce PV as rooftop type. Introducing PV into DS may cause multiple issues regarding voltage such as 1) the voltage rise and 2) the voltage fluctuation. An output of PV coincides with the decrease of load; hence voltage in DS becomes large compared to one without PV. Since voltage in DS is large due to Ferranti effect even in the current situation [5], voltage may exceed an upper limit of allowable range in case of PV interconnection. To prevent this problem, modifying the classical method for voltage management is indispensable. Furthermore, PV can cause voltage fluctuation in DS. As existing facilities in the power grid are not designed for compensating rapid and frequent voltage change, voltage might not be properly controlled in that case. One of way for solving these issues is to replace the existing obsolete facilities to novel functional devices such as Static Var Compensator (SVC). However, introducing new facilities leads to an increase of cost and may cause rising of electricity charges that is difficult because an electric power system is a public infrastructure. It is important to prevent these issues mentioned above with few additional costs.

One of effective measures against these problems is utilizing information in DS obtained through high-speed communication. With information in DS including voltage magnitude, voltage phase angle, current magnitude, and current phase angle, voltage can be managed in an efficient manner even if using the obsolete facilities. In recent years, many DSOs are trying to introduce multiple sensors to get useful information on DS. Some DSOs begins to install smart meters into consumers for meter-reading. In the present circumstances, however, many sensors do not have an ability to communicate in real-time. This means that it is difficult for current DSO to get precise information in DS. An important issue to be solved is how to properly control voltage with insufficient information.

1.3.2 Issues occurred in transmission system

A distribution substation has multiple DSs, and a Transmission System (TS) has many distribution substations. As many distribution substations are connected each other through transmission lines, fluctuation of load and PV's output in a DS may make adverse impact regarding to voltage on other DSs. In conventional way, voltage in TS is kept close to constant value using transformers and phase modifying equipment by Transmission System Operator (TSO). However, a large amount of PV in DS can vary voltage not only in DS, but also in TS. Voltage profile in the transmission line can become complex in that case. Since classical facilities in TS for voltage control do not assume PV penetration, these facilities might not keep voltage close to constant. This fluctuation of primary voltage at the distribution substation leads to the fluctuation of voltage in DS. Therefore, with PV penetration, voltage fluctuation in DS is due to both DS and TS. Controlling voltage in TS is critically important. The number of researches about voltage control in TS is small. In particular, an impact of PV on voltage in TS has not been sufficiently studied. It is necessary to investigate the impact of PV in TS. Furthermore, an efficient control strategy for voltage in TS with many PV should be developed.

1.4 Previous work

Conventional control methods for voltage in DS cannot manage voltage fluctuation caused by DG. These issues have been tackled in [6] ~ [22]. In [6] ~ [13], the maximum PV capacity which does not cause voltage violation from an adequate range is calculated. It is important to estimate the allowable capacity of PV installed in a DS because additional measures are indispensable if voltage violation is occurred. In [14] [15], by using power electronics devices including SVC and STATic synchronous COMpensator (STATCOM), voltage fluctuated by PV can be made stable and controlled within the adequate range. These devices recently attract attention. In [16] ~ [19], Power Conditioning System (PCS) is focused on because it is able to inject not only active power but also reactive power into the network. In [20] [21], multiple sensors and communication are employed to get information about voltage and current in DS to calculate optimal operation of the control devices.

As mentioned above, there are many researches for voltage management in case of PV interconnection. However, most of them assume that additional devices are necessary to control voltage. It is necessary to research a way to manage voltage for PV interconnection and develop a suitable control method with few additional costs.

1.5 Overview

This thesis focuses on voltage control for properly managing voltage in DS. The overview of this thesis is shown in Figure 1.3. Since the measures for PV interconnection should be changed according to development of power system, the content of each chapter are changed in accordance with time and situation.

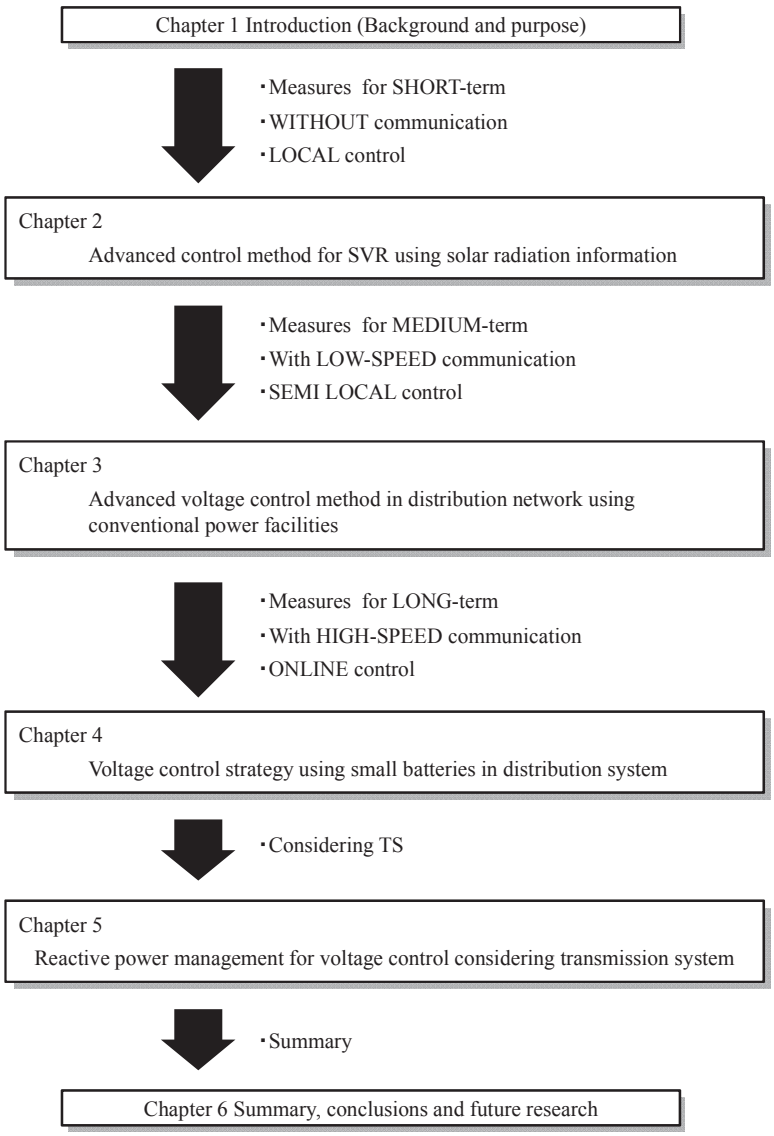

Figure 1.3 Contents and relations of each chapter in this thesis.

First of all, as measures for short-term, a local control method for SVR is proposed in chapter 2. Since chapter 2 assumes DS in near future, high cost devices should not be used as much as possible. The purpose of chapter 2 is to manage voltage fluctuated by PV in DS with SVR and little additional equipment.

With low-functional facilities, voltage is controlled based on local control. In chapter 3, a novel control method for existing facilities such as SVR and a few sensors in DS is proposed. Compared with chapter 2, chapter 3 targets the further future electric power network with functional device for voltage control. Chapter 4 targets rapid voltage fluctuation in DS unlike in chapters 2, and 3. This chapter assumes the power system with real-time communication and multiple functional devices. Under this condition, power system can perform online control. Batteries in the residences and Electric Vehicles (EV) are employed to compensate for the time delay of SVR. Finally, in chapter 5, a control method for reducing voltage fluctuation in TS that uses multiple SVCs is proposed. It is necessary to keep sending voltages in distribution substations close to constant.

(1) Chapter 2: Advanced control method of SVR using solar radiation information

Existing facilities for voltage control in DS such as SVR have low functionality because, for example, SVR observes only local voltage and sending current at PCC (Point of Common Coupling). Though this control method is suitable for DS without DG, it is unsuited for with DG. Hence, modifying the obsolete control method of existing facilities is indispensable to introduce DG into DS. This chapter studies a novel control method of SVR with little additional equipment to decrease cost. SVR in the proposed method is controlled corresponding to solar radiation information obtained from solar radiation sensor installed in SVR.

(2) Chapter 3: Advanced voltage control method in distribution network using conventional power facilities

Because current DS has few sensors embedded in section switches on distribution lines, DSO can obtain information in DS. Using information such as voltage and current on the distribution line, a better control method can be developed. However, communication speed between sensors is very slow, not in real-time. Therefore, a feasible control method for SVR using sensors with slow communication is proposed in this chapter. The proposed method uses SVR, few Voltage Sensor (VS), and low-speed communication between SVR and VS. It will be shown that developing control method with few additional facilities can properly manage voltage in this chapter.

(3) Chapter 4: Voltage control strategy using small batteries in distribution system

Transitional voltage fluctuation will be caused by PV. As discussed previously, current SVR does not have an ability to mitigate rapid voltage fluctuation since there is no rapid voltage fluctuation in the conventional DS. This quick phenomenon may cause tentative voltage violation from the allowable range. Though SVC and Thyristor Voltage Regulator (TVR) using power electronics technology are suitable to suppress this issue, these facilities have highly cost. Utilizing user-owned equipment such as a PCS and a battery is a valid way to resolve this issue. Many voltage control methods using PCS owned by users in DS

have been studied to date. In [16] ~ [19], user-owned PCSs control reactive power output and maintain voltage on distribution line within the adequate range. Tsuji et al employ user-owned PCSs to achieve a goal that is to minimize distribution loss and maintain voltage within the adequate range [17] ~ [19]. On the other hand, this thesis focuses on a user-owned battery.

Japan has been in a situation where there is lack of electric power caused by loss of nuclear power plants due to the Great East Japan Earthquake at 11.3.2011. This calamity made people in Japan attract attention for tight supply and demand of electric power. Smart grid is also focused on than before to eliminate waste of power and people pay attention to the battery in a smart house. Smart house can efficiently utilize electric power using PV and a storage device. A battery in house can be used as an electricity power source for emergency situation that is outage for instance. A battery can flexibly charge and discharge active power and control rapid voltage change in DS [22] ~ [25]. Hence, a lot of batteries in DS owned by users can be used as effective voltage control devices without additional highly cost. However, it is necessary to prevent user's detriment. If DSO occupies the user-owned batteries, the users cannot make use of the batteries. In order to prevent this situation, a novel control method for battery that uses a little part of user-owned battery is proposed in this chapter.

(4) Chapter 5: Reactive power management for voltage control considering transmission system

To handle problems such as voltage fluctuation in DS, many researches have been studied in literatures [17] ~ [19] [26] ~ [30]. These literatures assumed that a primary voltage of distribution substation is close to constant because the primary voltage is properly managed using multiple facilities on TS. However, when many PVs are introduced into DS, it is expected that the primary voltage fluctuates and the fluctuation makes impact on transformers in distribution substations. It is necessary to analyze voltage problems due to PV in TS as well as DS.

In this chapter, a power system model including both TS and multiple DSs will be built, and it is analyzed what problems are arisen in case that many PVs are connected into the power system. By investigating voltage behavior on this model, the voltage fluctuation on TS caused by PVs is found to be a serious problem. To prevent this issue, a novel control method of SVCs that are installed into distribution substations is proposed. It will be shown that the proposed method can compensate for PV's an adverse impact on TS and other DSs.

1.6 References

[1] Masahiro Takasaki, “Recent Power Quality Technology Employing Power Electronics Devices”, IEEJ Transactions on Power and Energy, Vol. 124, No. 7, pp. 902-905, 2004 (in Japanese)

[2] Mutsumu Okumura, and Naoki Kobayashi, “Recent Power Quality Technology”, IEEJ Transactions on Power and Energy, Vol. 125, No. 7, pp. 643-646, 2005 (in Japanese)

[3] “Long-term energy supply-demand outlook”, Ministry of Economy, Trade and Industry, May 2008 (in Japanese)

[4] “Long-term energy supply-demand outlook (revise)”, Ministry of Economy, Trade and Industry, August, 2009 (in Japanese)

[5] Technical committee for power factor problems in distribution network, “Power Factor Problems and Measures in Distribution Network”, Report of Electric Technology Research Association, Vol. 66, No. 1, Electric Technology Research Association, 2011 (in Japanese)

[6] Anderson Hoke, Rebecca Butler, Joshua Hambrick, and Benjamin Kroposki, “Steady-State Analysis of Maximum Photovoltaic Penetration Levels on Typical Distribution Feeders”, IEEE Transactions on Sustainable Energy, Vol. 4, No. 2, pp. 350-357, 2013

[7] Chia-Hung Lin, Wei-Lin Hsieh, Chao-Shun Chen, Cheng-Ting Hsu, and Te-Tien Ku, “Optimization of Photovoltaic Penetration in Distribution Systems Considering Annual Duration Curve of Solar Irradiation”, IEEE Transactions on Power Systems, Vol. 27, No. 2, pp. 1090-1097, 2012

[8] Yoshiyuki Kubota, Takamu Genji, Shinichi Takayama, and Yoshikazu Fukuyama, “Influence of Distribution Voltage Control Methods to Maximum Capacity of Distributed Generators”, IEEJ Transactions on Power and Energy, Vol. 124, No. 1, pp. 7-14, 2004 (in Japanese)

[9] Yasuhiro Hayashi, Junya Matsuki, Yuji Hanai, Shinpei Hosokawa, and Naoki Kobayashi, “Computation of Locational and Hourly Maximum Output of a Distributed Generator Connected to a Distribution Feeder”, IEEJ Transactions on Power and Energy, Vol. 126, No. 10, pp. 1023-1031, 2006 (inJapanese)

[10] Yoshiyuki Kubota, and Takamu Genji, “A Theory of Maximum Capacity of Distributed Generators Connected to a Distribution System Using Electric Power Density Model”, IEEJ Transactions on Power and Energy, Vol. 125, No. 5, pp. 475-484, 2005 (in Japanese)

[11] Yoshiyuki Kubota, and Takamu Genji, “A Study of Maximum Capacity of Distributed Generators Connected to a Distribution System with a Step Voltage Regulator Using Electric Power Density Model”, IEEJ Transactions on Power and Energy, Vol. 126, No. 9, pp. 878-886, 2006 (in Japanese)

[12] Panagis N. Vovos, Aristides E. Kiprakis, A. Robin Wallace, and Gareth P. Harrison, “Centralized and Distributed Voltage Control: Impact on Distributed Generation Penetration”, IEEE Transactions on Power Systems, Vol. 22, No. 1, pp. 476-483, 2007

[13] Luis F. Ochoa, Chris J. Dent, and Gareth P. Harrison, “Distribution Network Capacity Assessment: Variable DG and Active Networks”, IEEE Transactions on Power Systems, Vol. 25, No. 1, pp. 87-95,

2010

[14] Naoto Yorino, Takahiro Miki, Yuuki Yamato, Yoshifumi Zoka, and Hiroshi Sasaki, "A Time Scale Separation Method for the Coordination of Voltage Controls for SVC and SVR", IEEJ Transactions on Power and Energy, Vol. 124, No. 7, pp.913-919, 2004 (in Japanese)

[15] Junbiao Han, Sarika Khushalani-Solanki, Jignesh Solanki, and Jens Schoene, "Study of unified control of STATCOM to resolve the Power quality issues of a grid-connected three phase PV system", Innovative Smart Grid Technologies (ISGT), 2012 IEEE PES, pp. 1-7, 2012

[16] Xiangdong Zong, and Peter W. Lehn, "Reactive power control of single phase grid tied Voltage Sourced Inverters for residential PV application", IECON 2012 - 38th Annual Conference on IEEE Industrial Electronics Society, pp. 696-701, 2012

[17] Takao Tsuji, Takuhei Hashiguchi, Tadahiro Goda, Takao Shinji, and Shinsuke Tsujita, "A Study of Autonomous Decentralized Voltage Profile Control Method considering Control Priority in Future Distribution Network", IEEJ Transactions on Power and Energy, Vol. 129, No. 12, pp. 1533-1544, 2009 (in Japanese)

[18] Takao Tsuji, Tsutomu Oyama, Takuhei Hashiguchi, Tadahiro Goda, Takao Shinji, and Shinsuke Tsujita, "A Study of Autonomous Decentralized Voltage Profile Control Method considering Power Loss Reduction in Distribution Network", IEEJ Transactions on Power and Energy, Vol. 130, No. 11, pp. 941-954, 2010 (in Japanese)

[19] Akira Koide, Takao Tsuji, Tsutomu Oyama, Takuhei Hashiguchi, Tadahiro Goda, Takao Shinji, and Shinsuke Tsujita, "A Study on Real-Time Pricing Method of Reactive Power in Voltage Control Method of Future Distribution Network", IEEJ Transactions on Power and Energy, Vol. 132, No. 4, pp. 359-370, 2012 (in Japanese)

[20] Eng-Kiat Chan, and Horst Ebenhoh, "The implementation and evolution of a SCADA system for a large distribution network", IEEE Transactions on Power Systems, Vol. 7, No. 1, pp. 320-326, 1992

[21] Tetsuo Otani, and Hiromu Kobayashi, "A SCADA System Using Mobile Agents for a Next-Generation Distribution System", IEEE Transactions on Power Delivery, Vol. 28, No. 1, pp. 47-57, 2013

[22] Kejun Qian, Chengke Zhou, Malcolm Allan, and Yue Yuan, "Modeling of Load Demand Due to EV Battery Charging in Distribution Systems", IEEE Transactions on Power Systems, Vol. 26, No. 2, pp.802-810, 2011

[23] Mukesh Singh, Praveen Kumar, and Indrani Kar, "Implementation of Vehicle to Grid Infrastructure Using Fuzzy Logic Controller", IEEE Transactions on Smart Grid, Vol. 3, No. 2, pp. 565-577, 2012

[24] Joshua Traube, Fenglong Lu, Dragan Maksimovic, Joseph Mossoba, Matthew Kromer, Peter Faill, Stan Katz, Bogdan Borowy, Steve Nichols, and Leo Casey, "Mitigation of Solar Irradiance Intermittency in Photovoltaic Power Systems With Integrated Electric-Vehicle Charging Functionality", IEEE Transactions on Power Electronics, Vol. 28, No. 6, pp. 3058-3067, 2013

[25] Jeroen Tant, Frederik Geth, Daan Six, Peter Tant, and Johan Driesen, “Multiobjective Battery Storage to Improve PV Integration in Residential Distribution Grids”, IEEE Transactions on Sustainable Energy, Vol. 4, No. 1, pp. 182-191, 2013

[26] Shigenori Naka, Sakae Toune, Takamu Genji, Toshiki Yura, Shinichi Takayama, and Yoshikazu Fukuyama, “Optimal Setting for Control Equipment Considering Interconnection of Distributed Generators”, IEEJ Transactions on Power and Energy, Vol. 120, No. 12, pp. 1558-1565, 2000 (in Japanese)

[27] Yuji Hanai, Yasuhiro Hayashi, Junya Matsuki, and Masanori Kurihara, “Proposal and Experimental Verification of Distribution Voltage Estimation and Control Method using Measured Data from IT Switches”, IEEJ Transactions on Power and Energy, Vol. 130, No. 10, pp. 859-869, 2010 (in Japanese)

[28] Yuji Hanai, Yasuhiro Hayashi, and Junya Matsuki, “Experimental Verification of Application of Looped System and Centralized Voltage Control in a Distribution System with Renewable Energy Sources”, IEEJ Transactions on Power and Energy, Vol. 130, No. 11, pp. 932-940, 2010 (in Japanese)

[29] Hideharu Sugihara, Tsuyoshi Funaki, Yasuo Matsuura, Tomohiko Morita, and Masahiro Minami, “An Analysis on Relationship between Installable Capacity and Spatial Distribution of Distributed Generators under Customer-side Voltage Constraints in Medium and Low Voltage Distribution Networks—In Case of the DG's Rated Output—”, IEEJ Transactions on Power and Energy, Vol. 133, No. 3, pp. 229-236, 2013 (in Japanese)

[30] Tsuyoshi Udagawa, Yasuhiro Hayashi, Naoyuki Takahashi, Yasuo Matsuura, Tomohiko Morita, and Masahiro Minami, “Evaluation of Voltage Control Effect of Acquisition Period for IT Switch Data”, IEEJ Transactions on Power and Energy, Vol. 133, No. 4, pp. 324-332, 2013 (in Japanese)

Chapter 2
Advanced control method of SVR using solar radiation information

2.1 Introduction

In traditional sense, SVR is installed into DS to manage voltage within the allowable range. Its installation location and control parameters such as basis voltage of dead band, width of dead band, and settling time are usually determined under the condition without any DGs in DS and reverse power flow. However, when a large amount of PV is connected to DS, several technical issues arise. 1) One is operation delay for changing tap of SVR against voltage fluctuation. Since SVR is a transformer with mechanical structure, it needs operational delay against voltage fluctuation to avoid deterioration due to switching operations. In case that PV is connected to DS, line voltage may rapidly fluctuate due to sudden change of weather condition. Since conventional SVR does not suppose the rapid voltage fluctuation, SVR could not compensate for this rapid change. 2) The other is lack of information for switching operation to adequately compensate for the voltage fluctuation in DS, because conventional SVR operates based on only the monitored secondary voltage. DSO usually manages voltage under the assumption that a load pattern in DS is almost same every day. However, when PV is connected, the load pattern randomly fluctuates and voltage profile becomes complex. In that case, voltage at the secondary node of SVR is insufficient for proper management of voltage because SVR with local control cannot precisely estimate voltage profile in the distribution line.

Meanwhile, functional facilities such as SVC and PCS can compensate for rapid voltage change due to PV [1] ~ [10]. These facilities can prevent voltage fluctuation and compensate for complex voltage profile. However, using these devices leads to increase cost that should be avoided. Therefore, it is important to propose a novel control method to only utilize existing facilities such as SVR without additional installation of devices for voltage control even when PVs are connected to DS. Moreover, it is necessary to suppress useless switching operation of SVR for avoiding deterioration even when voltage in DS frequently changes. Under this background, in this chapter, an intelligent control method of conventional SVR is proposed to achieve these purposes. The proposed method defines “Voltage Margin (VM)” as an index of difficulty of voltage violation from the allowable range caused by PV. VM is obtained based on estimated output of PV using solar radiation information from a solar radiation sensor. By increasing VM, voltage violation and useless operation of SVR can be suppressed. Numerical simulation example is to demonstrate the effectiveness of proposed method. This simulation uses an actual scale DS model for

precise analysis.

2.2 Voltage issues caused by PV interconnection

2.2.1 Simulation model

Many literatures have studied about voltage management issue that is expected to occur when many PVs are introduced into DS. However, many studies use simple DS models without SVR and many nodes. It is insufficient to reveal the issues that actually occur in case of PV interconnection. From this, this section investigates the voltage issue by PV using an actual scale DS model shown in Figure 2.1, where network configuration including positions of SVRs and turn ratio of pole transformers is based on real DS data. Detail parameters such as load capacity and line impedance are shown in Appendices A3.

Four SVRs are installed in this model shown in Figure 2.1. The arrow represents a load, and PV is installed in all load nodes assuming PV introduced on roof of residences. The line voltage (Rated voltage: 6600V) in DS is transformed to low voltage (Rated voltage: 100V) by pole transformers. Its turn ratio N_{tr} is usually set as 6600/105 (High side/Low side), but turn ratios of some pole transformers are set to be lower to compensate for voltage drop. Since there are many users on from node #42 ~ #116 in Figure 2.1, N_{tr} on those nodes are set as 6450/105 so that primary voltage of SVR2 and SVR4 and the voltage at the end of feeder do not exceed the lower limit of allowable range. Numerical simulation is executed to represent voltage fluctuation caused by PVs using MATLAB/Simulink.

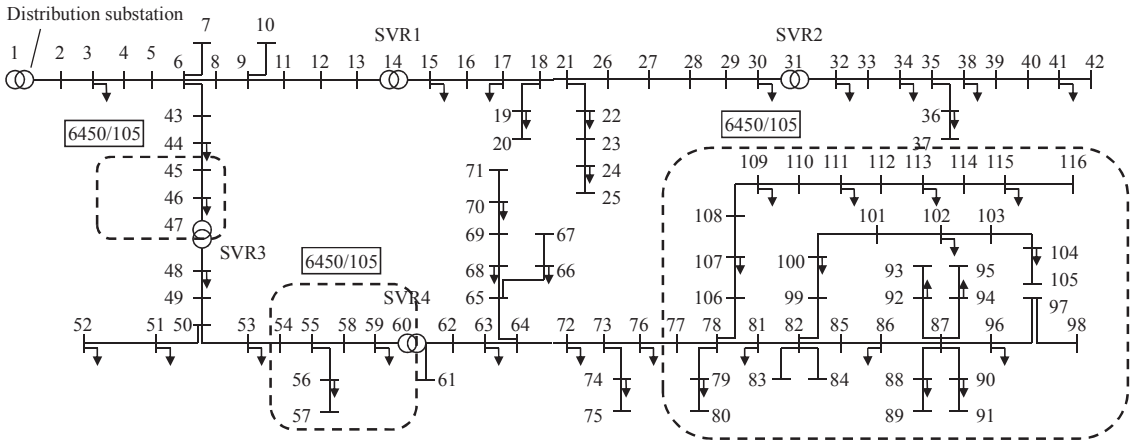

Figure 2.1 Actual scale distribution system model.

2.2.2 Simulation conditions

Table 2.1 shows simulation conditions in which parameters of SVR are employed in actual DS.

Table 2.1 Simulation conditions.

Sampling time *dt*			2s
Simulation period *T*			86400s (24h)
Allowable range (Low-side)			101 ~ 107V
Sending voltage of substation			6600
SVR	Basis voltage of dead band V_{basis}		6600V
	Settling time T_{settle}	SVR1, SVR3	60s
		SVR2, SVR4	90s
	Width of dead band V_{db}		189V
	Width of tap		150V

Simulation is executed to analyze voltage behavior over a day considering the load pattern and solar radiation. Real measured data in cloudy day is used for solar radiation and a typical resident load is used for the load pattern at each node. Sum of the active power *P* and the reactive power *Q* of load in the entire DS model are shown in Figure 2.2. Total output of PVs and solar radiation are represented in Figure 2.3. The output of PV rapidly and frequently fluctuates in proportion to solar radiation *S* assuming that PV outputs active power with power factor 1.0 and PV capacity is set as same as load capacity. It is assumed that PVs are connected at all nodes considering a large amount of PV interconnection. Sending voltage in the distribution substation controlled by LRT is set as constant 6600V to evaluate the impact of only PV on voltage not of sending voltage.

2.2.3 Simulation results

As examples of voltage violation out of the allowable range, the voltage at secondary nodes of SVRs V_{SVR} and the end of distribution line (node #42, #116) are shown in Figure 2.4 and Figure 2.5, respectively. High-side voltage at node #42 and #116 are transformed into low-side voltage using N_{tr} (#42: 6600/105, #116: 6450/105) in Figure 2.5. In Figure 2.4, the light gray lines represent the limits of dead band. In both Figure 2.4 and 2.5, the gray lines represent the limits of allowable range. In Figure 2.4, V_{SVR} of SVR2 and SVR4 exceed the upper limit of allowable range. This is because basis voltages of dead band V_{basis} are set as high position (=6600V) considering voltage drop on the distribution line (Allowable range: 6726V~6349V). Moreover, after V_{SVR} deviates from the dead band, the tap position is changed with a few settling time (T_{settle}). This is due to that frequent switching operations causes deterioration of SVR. T_{settle} causes transient voltage violation out of both the dead band and allowable range.

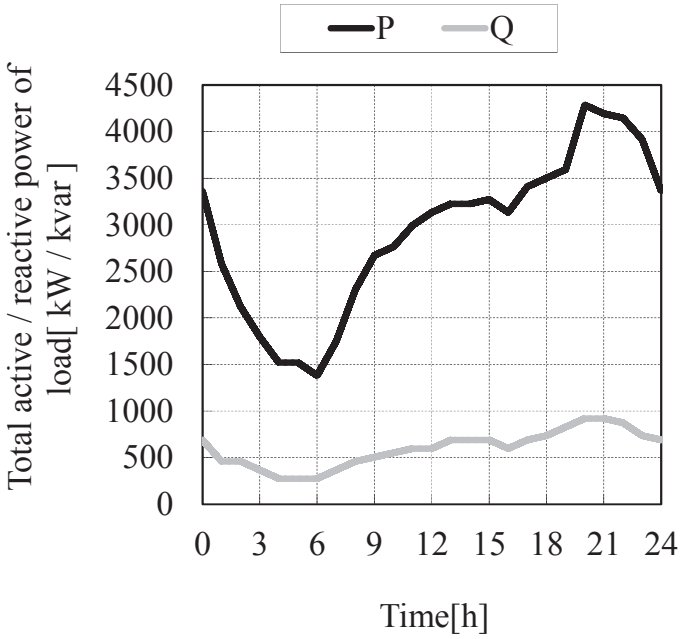

Figure 2.2 Trend of load active and reactive power.

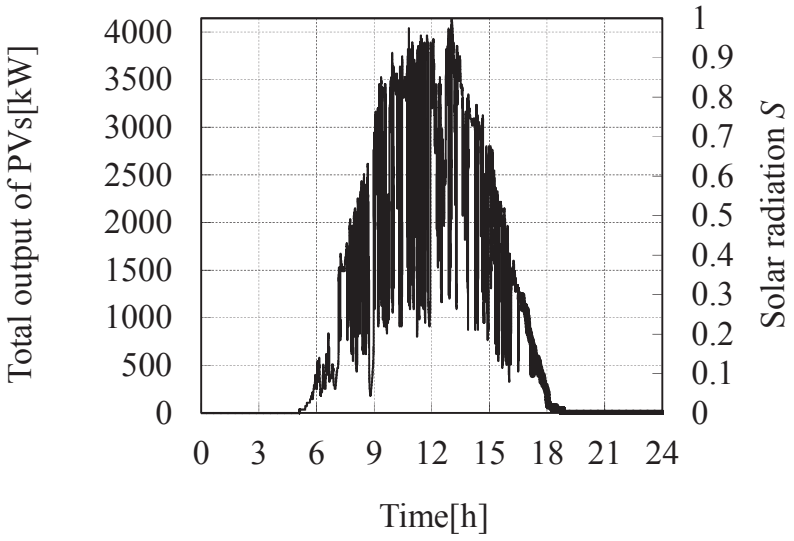

Figure 2.3 Trend of PV output and solar radiation.

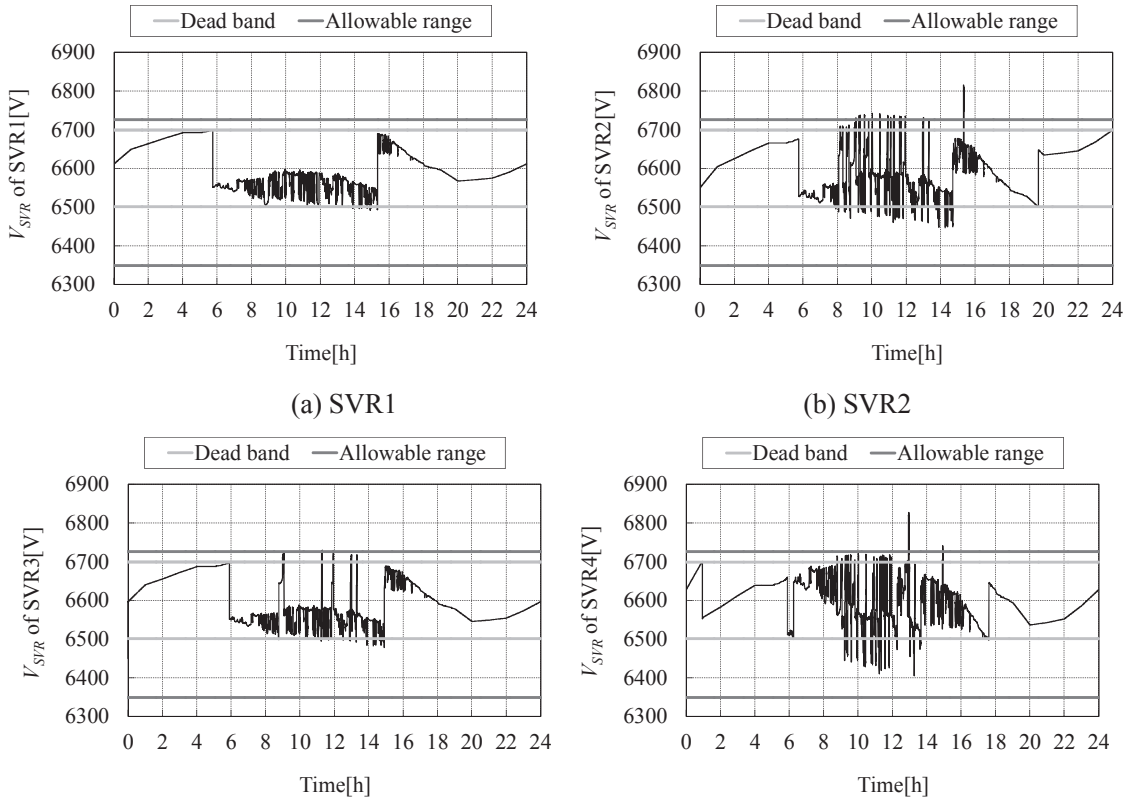

(a) SVR1 (b) SVR2

(c) SVR3 (d) SVR4

Figure 2.4 V_{SVR} in conventional method.

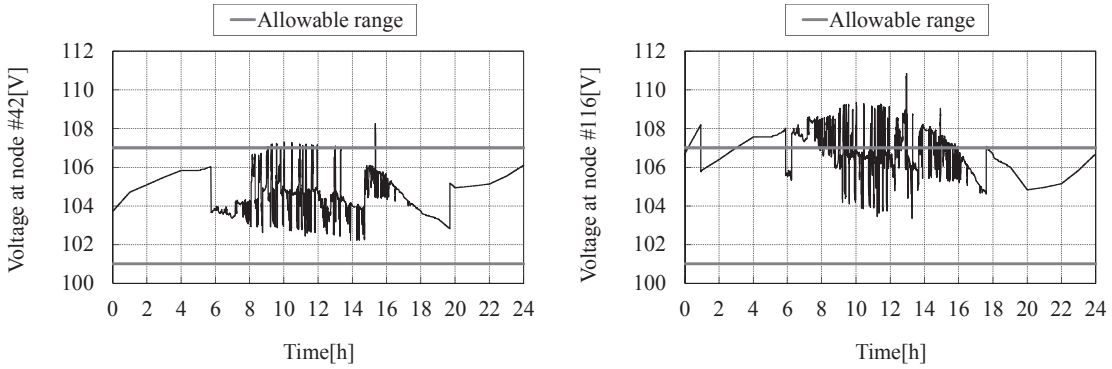

(a) Node #42 (b) Node #116

Figure 2.5 Low voltage at end of distribution line in the conventional method.

Thus, the voltage violation is not compensated owing to the time delay of switching operation, and hence voltage may continue to deviate from allowable range for a short time in Figure 2.4. Low voltage at end of distribution line in Figure 2.5 (a) exceeds the upper limit of allowable range (107V) in a similar way. This problem is mainly caused by two factors. One is improper settings of control parameters of SVR such as an install node, dead band, and settling time mentioned above. The other is improper settings of N_{tr}. The latter is the reason why the turn ratio of pole transformer 6450/105 is set corresponding to usual voltage drop in distribution line without considering the fact that voltage at node #116 rises due to PV.

Making T_{settle} small to improve the time delay of SVR may lead to increase of hunting of SVRs. It is caused by the frequent switching of SVR. For example, the simulation results are shown in case that T_{settle} is set as 1/10 of previous case in Table 2.1. In the same way as Figure 2.4 and 2.5, the V_{SVR} and the end of distribution line (node #42, #116) with small settling time are shown in Figure 2.6 and 2.7, respectively. In Figure 2.6 and 2.7, voltage violation from the allowable range is occurred even though T_{settle} is smaller than previous case. From these results, small T_{settle} does not influence enough for reducing voltage violation. In order to quantitatively evaluate these results, the amounts of voltage violation from the allowable range, time of voltage violation and the number of switching operation of SVR are calculated. Indices for evaluation of voltage violation are defined. An integration of voltage violation VD is obtained by integrating the amount of voltage violation from the allowable range (101~107V) with time as follows:

$$VD = \sum_{t=0}^{T} \sum_{n=1}^{n_{\max}} e_V(t,n) \tag{2.1}$$

$$e_V(t,n) = \begin{cases} V(t,n) - 107 & (V(t,n) > 107) \\ 101 - V(t,n) & (V(t,n) < 101) \end{cases}$$

where $V(t,n)$ shows low-side voltage at time t and node #n, and the total number of nodes n_{max} is 116. Voltage violation time from the adequate range VD_{time} is obtained by integrating time at which voltage deviates from the allowable range as follows:

$$VD_{time} = \sum_{t=0}^{T} \sum_{n=1}^{n_{\max}} e_T(t,n) \tag{2.2}$$

$$e_T(t,n) = \begin{cases} dt & (V(t,n) > 107) \\ dt & (V(t,n) < 101) \end{cases}$$

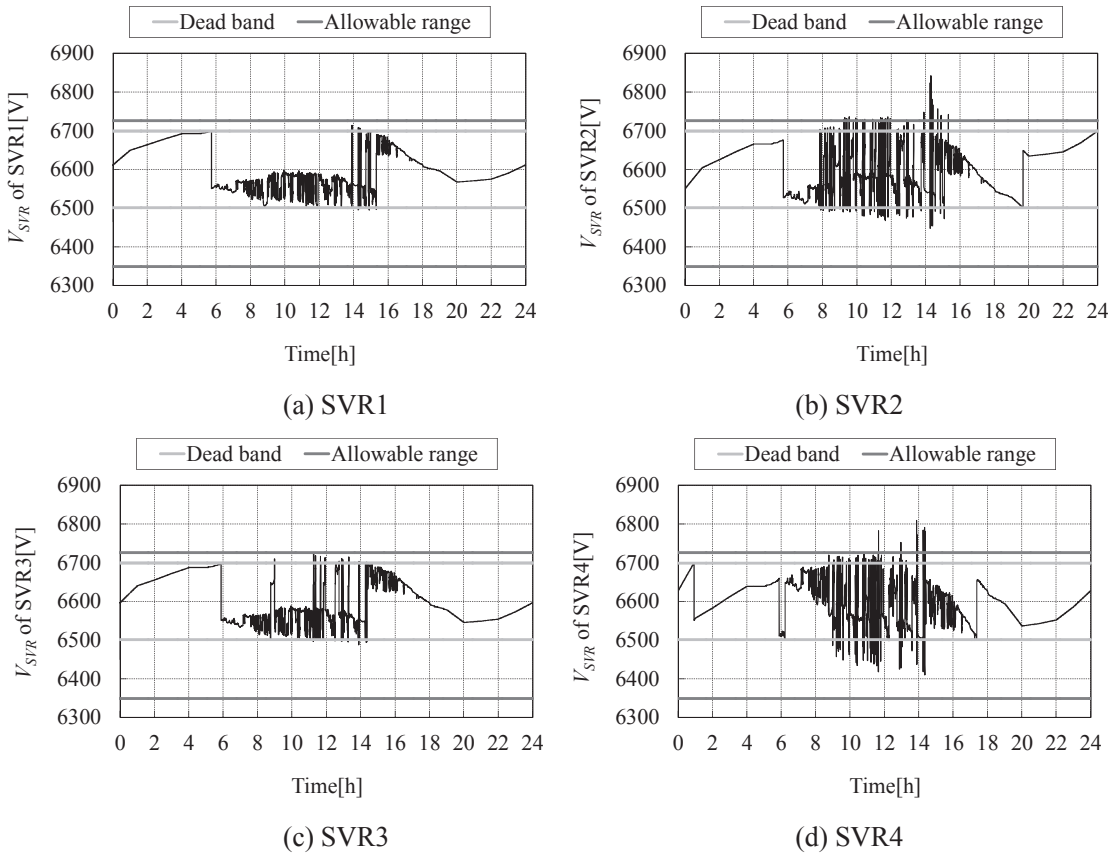

(a) SVR1 (b) SVR2

(c) SVR3 (d) SVR4

Figure 2.6 V_{SVR} with small T_{settle}.

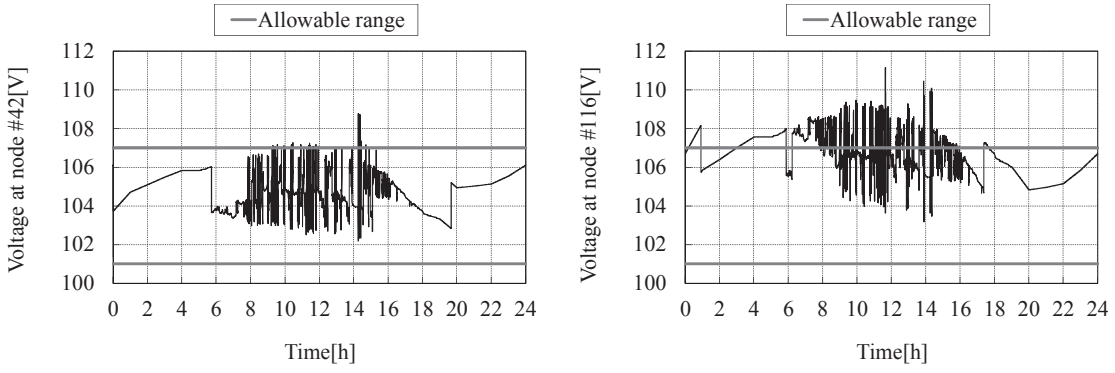

(a) Node #42 (b) Node #116

Figure 2.7 Low voltage at end of distribution line with small T_{settle}.

Table 2.2 shows qualitative evaluation results comparing two cases of conventional T_{settle} and small T_{settle}. "Differences" in Table 2.2 represents that variation value using small T_{settle} compared to the conventional method.

Table 2.2 Quantitative evaluation results.

		Conventional	Small settling time	Differences
VD		1224×10^2 Vs	1110×10^2 Vs	-9.3%
VD_{time}		1582×10^2 s	1522×10^2 s	-3.8%
The number of switching operation of SVR	SVR1	2	18	+16
	SVR2	22	106	+84
	SVR2	12	22	+10
	SVR4	28	88	+60

Table 2.2 shows that even if T_{settle} is set smaller, both *VD* and VD_{time} cannot be almost improved. On the other hand, the number of switching operation of SVR largely increases since the secondary voltages of all SVRs fluctuate largely and frequently, particularly in SVR2 and SVR4. Moreover, in Figure 2.6, the secondary voltage of SVR2 and SVR4 frequently fluctuate corresponding to the operation of upper SVRs (SVR1, SVR3). Such frequent operations of lower SVRs continually occur in daytime hours in which solar radiation frequently fluctuates. Thus, small T_{settle} causes the frequent switching operation of SVR, voltage violation, and deterioration of SVR. Hence, it can be seen that it is difficult to properly manage voltage fluctuated due to PV using only SVR controlled by a conventional method. It is easy to properly control voltage using reactive power control with PCS and Flexible AC Transmission System (FACTS) devices such as SVC. However, introducing many SVC into DS is difficult due to its highly cost, and few PCSs cannot output reactive power enough to control voltage. Moreover, even if it is possible to use many PCSs in DS, it needs a cooperative control method which is hard to achieve.

For this reason, the new control method utilizing existing SVR is proposed by modifying the existing control algorithm slightly, which is effective to handle the voltage issue in case of many PVs interconnection with reducing installation cost of additional facilities.

2.3 Proposed control method

2.3.1 Fundamental idea for proposed method

A key concept of the proposed method is managing voltage fluctuated by PV using the existing SVR as well as suppressing the frequent switching operations of SVR. The goal is to reduce *VD*, VD_{time}, and the number of switching operation of SVR. To do this, it is necessary to increase a margin of voltage for upper and lower limits of allowable range so that voltage does not deviate from the adequate range even if output of PV changes rapidly. In this chapter, this margin is called VM. Difference of voltage behavior due to difference of VM is shown in Figure 2.8.

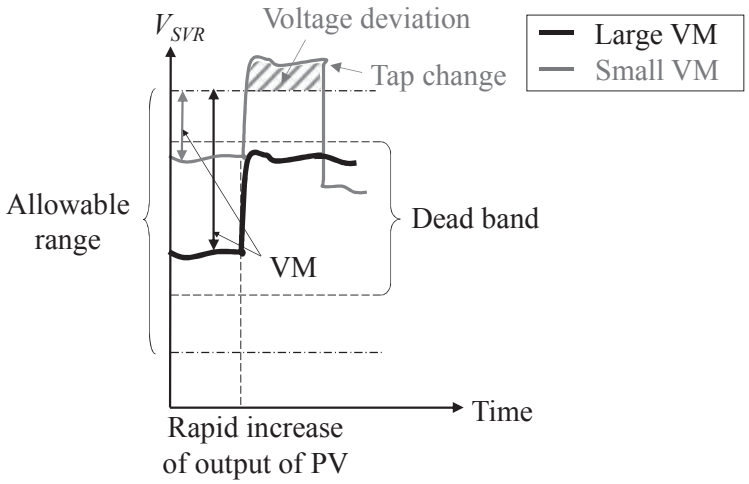

Figure 2.8 Effect of large VM.

In Figure 2.8, gray line represents V_{SVR} with small VM and Black line represents V_{SVR} with large VM. With small VM, voltage easily deviates from the allowable range due to rapid change of PV's output. Voltage violation occurred in Figure 2.5 and 2.6 is due to mainly small VM. On the other hand, with large VM, voltage violation can be suppressed because V_{SVR} tends to be kept within the dead band, and SVR does not change the tap position even though the output of PV changes rapidly. Because it is necessary to predict the fluctuation of PV's output in order to increase VM in advance, in this chapter, the method for estimating the output fluctuation is proposed by using solar radiation from the solar radiation sensor installed in SVR. The output of PV is in proportion to solar radiation. Therefore, it is assumed that solar radiation has a same value in an area in which SVR manages. This assumption is extended to the case that it might be possible to estimate the output of PV in each residence using the solar radiation sensor. In the proposed strategy, SVR increases V_{SVR} in advance if solar radiation has large value because voltage may rapidly decrease corresponding to solar radiation. On the other hand, SVR makes V_{SVR} decrease in advance if solar radiation has small value because voltage may rapidly increase corresponding to solar radiation.

2.3.2 Control algorithm

The center voltage of dead band in SVR V_{center} is controlled corresponding to solar radiation to achieve the proposed strategy mentioned above. Figure 2.9 shows the concept of proposed algorithm. Solar radiation information obtained from sensor is normalized as S using the maximum solar radiation value at a node with sensor. The maximum solar radiation is determined considering the mounting angle of PV array and other conditions. dV is the deviation of V_{center} from the base voltage V_{basis} of the allowable range, which is determined corresponding to S. While the dead band is also shifted with V_{center}, the width of dead band V_{db} is not changed. V_{basis} is set as the normal voltage in DS (=6600V) and V_{center} becomes equal to V_{basis} when $S = 0.5$. In that case, the dead band position is same as in the conventional method.

The amount of dV should be determined using both the solar radiation information and voltage fluctuation due to PV. The reason is that, for example, an unnecessary operation of SVR might occur if V_{center} is controlled corresponding to only solar radiation in spite of small voltage fluctuation due to PV as shown in Figure 2.10 (a). The unnecessary operation of SVR leads to voltage violation as mentioned above. Hence, when the voltage fluctuation is small due to PV, conventional settings of dead band should be employed that has been properly modified by DSO and the dead band should not be shifted as shown in Figure 2.10 (b). Hence, V_{center} is determined considering not only solar radiation but also an impact of PV on voltage in DS. This impact is calculated using the maximum voltage V_{max_mem} and the minimum voltage V_{min_mem} at the primary node of SVR for T_{mem}, a period in the past. dV is determined using equation (2.3) and V_{center} is obtained as equation (2.4).

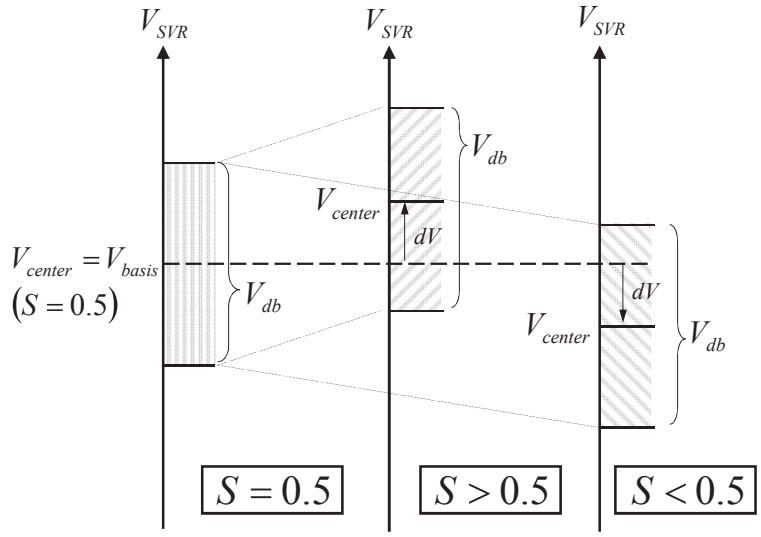

Figure 2.9 Movement of dead band corresponding to solar radiation.

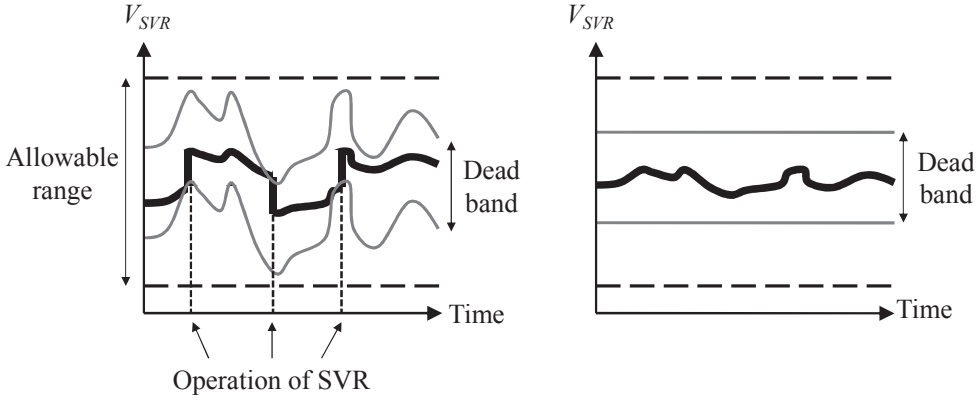

(a) dV controlled corresponding to S (b) dV=0 regardless of S

Figure 2.10 Unnecessary operation of SVR and its measure.

$$dV = \left(V_{max\_mem} - V_{min\_mem}\right)\left(S - 0.5\right) \tag{2.3}$$

$$V_{center} = V_{basis} + dV \tag{2.4}$$

The position of the dead band should be controlled by the amount of voltage fluctuation. However, since voltage fluctuation is caused by not only PV's output but also loads, the fluctuation due to loads should be separated from one due to PV. Therefore, T_{mem} in which SVR monitors ($V_{max\_mem} - V_{min\_mem}$) is set as short time enough to ignore load fluctuation. The output of PV increases and decreases to some extent during this periods. ($V_{max\_mem} - V_{min\_mem}$) is updated each period T_{mem}.

2.3.3 Dead band control considering the allowable range

The dead band position should be controlled considering the allowable range in the proposed method. Moreover, voltage drop at nodes downstream of SVR should also be considered. Assuming that downstream voltage does not exceed upstream voltage in the distribution line, in the proposed method, the allowable dead band range is determined. Under this assumption, the maximum voltage of dead band V_{SVR_MAX} is set as same as the upper limit of adequate range V_{MAX}. Considering voltage drop, the lower limit of dead band V_{SVR_MIN} is larger than the lower limit of allowable range V_{MIN} by a bias voltage V_{bias}. V_{SVR_MAX} and V_{SVR_MIN} can be expressed as follows.

$$V_{SVR\_MAX} = V_{MAX} \tag{2.5}$$

$$V_{SVR\_MIN} = V_{MIN} + V_{bias} \tag{2.6}$$

The band defined by both V_{SVR_MAX} and V_{SVR_MIN} is called as an available range shown in Figure 2.11. As the amount of voltage drop is changed due to PV, V_{bias} can be represented as a function of S shown in equation (2.7). K_{bias} represents V_{bias} when S=0.0, in this case, voltage drop becomes maximum value.

$$V_{bias} = K_{bias}\left(1 - S\right) \tag{2.7}$$

where K_{bias} is Bias gain.

If V_{SVR_MAX} exceeds V_{MAX}, V_{SVR_MAX} becomes equal to V_{MAX}. If V_{SVR_MIN} is smaller than V_{MIN}, V_{SVR_MIN} becomes equal to V_{MIN}. Hence, if the upper limit of dead band $V_{center} + V_{db}/2$ exceeds V_{SVR_MAX}, V_{center} is modified using equation (2.8). Similarly, if the lower limit of dead band $V_{center} - V_{db}/2$ is less than V_{SVR_MIN}, V_{center} is modified using equation (2.9).

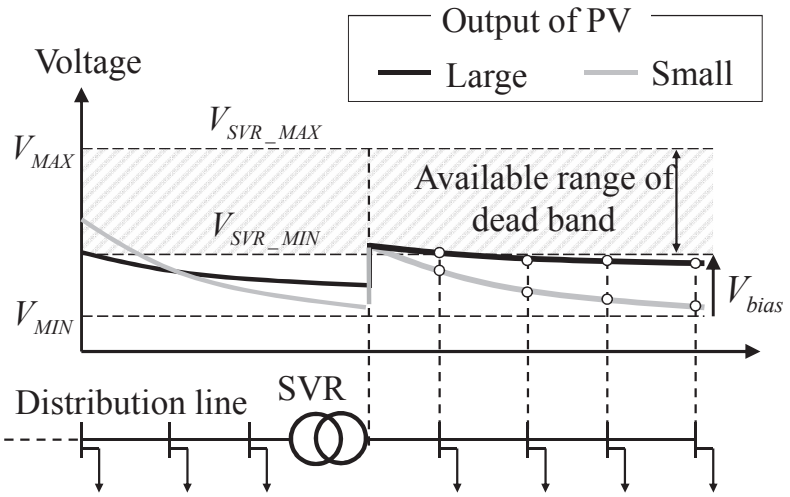

Figure 2.11 Restricted allowable range of dead band.

$$V_{center} + V_{db}/2 > V_{SVR\_MAX} \rightarrow \quad V_{center} = V_{SVR\_MAX} - V_{db}/2 \tag{2.8}$$

Upper limit of dead band: V_{SVR_MAX}

Lower limit of dead band: $V_{SVR\_MAX} - V_{db}$

$$V_{center} - V_{db}/2 < V_{SVR\_MIN} \rightarrow \quad V_{center} = V_{SVR\_MIN} + V_{db}/2 \tag{2.9}$$

Upper limit of dead band: $V_{SVR\_MIN} + V_{db}$

Lower limit of dead band: V_{SVR_MIN}

2.3.4 Reducing time delay for the operation

As mentioned above, the time delay of SVR is a prime cause of voltage violation. Hence, T_{settle} should be reduced to avoid voltage violation. In the conventional control algorithm of SVR, the number of switching operation of SVR substantially increases with small T_{settle}. On the other hand, in the proposed method, SVR does not frequently operate despite of small T_{settle} because VM is large. When multiple SVRs are installed on a distribution line in series, the proposed method is effective for suppressing hunting of multiple SVRs.

2.4 Case study

2.4.1 Simulation conditions

Numerical Simulation using an actual scale distribution system model shown in Figure 2.1 is executed to compare the proposed method with the conventional control method of SVR. Simulation is performed not only under cloudy conditions but also sunny and rainy shown in Figure 2.12.

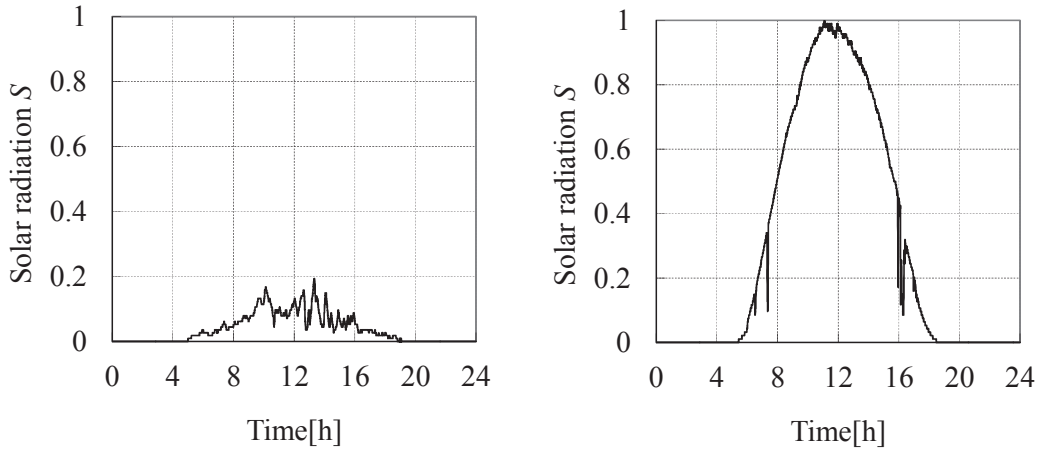

(a) Sunny (b) Rainy

Figure 2.12 Trend of solar radiation.

Sunny and rainy data are actually measured as well as cloudy data. Simulation conditions and parameters of the conventional control method are as same as Table 2.1. The width of tap and dead band in the conventional method are also employed in the proposed method because the proposed method is for effectively utilizing existing SVR with slight modification. T_{settle} in the proposed method is 1/10 compared to the conventional method because it is desirable to respond rapid change of PV's output for reducing voltage violation. T_{mem} is set as 400s. K_{bias} is set as 150V. Since voltage tends to deviates from allowable range at a node in which N_{tr} is 6450/105, N_{tr} is set as 6600/105 on entire DS in this simulation.

2.4.2 Simulation results

In order to compare two control methods of SVR, i) VD, ii) VD_{time}, iii) the maximum voltage during simulation, iv) the minimum voltage during simulation v) the number of switching operation of SVR are used as indices of evaluation for simulation results. Simulation results are shown on Tables 2.3, 2.4, and 2.5. In Tables 2.3, 2.4, and 2.5, VD and VD_{time} in the proposed method are reduced more than 80% compared to the conventional method at any climate conditions. The maximum voltage in the proposed method does not exceed one in the conventional method at any climate conditions. Similarly, the minimum voltage is not less than one in the conventional method. These results demonstrate that a voltage fluctuation in the proposed method is smaller than one in the conventional method.

The number of operations of SVRs in the proposed method is not largely increased compared to the conventional method in spite of small T_{settle}. V_{SVR} in the proposed method are shown in Figure 2.13, 2.14, and 2.15. In Figure 2.13, the dead band is shifted corresponding to both solar radiation and voltage fluctuation. On the other hand, in Figure 2.14 and 2.15, the position of dead band is almost not moved. This is caused by small voltage fluctuation for T_{mem} under sunny and rainy conditions.

Table 2.3 Simulation results in cloudy.

		Conventional	Proposed	Differences
VD		4.3×10^3Vs	0.062×10^3Vs	-98.6%
VD_{time}		14×10^3s	1.1×10^3s	-92.1%
Maximum voltage		108.6V	107.2V	-1.4V
Minimum voltage		101.0V	101.6V	+0.6V
Number of operation of SVR	SVR1	2	2	±0
	SVR2	22	26	+4
	SVR3	12	4	-8
	SVR4	28	18	-10
	Total	64	50	-14

Table 2.4 Simulation results in sunny.

		Conventional	Proposed	Differences
VD		0.26×10^3Vs	0.011×10^3Vs	-95.8%
VD_{time}		1.5×10^3s	0.13×10^3s	-91.3%
Maximum voltage		107.6V	107.2V	-0.4V
Minimum voltage		101.7V	101.7V	±0
Number of operation of SVR	SVR1	2	2	±0
	SVR2	2	4	+2
	SVR3	2	2	±0
	SVR4	6	6	±0
	Total	12	14	+2

Table 2.5 Simulation results in rainy.

		Conventional	Proposed	Differences
VD		0.27×10^3Vs	0.029×10^3Vs	-89.3%
VD_{time}		1.1×10^3s	0.18×10^3s	-83.6%
Maximum voltage		107.4V	107.4V	±0
Minimum voltage		101.7V	101.7V	±0
Number of operation of SVR	SVR1	2	2	±0
	SVR2	2	4	+2
	SVR3	0	0	±0
	SVR4	2	2	±0
	Total	6	8	+2

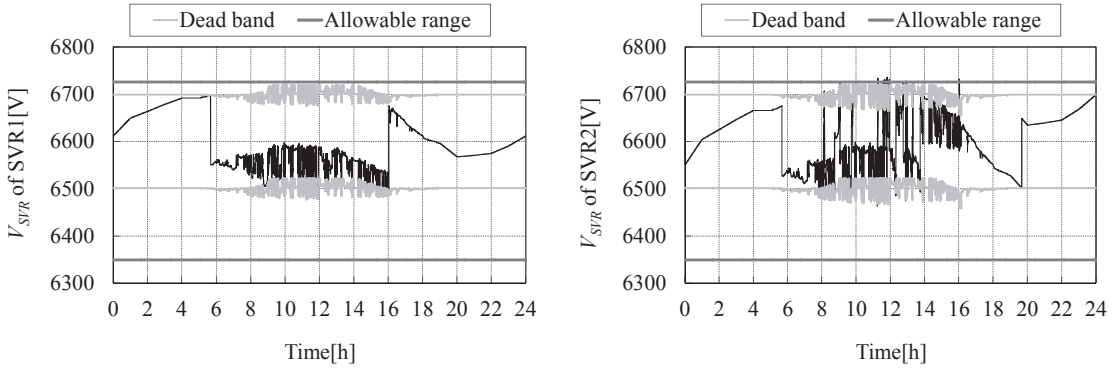

(a) SVR1

(b) SVR2

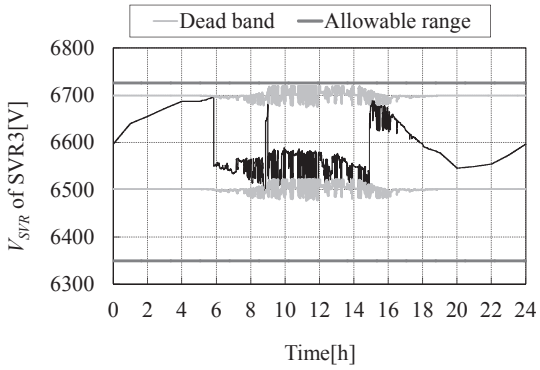

(c) SVR3

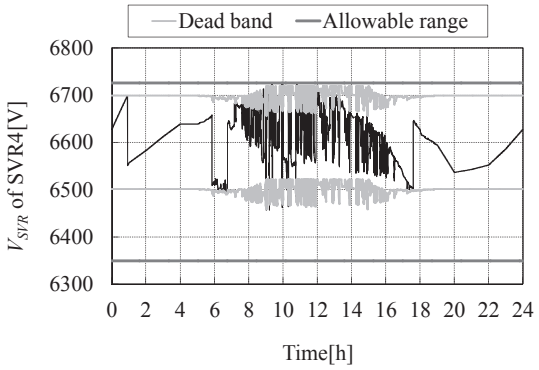

(d) SVR4

Figure 2.13 V_{SVR} in cloudy.

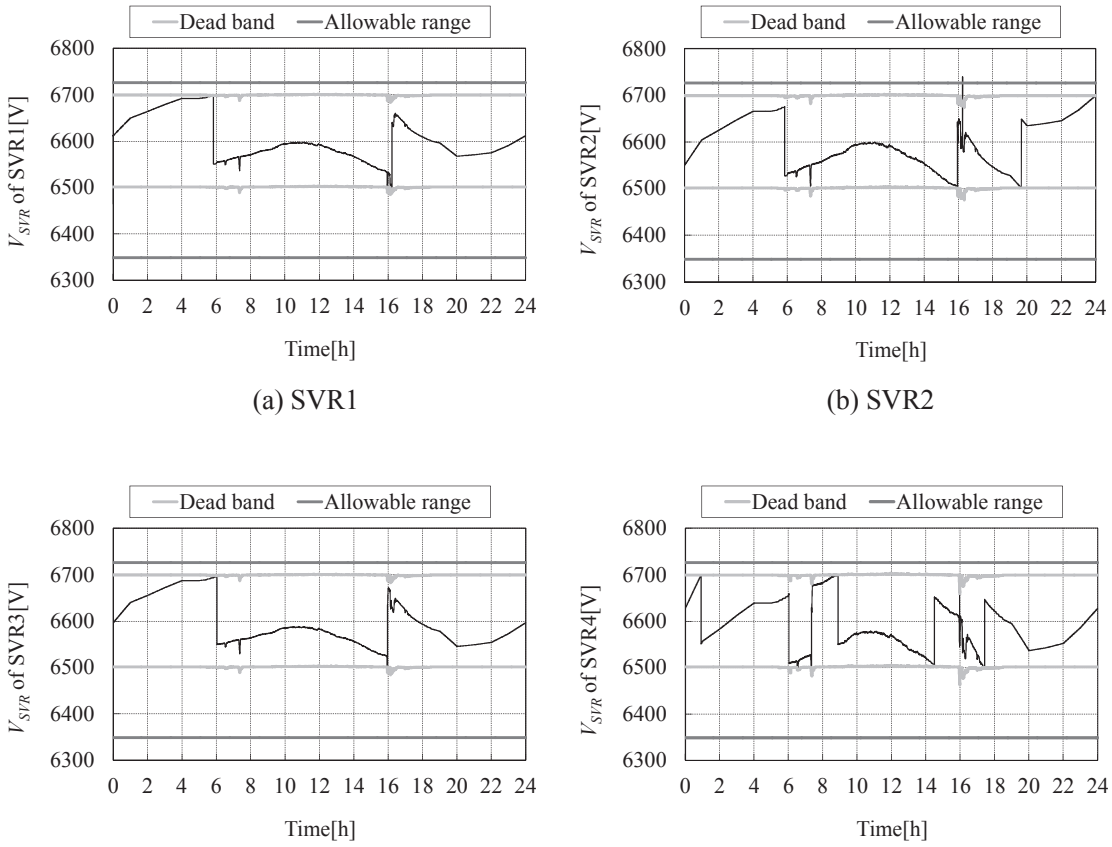

(a) SVR1 (b) SVR2

(c) SVR3 (d) SVR4

Figure 2.14 V_{SVR} in sunny.

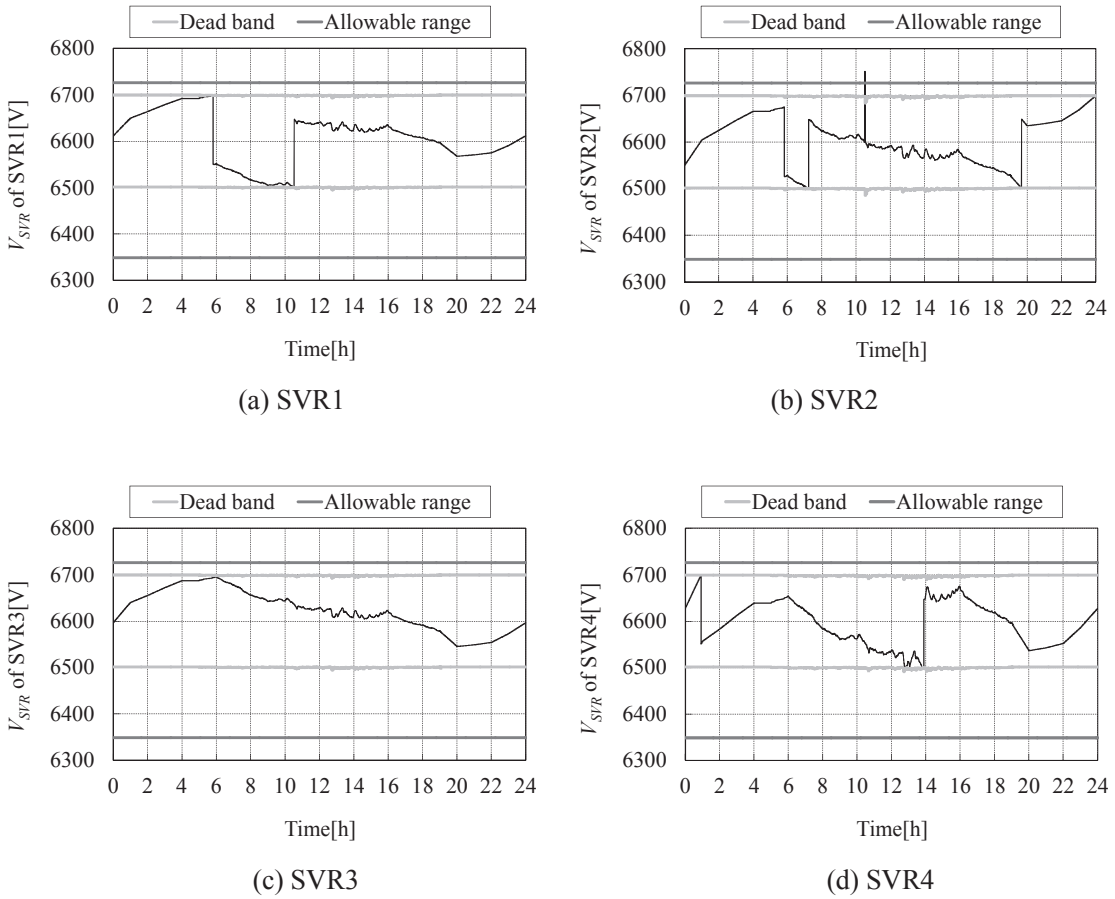

(a) SVR1 (b) SVR2

(c) SVR3 (d) SVR4

Figure 2.15 V_{SVR} in rainy.

Next, as an example, V_{SVR} of SVR4 in the proposed method and the conventional method at cloudy are shown in Figure 2.16. In Figure 2.16, voltage changed due to the operation of SVR is enclosed in a gray circle. SVR with the conventional method changes the tap position in Figure 2.16 (a). However, SVR in the proposed method does not change the tap position in Figure 2.16 (b). This is due to a shift of dead band in the proposed method. From this result, it can be seen that the proposed method is suitable for avoiding the deterioration of SVR. On the other hand, voltage violation is not perfectly prevented even though the proposed method is employed. This is due to an impact of upper SVR on lower SVR that is called hunting. It is important to prevent hunting for reducing voltage violation. To avoid hunting, a coordination of multiple SVRs is effective and indispensable. Meanwhile, because the proposed method can reduce the number of switching operation of upper SVR, the hunting operation also can be reduced. This is also an advantage of the proposed method.

It can be seen that, using the proposed method, voltage violation can be suppressed without the operation of SVR. Furthermore, the proposed method shows good performance at any climate conditions such as sunny, cloudy, and rainy. However, a coordination of multiple SVRs is necessary to avoid hunting of SVRs.

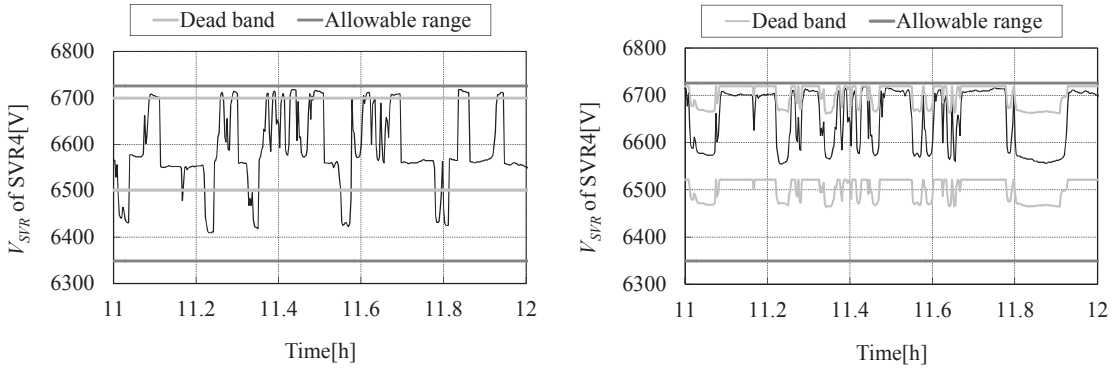

(a) Conventional method (b) Proposed method

Figure 2.16 V_{SVR} of SVR4 in cloudy.

2.5 Discussion and summary

Through the numerical simulation, it can be seen that voltage fluctuation due to PV leads to voltage violation and the frequent switching operation of SVR. The frequent switching operation of SVR makes SVR deteriorate. In this chapter, the authors have developed a novel control algorithm of SVR to suppress the voltage violation and the frequent operation of SVR. The proposed method increases the voltage margin using solar radiation information from the sensor installed in SVR, and hence voltage remains within both the dead band and adequate range. The effectiveness of proposed method is verified through the numerical simulation with multiple weather conditions. The purpose of this chapter is to improve the control algorithm of the conventional SVR through just adding solar radiation sensors into SVR not any additional devices with high cost.

The proposed method does not employ communication with sensors installed on the distribution line. However, with sensors for obtaining information in DS such as voltage, it might be possible to control SVR more effectively. The control method of SVR using sensors that have been already installed in DS should be developed for proper control of voltage. In this chapter, it is assumed that solar radiation in DS has same value to simulate. However, actual solar radiation is different from one at other point. It is necessary to verify the effectiveness of proposed method in that case for appropriate voltage management.

2.6 References

[1] Daisuke Iioka, Kuniaki Sakakibara, Yasunobu Yokomizu, Toshiro Matsumura, and Norihisa Izuhara, "Distribution Voltage Rise at Dense Photovoltaic Power Generation Area and its Suppression by SVC", IEEJ Transactions on Power and Energy, Vol. 126, No. 2, pp. 153-158, 2006 (in Japanese)

[2] Taro Kondo, Jumpei Baba, and Akihiko Yokoyama, "Voltage Control of Distribution Network with a Large Penetration of Photovoltaic Generations using FACTS Devices", IEEJ Transactions on Power and Energy, Vol. 126, No. 3, pp. 347-358, 2006 (in Japanese)

[3] Naoto Yorino, Takahiro Miki, Yuuki Yamato, Yoshifumi Zoka, and Hiroshi Sasaki, "A Time Scale Separation Method for the Coordination of Voltage Controls for SVC and SVR", IEEJ Transactions on Power and Energy, Vol. 124, No. 7, pp. 913-919, 2004 (in Japanese)

[4] Junji Kondoh, "Evaluation on Reduction of Output Suppression Loss by Cooperative Control of Voltage Profile in a Distribution System with a Large Amount of Photovoltaic Power Generation", IEEJ Transactions on Power and Energy, Vol. 130, No. 11, pp. 981-988, 2010 (in Japanese)

[5] Masato Oshiro, Tomonobu Senjyu, Atsushi Yona, Naomitsu Urasaki, and Toshihisa Funabashi, "Voltage Control in Distribution Systems Considered Reactive Power Output Sharing", IEEJ Transactions on Power and Energy, Vol. 130, No. 11 , pp. 972-980, 2010 (in Japanese)

[6] Takao Tsuji, Tadahiro Goda, Kazushige Ikeda, and Seiji Tange, "A Study of Autonomous Decentralized Voltage Profile Control of Distribution Network considering Economic Efficiency", IEEJ Transactions on Power and Energy, Vol. 128, No. 1, pp. 174-185, 2008 (in Japanese)

[7] Takao Tsuji, Tsutomu Oyama, Takuhei Hashiguchi, Tadahiro Goda, Takao Shinji, and Shinsuke Tsujita, "A Study of Autonomous Decentralized Voltage Profile Control Method considering Power Loss Reduction in Distribution Network", IEEJ Transactions on Power and Energy, Vol. 130, No. 11, pp. 941-954, 2010

[8] Takao Tsuji, Takuhei Hashiguchi, Tadahiro Goda, Takao Shinji, and Shinsuke Tsujita, "A Study of Autonomous Decentralized Voltage Profile Control Method considering Control Priority in Future Distribution Network", IEEJ Transactions on Power and Energy, Vol. 129, No. 12 pp. 1533-1545, 2009 (in Japanese)

[9] Noriyuki Uchiyama, Hiroaki Miyata, Tomomichi Ito, and Hiroo Konishi, "Reactive Power Control Method for Reducing Voltage Fluctuation in Large-scale Photovoltaic Systems", IEEJ Transactions on Power and Energy, Vol. 130, No. 3, pp. 297-304, 2009 (in Japanese)

[10] Shunsuke Tanaka, and Hirokazu Suzuki, "A Study on Voltage Compensation Method using Autonomous Decentralized Control of Distributed Generators", IEEJ Transactions on Power and Energy, Vol. 129, No. 7, pp. 869-879, 2009 (in Japanese)

Chapter 3

Advanced voltage control method in distribution network using conventional power facilities

3.1 Introduction

Conventional control devices such as SVR have a lack of ability to compensate for voltage fluctuation due to PV. To solve this issue, in the previous chapter, a novel control method of SVR with a solar radiation sensor is proposed. This is for reducing additional cost. However, as shown in previous chapter, it is hard to completely prevent voltage violation with slight modified SVR. To control voltage fluctuation due to PV, functional devices using power electronics technology such as SVC and battery are effective and hence being focused on in recent years. Meanwhile, because there have been a lot of existing facilities for voltage regulation, replacing them with novel facilities requires the enormous additional cost. For voltage management, it is necessary to effectively make use of these existing facilities as much as possible. As the existing facilities in current DS, there are VS and low-speed communication line. Since current DS has few sensors embedded in section switches on a distribution line, voltage information from these existing sensors is available for voltage control. For more efficient voltage management, existing facilities with communication function should be utilized.

To date, multiple voltage control method using existing facility in DS with PV have been proposed [1] ~ [6]. In [1], however, existing facilities are controlled based on voltage information from sensors embedded in section switches installed on a distribution line. This method cannot control voltage if communication is disrupted. Although voltage profile can be improved using sensors in [1], introducing many VSs as well as high-speed communication lines may be difficult in regards to cost. It is necessary to develop a novel method for voltage regulation using few VSs and slow speed communication. Therefore, in this chapter, a control method of SVR using local voltage data with restricted global voltage data from sensor is proposed. In the proposed method, SVR gets information from VS on DS through low-speed communication. Advantages of the proposed method are to need only few sensors and low-speed communication, and also to be able to control voltage even if communication is disrupted because the proposed method is based on local information.

This chapter is organized as follows. First, in case of PV interconnection, several issues caused by SVR will be shown. It will be also shown that modification of the control method of SVR is indispensable in that case. Next, a novel control method of SVR suitable for voltage management in case of PV interconnection is presented. In section 3.3, the effectiveness of the proposed method is verified through

numerical simulation using DS model with multiple SVRs. Finally, this chapter is overviewed.

3.2 Issues caused by SVR with a large amount of PV

When many PVs are connected to DS, rapid voltage change may occur due to weather conditions. SVR could not compensate for the rapid voltage fluctuation. Because a DS with SVR has many consumers and/or long distribution line, voltage fluctuation due to PV tends to be large. In such a case, voltage control within the proper range may be more difficult than in a DS without SVR. Under this background, a study about issues caused by PV in a DS with SVR has been done, especially with multiple SVRs [4]. In this study, two factors of the voltage problem in DS with many PVs and multiple SVRs have revealed, one is the time delay of operation of SVR and the other is the constant dead band parameters of SVR. These are explained as below in detailed.

(1) Time delay of SVR

SVR changes its tap position after V_{SVR} deviates from the dead band for T_{settle}. $T_{operate}$ is necessary to finish the tap change operation even if the amount of above deviation count becomes T_{settle}. Thus, though voltage in DS deviates from the allowable range due to PV, SVR cannot immediately change its tap position and hence voltage violation continues until the finish of tap operation.

(2) Constant dead band parameters of SVR

Generally, voltage drop can be estimated using load-curve; hence DSO has set parameters of dead band such as V_{basis}, V_{db}, and T_{settle} based on measured load curve to keep voltage within the proper range. However, with a lot of PVs, voltage profile is changed and becomes complex. In that case, it is expected that a proper control of voltage using conventional dead band parameters is difficult. By investigating these issues through numerical simulation in detail, it can be confirmed that the switching operation of SVR may lead to increase of voltage violation according to the situation. This phenomenon is illustrated in Figure 3.1.

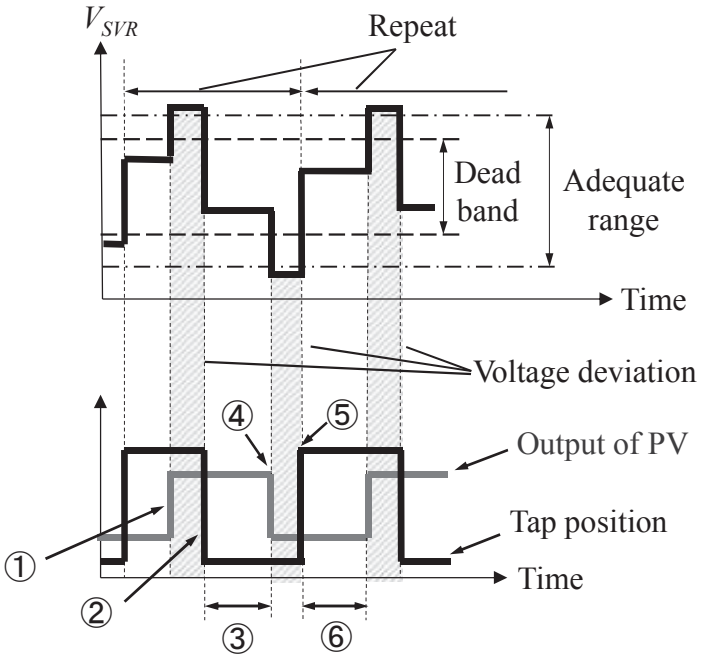

Figure 3.1 Voltage violation caused by ROS.

In Figure 3.1, following cycles (Repeat Operation of SVR: ROS) is repeated.

① An increase of PV's output leads to voltage rising.

② SVR moves its tap position downwards after voltage violation due to the time delay of SVR (T_{settle} and $T_{operate}$) is occurred.

③ Voltage returns into the allowable range by SVR's operation.

④ A rapid change of weather condition causes decrease of PV's output and hence a sudden voltage drop.

⑤ SVR moves its tap position upwards after voltage violation due to the time delay of SVR is occurred.

⑥ Voltage returns into the allowable range by SVR's operation.

One cycle of ROS leads to voltage violation. Hence voltage frequently deviates from the adequate range in cloudy with frequent fluctuation of PV's output. This is because the conventional SVR tries to make V_{SVR} near V_{basis}. Because ROS is not occurred if there are no frequent operation of SVR against voltage fluctuation, it is effective to expand the width of dead band and prevent the switching operation of SVR. However, expanding the width of dead band too much may lead to voltage violation from the proper range. It is indispensable to properly set dead band parameters and to expand the width of dead band not to occur voltage violation. Furthermore, in case that multiple SVRs are installed in series into a DS, ROS tends to be occurred because the switching operation of upper SVR causes a step voltage change at downstream nodes resulting in a cascading operation of lower SVRs. To prevent ROS, suppressing the

switching operation of SVR is effective for the case of multiple SVRs in series at DS.

Voltage in DS with multiple SVRs tends to be fluctuated; hence voltage violation tends to occur when many PVs are connected to DS. List of these causes and those measures for voltage violation due to SVR are shown in Table 3.1.

Table 3.1 Causes and measures of voltage violation related to SVR.

	Cause	Measure
1	The time delay of SVR	Make T_{settle} shorter Make the width of dead band smaller
2	Setting of the dead band	Make parameters of dead band proper Make the width of dead band become wide

For restriction of voltage violation due to SVR, it is necessary (1) to compensate the time delay of SVR and (2) to modify parameters of SVR.

3.3 Suitable control method of SVR for PV interconnection

3.3.1 Install of voltage sensors

Conventional SVR observes only its secondary voltage V_{SVR} and cannot obtain voltage information at distant nodes from SVR. For proper voltage regulation, it is indispensable to estimate voltage at remote nodes from SVR. As voltage estimation method on distribution line, there is Line Drop Compensator (LDC) method that monitors only V_{SVR}. However, because voltage profile on distribution line becomes complex due to PV interconnection, estimation of the system state by using only V_{SVR} is difficult. It is necessary to utilize voltage information on DS from VS such as the sensor embedded in section switch installed in DS. There are many studies for estimation of voltage on a distribution line using VS [1] [7] [8]. In general, an estimation error is reduced in proportion to the number of VS in DS. At the same time, the cost for communication line and VS increase. Though it is expected that a development of VSs and communication line proceed in future, installing these high-cost facilities into many DSs is difficult. Besides, voltage control method using high-performance communication facility is yet trial level and it is expected to take time to apply this control method to actual DS. As an issue at hand, it is important to manage voltage using poor communication facility. While in these literatures a lot of VSs is adopted to estimate voltage, in this chapter few sensors are adopted to estimate voltage profile in DS for reducing additional cost. In the proposed method, SVRs observe voltage at PCC (primary and secondary nodes). SVR obtains voltage data from VS and estimates voltage based on voltage data obtained through communication. This estimation method will be explained in the next section.

3.3.2 Relation between the secondary voltage of SVR and voltage on distribution line

In the proposed method, SVR communicates with VS at regular time interval T_{commu}. SVR estimates voltage at node with VS during T_{commu} using V_{SVR} obtained in real time. The tap position of SVR is controlled based on V_{SVR} and the estimated voltage. How to estimate voltage at node with VS using a simple DS is shown in Figure 3.2.

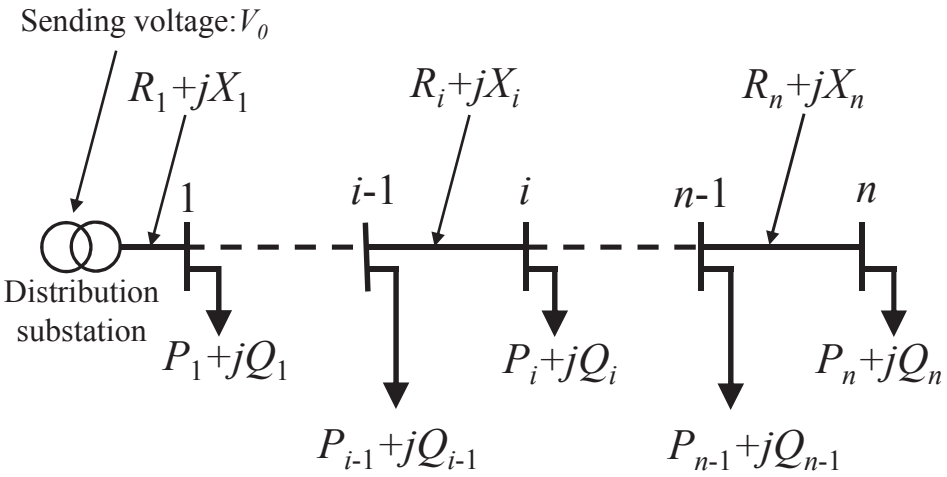

Figure 3.2 Simple distribution system.

R_i and X_i in Figure 3.2 are the resistance and reactance of the distribution line between node #i-1 and #i, respectively. V_0 represents sending voltage at the distribution substation. P_i and Q_i are an active and reactive power at node #i, respectively. Assuming that difference of two phase angles between V_i and V_0 is small, V_i can be approximately calculated as follows [9].

$$V_i \approx V_0 \left\{ 1 - \frac{\sum_{k=1}^{i} \left(R_k \sum_{l=k}^{n} P_l \right) + \sum_{k=1}^{i} \left(X_k \sum_{l=k}^{n} Q_l \right)}{V_0^{\,2}} \right\} \tag{3.1}$$

Voltage difference between node #i and #j on the distribution line are calculated as follows.

$$V_{ij} = V_i - V_j \approx \frac{\sum_{k=i+1}^{j} \left(R_k \sum_{l=k}^{n} P_l \right) + \sum_{k=i+1}^{j} \left(X_k \sum_{l=k}^{n} Q_l \right)}{V_0} \tag{3.2}$$

Equation (3.2) represents that V_{ij} depends on the load below node #*i*. In general, the load fluctuation during a short time is small, and hence a term related to reactive power in equation (3.2) can be regarded as a constant K_Q. Under this assumption, equation (3.2) can be rewritten as follows.

$$V_{ij} \approx \frac{\sum_{k=i+1}^{j}\left(R_k \sum_{l=k}^{n} P_l\right)}{V_0} + K_Q \tag{3.3}$$

If total active power of load below node #*i* can be expressed as $P_{sum}(i)$, the active power at each node P_l is given.

$$P_l = K_l P_{sum}(i) \tag{3.4}$$

$$\sum_{l=i+1}^{n} K_l = 1.0 \tag{3.5}$$

Assuming that the active power at each node changes corresponding to a same load curve, each K_l can be considered as constant and following equations can be obtained.

$$\begin{aligned} V_{ij} &\approx \frac{\sum_{k=i+1}^{j}\left(R_k \sum_{l=k}^{n} K_l P_{sum}(i)\right)}{V_0} + K_Q \\ &= K_P P_{sum}(i) + K_Q \end{aligned} \tag{3.6}$$

$$K_P = \frac{\sum_{k=i+1}^{j}\left(R_k \sum_{l=k}^{n} K_l\right)}{V_0} \tag{3.7}$$

In equation (3.6), V_{ij} is expressed as a linear function of $P_{sum}(i)$. K_P represents the gradient of linear function calculated using a resistance of distribution line and a load profile on DS. In a precise sense, equation (3.3) is not a linear function because K_P and K_Q change corresponding to fluctuation of Q_i and V_0. However, because multiple residences are usually connected to a pole transformer, it is expected that the load fluctuation at a pole transformer is smoothed and approximated to a typical residence load pattern. Moreover, V_0 can be considered as constant during a short time.

The output of each PV dispersedly connected to DS is different from others because solar radiation depends on the connected point. If correlation of whole solar radiation in DS is close to 1.0, voltage

fluctuation due to PV becomes large and voltage management becomes difficult. Therefore, in this chapter, the assumption (3.6) is necessary to control voltage within the allowable range even under this severe condition. If K_P and K_Q are calculated, V_j can be obtained using V_i and $P_{sum}(i)$ at node #*i*.

The proposed method estimates the voltage drop from SVR to VS, and V_{SVR} is controlled based on the estimated voltage drop. An advantage of the proposed method is being able to neglect an impact of voltage fluctuation caused by fluctuation of sending voltage and the tap change of SVR. This is because the proposed method does not calculate direct voltage but voltage drop between two points (SVR and VS).

3.3.3 Voltage estimation using principal component analysis

In order to obtain the best K_P and K_Q that represent the linear function, Principal Component Analysis (PCA) is used. PCA is an analytical approach to find components that minimize the loss of measured data. PCA regards information in multidimensional data as variance. In PCA, by setting components to maximize the variance of data, the characteristic of data can be effectively analyzed. Voltage estimation method using PCA is shown in Figure 3.3.

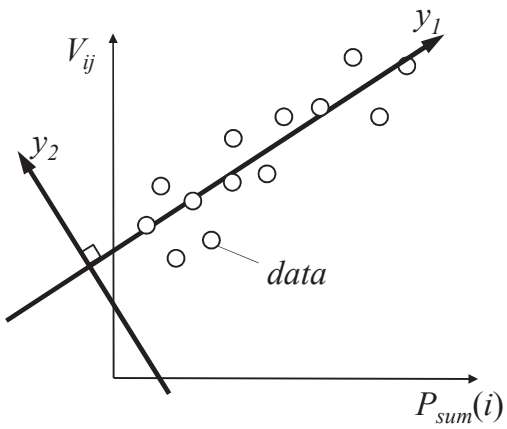

Figure 3.3 Analysis of relation between $P_{sum}(i)$ and V_{ij}.

Figure 3.3 shows that voltage difference V_{ij} between at a node #*i* with SVR and a node #*j* with a VS, and $P_{sum}(i)$. In Figure 3.3, the data set ($P_{sum}(i)$, V_{ij}) have variability and the best approximated line of relation between $P_{sum}(i)$ and V_{ij} is obtained by calculating the first principal component y_1. The second principal component y_2 is obtained that is an orthogonal oriented to y_1. Each principal component is calculated using a coefficient $w = w_{11}, \ldots, w_{22}$.

$$\begin{aligned} y_1 &= w_{11}P_{sum}(i) + w_{12}V_{ij} \\ y_2 &= w_{21}P_{sum}(i) + w_{22}V_{ij} \end{aligned} \qquad (y_1 \perp y_2) \tag{3.8}$$

As y_1 is the first principal component, the data on y_1 achieve equation (3.9).

$$\begin{aligned} y_2 &= w_{21} P_{sum}(i) + w_{22} V_{ij} \\ &= 0 \end{aligned} \tag{3.9}$$

That is,

$$V_{ij} = -\frac{w_{21}}{w_{22}} P_{sum}(i) \tag{3.10}$$

By using equation (3.10), the approximated V_{ij} can be estimated using V_{SVR} and the sending active power of SVR $P_{sum}(i)$. Data from VS may sometimes have large variability due to load fluctuation. PCA determines the principle component to maximize the variance of data set. The best line representing the characteristic of data can be obtained using PCA. Therefore, PCA is employed to estimate V_{ij} in this chapter. To hold equation (3.10), the origin of y_2 must fit the origin of ($P_{sum}(i)$, V_{ij}) plane. To do this, data standardization is processed and hence K_P and K_Q are obtained after normalized V_{ij} is transformed to original value. The following steps and Figure 3.4 describe voltage estimation process by each SVR (upper and lower). The lower SVR plays a role as VS that sends voltage information to the upper SVR, and VS sends information to the lower SVR.

[Voltage drop estimation process]

(i) Each SVR memorizes $P_{sum}(i)$ and V_i obtained in real time with time stamp, and holds these information during T_{mem}.
(ii) VS corresponding to SVR stores V_j with time stamp, and holds V_j during T_{commu}.
(iii)Each SVR receives V_j with time stamp from the VS corresponding the SVR at each T_{commu}.
(iv) Each SVR updates V_j at each T_{commu} based on received V_j and own V_i.
($P_{sum}(i)$ and V_i are stored in SVR for T_{mem} which is larger than T_{commu}. Old data is eliminated and new data is added to stored data at each T_{commu}.)
(v) To calculate K_P and K_Q, the relationship between $P_{sum}(i)$ and V_{ij} is analyzed using PCA.
(vi) Since SVR cannot receive information from VS until next communication, SVR estimates V_{ij} using $P_{sum}(i)$ observed in real time at local.

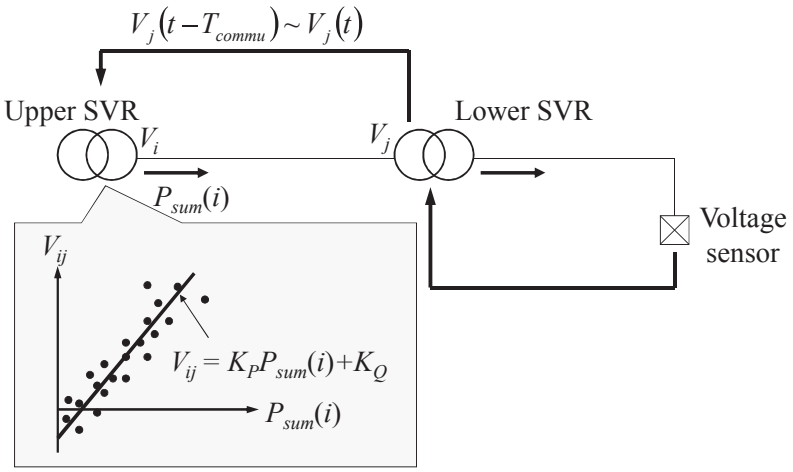

Figure 3.4 Determination of parameters by PCA.

The set of data ($P_{sum}(i)$, V_{ij}) obtained through communication is plotted on the plane; hence a linear function is obtained as shown in Figure 3.4. By finding K_P and K_Q using PCA, V_{ij} is calculated using equation (3.6). V_j at VS is obtained using equation (3.11).

$$V_j = V_i - V_{ij} \tag{3.11}$$

3.3.4 Voltage recording time

(K_P, K_Q) at light load and at heavy load may be different, hence it is necessary to modify K_P and K_Q according to load conditions. In addition, because K_P and K_Q depend on the load pattern, those values are changed corresponding to weekdays and holidays, and seasons. Therefore, T_{mem} is set as relatively short time and hence SVR flexibility responds to load fluctuation.

3.3.5 Settings of dead band

In the proposed method, the dead band of SVR is optimized using estimated voltage not to lead to ROS. SVR operates so that both V_i and V_j do not deviate from the allowable range. To do so, following conditions should be considered.

$$\begin{cases} V_i \le V_{MAX} \\ V_j \ge V_{MIN} \end{cases} \quad (V_{ij} \ge 0) \tag{3.12}$$

$$\begin{cases} V_i \ge V_{MIN} \\ V_j \le V_{MAX} \end{cases} \quad (V_{ij} < 0) \tag{3.13}$$

The dead band is set by considering above conditions. The method how to set the dead band is shown as follows (Figure 3.5). Shaded area in Figure 3.5 represents the dead band.

(a) In case of $V_{ij} \geqq 0$

In case of $V_{ij} \geqq 0$, the upper limit of dead band V_{db_MAX} is set to be equal to the upper limit of proper range V_{MAX}. The lower limit of dead band V_{db_MIN} is obtained by adding a bias voltage V_{ij} from the lower limit of the allowable range V_{MIN} considering voltage drop V_{ij}. Formula for V_{db_MAX} and V_{db_MIN} is shown in equation (3.14).

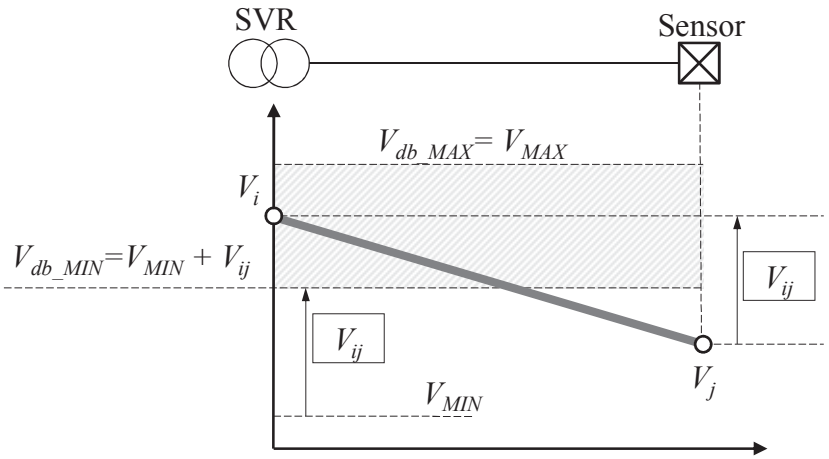

(a)$V_{ij} \geqq 0$

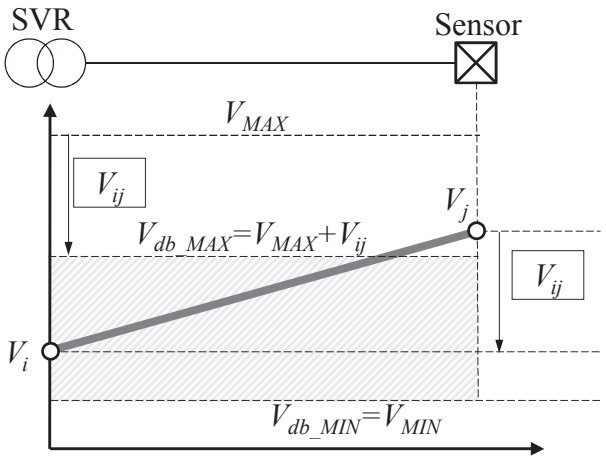

(b)$V_{ij} < 0$

Figure 3.5 Setting of the dead band in the proposed method.

$$\begin{cases} V_{db\_MAX} = V_{MAX} \\ V_{db\_MIN} = V_{MIN} + V_{ij} \end{cases} \quad \left(V_{ij} \geq 0\right) \tag{3.14}$$

(b) In case of V_{ij}<0

In case of V_{ij}<0, V_{db_MIN} is set to be equal to V_{MIN}. Besides, V_{db_MAX} is obtained by reducing as $|V_{ij}|$ from V_{MAX} considering voltage rising between SVR and VS. Formula for V_{db_MAX} and V_{db_MIN} is shown in equation (3.15).

$$\begin{cases} V_{db\_MAX} = V_{MAX} + V_{ij} & \left(V_{ij} < 0\right) \\ V_{db\_MIN} = V_{MIN} \end{cases} \tag{3.15}$$

3.3.6 Shorten the settling time

In the proposed method, that V_{SVR} deviates from the dead band means that voltage on the distribution line also deviates from the adequate range. It is desirable to make T_{settle} become the minimum value to prevent voltage violation. Although it is necessary to make T_{settle} large in the conventional method to suppress the switching operation of SVR, the proposed method can make T_{settle} smaller by adjusting the wide width of dead band. By setting T_{settle} as small value, the proposed method can minimize voltage violation due to the time delay of SVR.

3.4 Case study

3.4.1 Simulation model and parameters

(1) Distribution system model

A distribution system model with two SVRs installed in series is adopted in the numerical simulation aiming at verification for the effectiveness of the proposed method. There are two reasons for adopting this model. One is that this model tends to cause voltage issues when a lot of PVs are connected. The other is that there are relatively many DSs with two SVRs. Figure 3.7 shows the distribution system model and Table 3.2 shows the model parameters. This model has been created based on the actual systems with two SVRs. Also, the parameters of line impedance and SVR are set so that voltage at end of line is not below the lower limit of proper range when no PVs are connected.

Table 3.2 Parameters of distribution system model.

Distribution line parameters		
Line impedance		0.3+*j*0.3Ω/km
Feeder length		11km (Interval of consumers:1.0km)
Consumer parameters		
Load capacity	Node #3,5,7,9,10	113kVA
	Node #11,12	229kVA

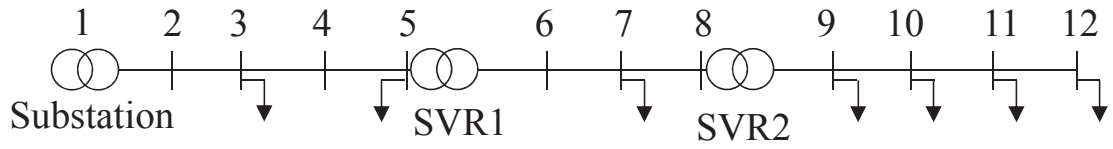

Figure 3.6 Distribution system model.

(2) Load model

Arrows in Figure 3.6 represent loads. All loads are residences because a large amount of PVs will be introduced on roof of residences. Load curve is set as a typical residential load pattern in this simulation. Figure 3.7 shows fluctuation of total active/reactive power of loads in the system. In Figure 3.8, random noise within ±10% is added to typical residential load patterns considering the small fluctuation of load. This random noise is set to be different at each node.

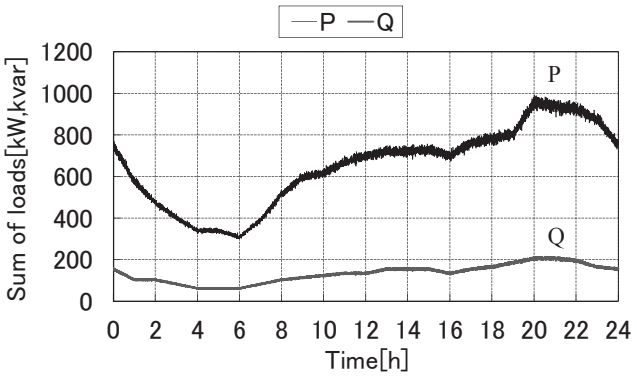

Figure 3.7 Load pattern.

(3)PV model

In the simulation, output of PV PV_{out} is in proportion to solar radiation. A measured solar radiation data is used. The capacity of each PV which is introduced to each node is set as same as the load capacity at each node to verify the effectiveness of proposed method even under the severe condition.

The solar radiation pattern includes (a) sunny with rare rapid change of solar radiation, (b) cloudy with frequent rapid change of solar radiation, (c) rainy with small solar radiation. However, the amount of solar radiation is set uniformly across the whole distribution system. This is for verifying the effectiveness of proposed method under the severe condition. Figure 3.8 shows the sum of PV_{out} in DS over 24h.

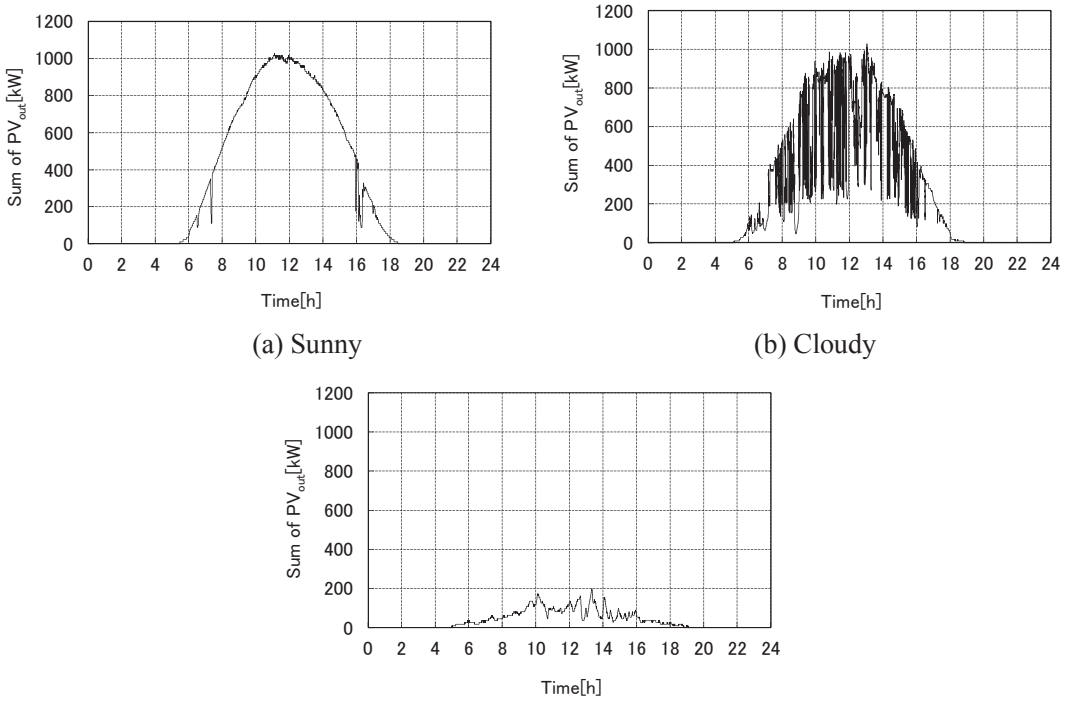

(a) Sunny (b) Cloudy

(c) Rainy

Figure 3.8 Pattern of output of PV.

(4) Simulation conditions

Conditions for simulation are shown in Table 3.3. V_{db} used in the conventional method is 3% (189V) of basis voltage 6600V that is actually used by DSO. Table 3.3 also shows the conventional control parameters of SVR, which are to compare with the proposed method. In the numerical simulation, power flow calculation is performed every 2s, and repeated over 24h. Though it is assumed that there is no sampling delay in controller of SVR in this simulation, it has been confirmed that simulation results are not affected by this assumption. T_{settle} in the proposed method is set to 0s for reducing the ill impact of time delay of SVR. Allowable range of low-side voltage in this simulation is 101 ~ 107V that is transformed from high-side to low-side. The tap ratio of each pole transformer is 105/6600 on entire DS. In order to compare the conventional method with the proposed method, in the simulation, only control algorithm of SVR is changed. The sending voltage at distribution substation is set to constant as 6600V considering LRT in distribution substation manage sending voltage close to constant.

Table 3.3 Simulation conditions.

Simulation interval				2.0s
Simulation time T				24h
Allowable range (Low voltage)			V_{MAX}	107.0V
			V_{MIN}	101.0V
Ratio of pole transformers				105/6600
Sending voltage at the substation				6600V
SVR	Width of Dead Band V_{db}		Conventional	189V
			Proposed	See Eq.(14)(15)
	Basis voltage of dead band in conventional method			6600V
	Settling time T_{settle}	Conventional	SVR1	60s
			SVR2	90s
		Proposed	SVR1	0s
			SVR2	0s
	Delay of tap change $T_{operate}$			8.0s
	Range of tap position			6300/6600～6900/6600
	Setting of the proposed method		T_{commu}	1.0min
			T_{mem}	30min

(5) Evaluation method of simulation result

Simulation results are evaluated using following indices.

(a) Voltage violation index

Voltage violation index *VD* is the amount of voltage violation from the proper range which is calculated integrating the amount of voltage violation from the allowable range e_V over simulation period. *VD* can be calculated using equation (3.16).

$$VD = \sum_{t=0}^{T} \sum_{i=1}^{12} e_V(t,i)$$
$$e_V(t,i) = \begin{cases} V(t,i) - V_{MAX} & (V(t,i) > V_{MAX}) \\ V_{MIN} - V(t,i) & (V(t,i) < V_{MIN}) \end{cases} \tag{3.16}$$

Where $V(t, i)$ represents low-side voltage at time t and node #i transformed from high-side voltage using the tap ratio of pole transformers.

(b) Maximum and minimum voltage in the simulation

In order to evaluate the magnitude of voltage fluctuation, the maximum and minimum voltages in simulation V_{MAX_sim}, V_{MIN_sim} are used as indices, respectively. On the other hand, the number of switching operation of SVR N_{SVR} is also used as an index of deterioration of SVR.

(6) Simulation cases

Table 3.4 shows simulation cases. First, it will be confirmed that voltage can be appropriately managed without PV using the conventional control method of SVR. Next, simulations with a lot of PV are executed.

Table 3.4 Simulation cases.

Case	Control of SVR	PV
1	Conventional method	No PV
2		Sunny
3		Cloudy
3		Rainy
5	Proposed method	Sunny
6		Cloudy
7		Rainy

3.4.2 Simulation results

(1) Conventional control method

First, in case 1, 2, 3, and 4, simulation results using the conventional control method of SVR are shown.

(a) Without PVs (case 1)

Table 3.5 shows simulation results when no PVs are connected to the DS model. From Table 3.5, it is found that voltage is properly managed because *VD* is 0Vs. The secondary voltage of SVR V_{SVR} is shown in Figure 3.9. In Figure 3.9, SVR controls voltage fluctuated due to load fluctuation within the dead band. Thus, when there are no PVs, voltage can be properly managed using SVR with time delay against voltage fluctuation.

Table 3.5 Simulation results in case 1.

VD		0Vs
V_{MAX_sim}		106.4V
V_{MIN_sim}		101.4V
N_{SVR}	SVR1	0
	SVR2	2

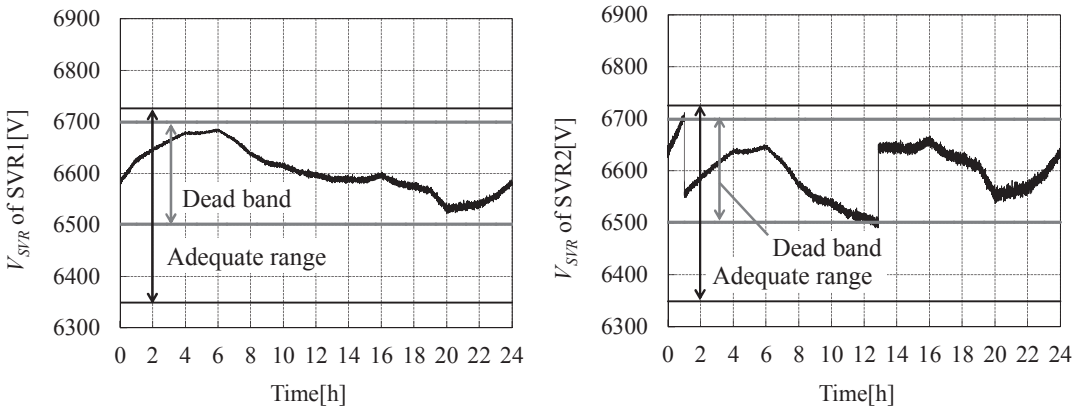

(a)SVR1 (upper) (b)SVR2 (lower)

Figure 3.9 V_{SVR} in case 1.

(b) With many PVs (case 2, 3, and 4)

Simulation is executed using the conventional control method when many PVs are introduced into the DS model. Simulation results in case 2, 3, and 4 are shown in Table 3.6.

Table 3.6 Simulation results using the conventional method.

Case		2	3	4
VD		93Vs	5851Vs	0Vs
V_{MAX_sim}		108.0V	108.4V	106.4V
V_{MIN_sim}		101.4V	101.0V	101.4V
N_{SVR}	SVR1	2	12	0
	SVR2	6	32	2
	Total	8	44	2

Table 3.6 shows that voltage deviates from the allowable range when a large amount of PVs are introduced into the DS model. In particular, *VD* and N_{SVR} greatly increase in case 3 of cloudy. This is because SVR with the time delay cannot compensate for rapid and frequent voltage fluctuation in cloudy condition. In sunny condition (case 2), rapid voltage fluctuation due to PV is hardly occurred because solar

radiation value is slowly changed. In rainy condition (case 4), because the output of PVs are very small, voltage fluctuation due to PV is also small. Therefore, in case 2 and case 4, *VD* and N_{SVR} are small compared to in case 3.

Figure 3.10 ~ 3.12 show V_{SVR} in case 2 ~ 4. In Figure 3.10 and Figure 3.12, since fluctuation of V_{SVR} is small, V_{SVR} does not frequently exceed the upper or lower limit of the dead band. Hence, the switching operation of SVR is hardly occurred. From Figure 3.11 (b), on the other hand, it can be seen that V_{SVR} of SVR2 frequently deviates from the dead band. This is due to ROS. From the simulation results, the conventional control method of SVR is found to be not suitable for voltage control in case of PV penetration.

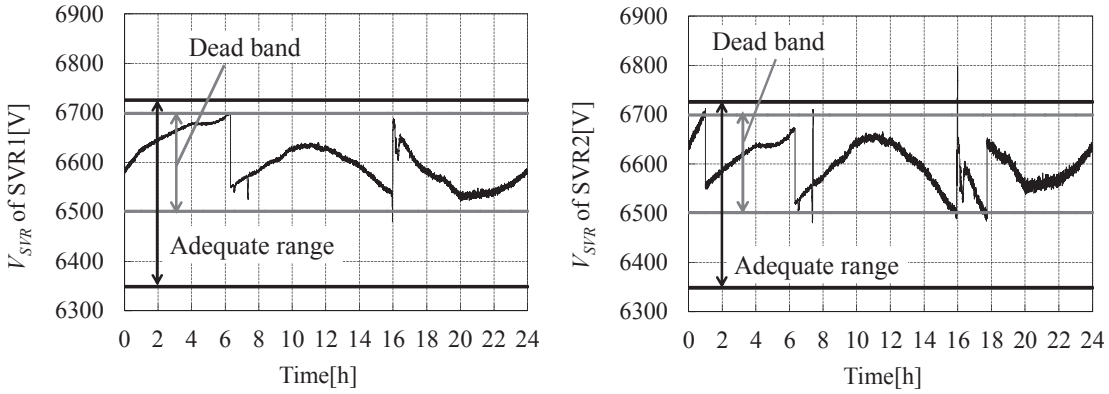

(a) SVR1 (upper) (b) SVR2 (lower)

Figure 3.10 V_{SVR} in case 2.

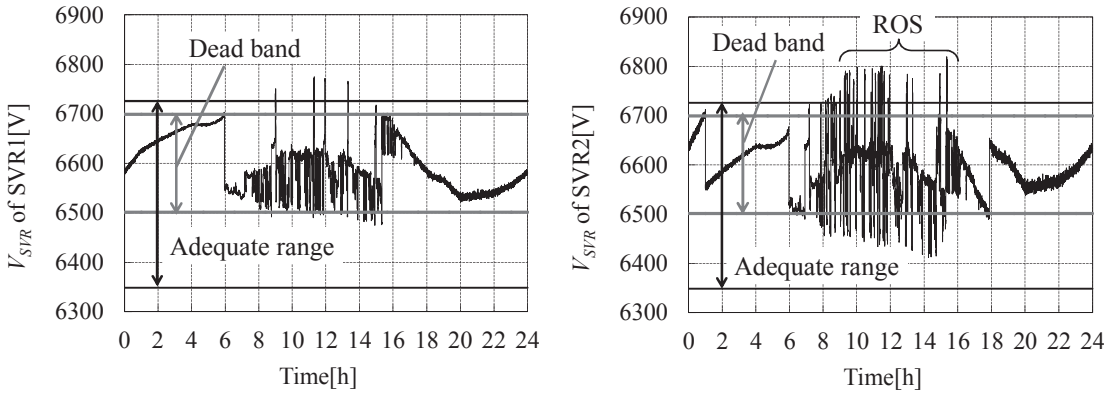

(a) SVR1 (upper) (b) SVR2 (lower)

Figure 3.11 V_{SVR} in case 3.

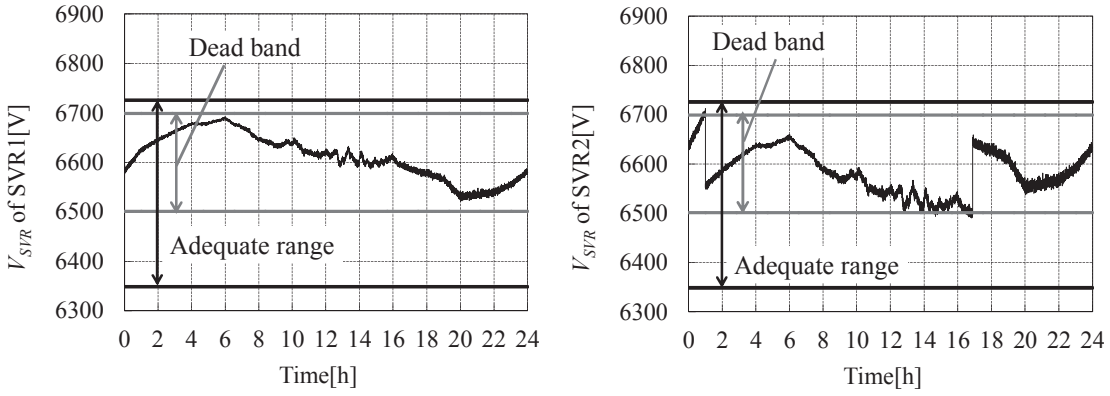

(a) SVR1 (upper) (b) SVR2 (lower)

Figure 3.12 V_{SVR} in case 4.

(2) Proposed control method of SVR

Simulation results using the proposed control method are shown on Table 3.7. Table 3.7 shows that the proposed method can greatly reduce *VD* and N_{SVR} compared to the conventional method. This is because ROS is restricted by expanding the width of dead band using information from VS. Though V_{MIN_sim} in the proposed method is smaller than in the conventional method, the proposed method is more suitable than the conventional one to reduce V_{MAX_sim}. Figures 3.14, 3.15, and 3.16 show V_{SVR} in case 5, 6, and 7. From these figures, it can be seen that the expanding width of dead band can restrain V_{SVR} from exceeding the upper or lower limit of dead band. Hence, ROS can be avoided using the proposed method. Since step voltage change due to the operation of upper SVR is also restricted, an adverse impact on the lower SVR by upper SVR can be suppressed. Under the multiple weather conditions, the feasibility and effectiveness of the proposed method for reducing *VD* and N_{SVR} is verified.

Table 3.7 Simulation results using the proposed method.

Case		5	6	7
VD		0.30Vs	3.88Vs	0.03Vs
V_{MAX_sim}		107.0V	107.2V	106.7V
V_{MIN_sim}		100.9V	100.8V	101.0V
N_{SVR}	SVR1	2	2	0
	SVR2	2	6	2
	Total	4	8	2

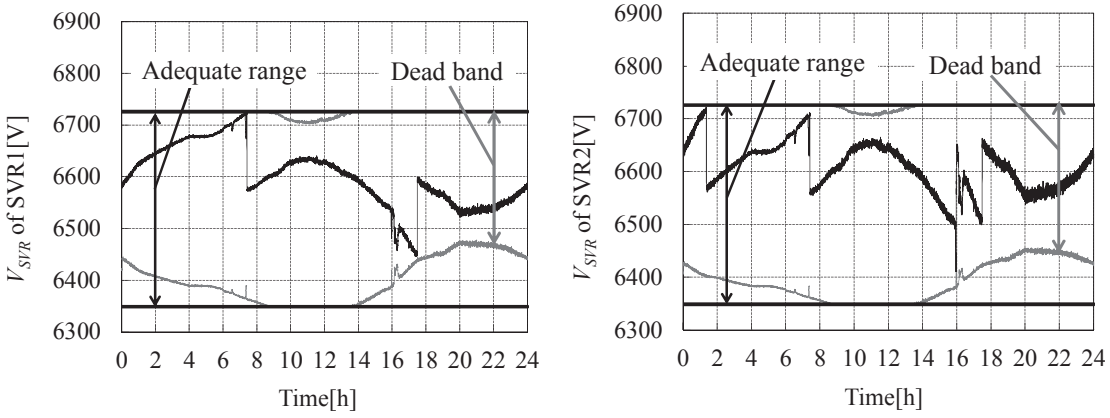

(a) SVR1 (upper) (b) SVR2 (lower)

Figure 3.13 V_{SVR} in case 5.

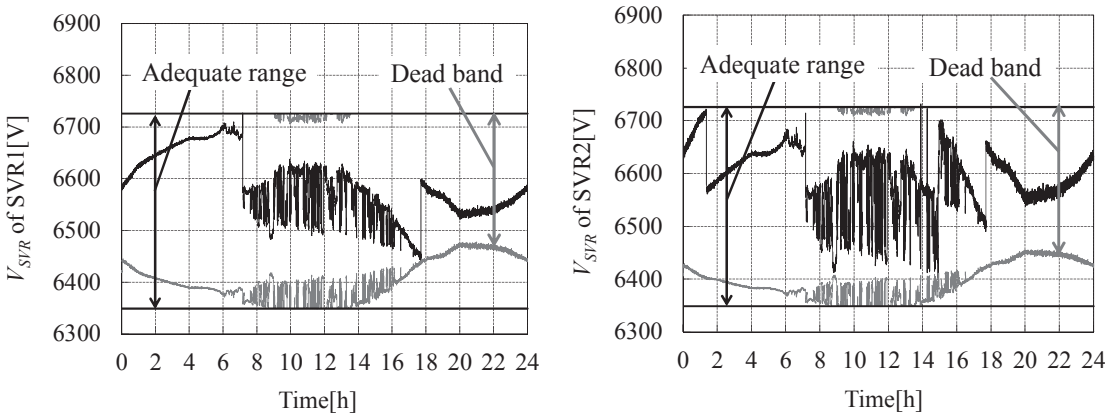

(a) SVR1 (upper) (b) SVR2 (lower)

Figure 3.14 V_{SVR} in case 6.

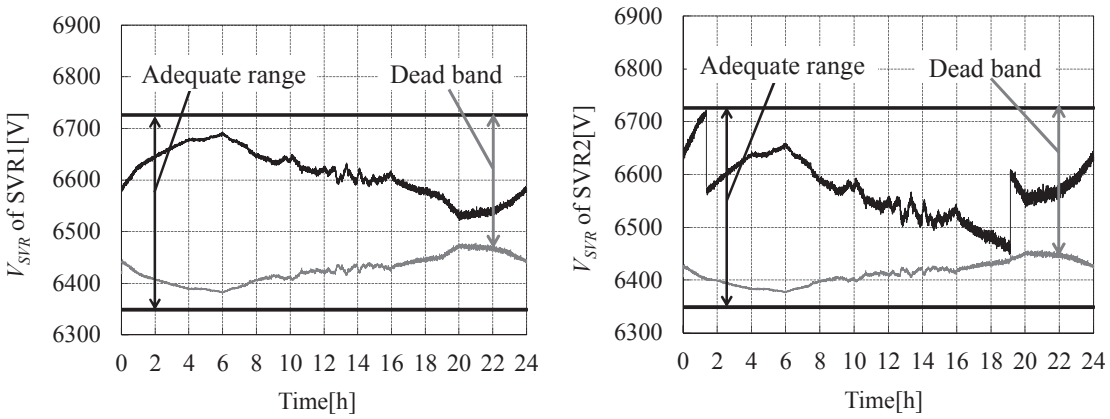

(a) SVR1 (upper) (b) SVR2 (lower)

Figure 3.15 V_{SVR} in case 7.

3.5 Discussion and summary

This chapter has proposed the suitable control method of SVR for voltage management using information from VS on the distribution line when a large amount PVs is introduced into DS. First, section 3.2 shows that it becomes difficult to manage voltage in DS with SVR and many PVs. In Particular, in a DS with multiple SVRs installed in series, the increase of switching operation of upper SVR leads to rapid and frequent voltage change at downstream nodes and hence makes an adverse impact on the operation of lower SVR. From this, the control method of SVR should be reviewed when many PVs are installed into DS. The suitable method for reducing voltage violation has been proposed. The proposed method appropriately controls the dead band parameters and expands the width of dead band utilizing information from VS installed on DS. The effectiveness of proposed method has been verified through the numerical simulation.

In this study, a simple distribution network model is employed assuming a trunk line without branches. This is because controlling voltage on the trunk line within adequate range is important in actual DS. With respect to managing voltage on the trunk line, the proposed method is found to be the effective control method. However, because of mechanical time delay of SVR, it is difficult to compensate for rapid voltage fluctuation due to PV. For more effective management of voltage, functional devices such as SVC and a battery that can rapidly control voltage are indispensable. A more effective and feasible control strategy of voltage in DS by combining these control facilities and the proposed method is necessary. This is the future work.

3.6 References

[1] Yuji Hanai, Yasuhiro Hayashi, Junya Matsuki, and Masanori Kurihara, “Proposal and Experimental Verification of Distribution Voltage Estimation and Control Method using Measured Data from IT Switches”, IEEJ Transactions on Power and Energy, Vol. 130, No. 10, pp. 859-869, 2010 (in Japanese)

[2] Yoshiki Nakachi, Satoshi Kato, and Hiroyuki Ukai, “Coordinated Voltage Control of Transformer Taps on account of Hierarchical Structure in Power System”, IEEJ Transactions on Power and Energy, Vol. 126, No. 5, pp. 525-531, 2006 (in Japanese)

[3] Yoshiki Nakachi, Ryosuke Maki, and Hiroyuki Ukai, “Coordination Scheme of Autonomous-decentralized Voltage Control on Step Voltage Regulator in Distribution Power System”, Journal of IEIEJ, Vol. 27, No. 5, pp. 392-400, 2007 (in Japanese)

[4] Yasuhiro Hayashi, Junya Matsuki, Ryoji Suzuki, and Eiji Muto, “Determination Method for Optimal Sending Voltage Profile in Distribution System with Distributed Generators”, IEEJ Transactions on Power and Energy, Vol. 125, No. 9, pp. 846-854, 2005 (in Japanese)

[5] Junji Kondoh, Hirohisa Aki, Hiroshi Yamaguchi, Akinobu Murata, and Itaru Ishii, “Study on Voltage Regulation Methods for Distribution Systems with Dispersed Generators”, IEEJ Transactions on Power and Energy, Vol. 124, No. 12, pp. 1432-1438, 2004

[6] Katsuhiro Matsuda, Masaru Wada, Masahiro Watanabe, and Reiji Takahashi, “Optimum Parameter Decision Method for Pole Transformer Tap Considering Distributed Resources”, IEEJ Transactions on Power and Energy, Vol. 127, No. 1, pp. 137-144, 2007 (inJapanese)

[7] Ilija Vujošević, Ervin Spahić, and Đorđije Rakočević, “One method for the estimation of voltage drop in distribution systems”, Power Engineering Society Summer Meeting, 2002 IEEE, vol. 1, pp. 566-569, 2002

[8] David Timothy Chessmore, Wei-Jen Lee, William E. Muston, Thomas L. Anthony, Frank Daniel,Jr., and Larry Kohrmann, “Voltage-Profile Estimation and Control of a Distribution Feeder”, Industry Applications, IEEE Transactions on Industry Applications, Vol. 45, No. 4, pp. 1467-1474, 2009

[9] Junji Kondoh, Hirohisa Aki, Hiroshi Yamaguchi, Akinobu Murata, Itaru Ishii, “Voltage Regulation in Distribution Systems by Hierarchically Cooperative Control”, IEEJ Transactions on Power and Energy, Vol. 126, No. 10, pp. 994-1002, 2006 (in Japanese)

Chapter 4
Voltage control strategy using small batteries in distribution system

4.1 Introduction

In previous chapters, novel methods for voltage control in DS using existing facilities such as SVR have been presented. The reason for utilizing those existing facilities is to reduce an additional cost. Though modifying control method of existing facilities in a smart manner can reduce voltage violation from the allowable range, it is difficult to completely prevent voltage violation due to those low functions. For more smart management of voltage, novel control devices with high functions using power electronics technologies should be required. This chapter focuses on a battery (BT) as a smart device to control voltage.

Triggered by power shortage attributed to the accident of nuclear power plant in Fukushima caused by the Great East Japan Earthquake, in Japan, the energy issue has quickly surfaced. Thus, the introduction of energy policy is progressed such as Renewable Energy Source (RES), energy saving, and realization of novel and flexible power system with ICT. In those a realization of next generation power system, so-called smart grid, is indispensable for efficient energy utilization. One of important factors to efficiently utilize electric energy is the spread of storage devices such as BT. On the other hand, recently, for efficient energy management in residences, efforts to spread HEMS (Home Energy Management System) using PV, EV (Electric Vehicle), and BT are developing. Since BT has ability to flexibly regulate its output (charge or discharge), it can be effective device not only for adjusting supply and demand of electric power but also for maintaining voltage. The purpose of this chapter is to propose the novel voltage control method suppressing voltage fluctuation by PV using BT, which is expected to be distributed into DS by users in future. On the other hand, however, since the charging and discharging cause deterioration in BT, reduction of the amount of BTs for voltage control is greatly important for user's advantage. Hence, in this chapter, the control method for voltage using only a small part of user's BTs is presented.

This chapter organized as follows. After proposing the novel method using BTs in section 4.2, in section 4.3 the modeling and the actual operation of user's BT in DS are represented. The effectiveness of proposed approach is verified through numerical simulation in section 4.4. Finally, a summary of this chapter is shown in section 4.5.

4.2 Voltage management in case of a large amount of PV interconnection

4.2.1 Utilizing small BTs

Demand Side energy Management (DSM) such peak shift and peak cut of power consumption is very important for efficient energy management in customers. In particular, recently Demand Response (DR) using ICT is focused on as a new technology to realize DSM. The key technology of DR is BT. HEMS including BT as control device is an effective energy management system in residence, and hence BT of residence is expected to become widespread in future. On the other hand, to realize a low-carbon society, EV attracts attention compared to classical vehicles that have internal combustion engine with low efficiency and high environmental impact. Recent technological innovations dramatically improve energy density of BT and it is expected that EV and PHV with large BT increase in future as shown in Figure 4.1.

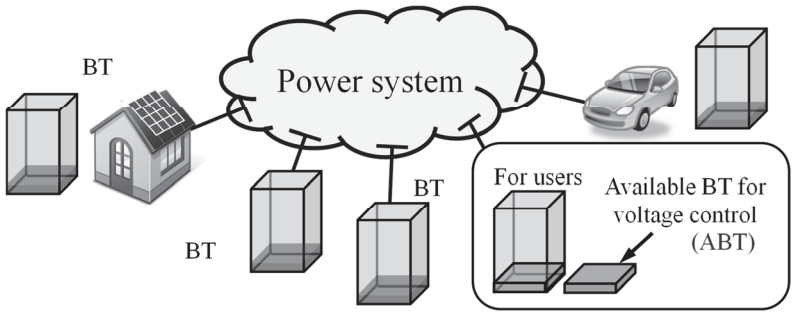

Figure 4.1 Introduction of many PVs to power system.

In case of PV interconnection, voltage management becomes easier by utilizing these many BTs dispersively installed in DS. Meanwhile, considering user's convenience, most part of user's BT should be used for user. Hence, a proposed strategy controls voltage using available capacity of BT (Available BT: ABT) that is a part of BT provided by users to DSO as shown in Figure 4.1.

Recently, many literatures employ user's facilities based on a concept of DR. In [1] [2], DSO controls charging and discharging of BTs in residences and EV for electric-load leveling and suppression of frequency fluctuation. Besides, in order to suppress voltage fluctuation due to PV, many researches regarding reactive power control using PCS system for interconnection of user's PV have been done [3] ~ [5]. Furthermore, in [6] [7], DR is used as load shaping which is useful for load leveling. In [8] ~ [10], loads are efficiently controlled using DR. Thus, the effectiveness of employing user's facilities has been widely recognized. By not only DSO but also users, it is possible to realize more efficient operation of power system. Although reactive power control by PCS is known to be an efficient control method for voltage regulation, this approach makes large adverse impact on upper transmission system with large X/R

ratio of line. From this point of view, this chapter focuses on active power control by BT not using reactive power. Though it is necessary to compare the proposed approach with the reactive power control by PCS, this chapter mainly focuses on voltage control using active power. Since DSO uses only a part of user's BT in the proposed method, the most part of user's BT can be used by user. Furthermore, though charge and discharge of BT causes degradation of BT, the proposed method can reduce active power being charged and discharged and suppress degradation of BT.

4.2.2 Control method of ABT

In case of employing BT for voltage control, SOC (State Of Charge) of BT should be considered. Since an available capacity of user's BT is small, SOC of ABT (ASOC: Available SOC) tends to become 0% or 100%. This means that ABT tends to fall into a state in which ABT cannot charge and discharge to regulate voltage. When ABT falls into this state, ABT cannot operate corresponding to command from DSO and voltage control may become difficult. To avoid this issue, the proposed method by ABT suppresses only rapid voltage fluctuation (Rapid Voltage Fluctuation Repression: RVFR method). The conceptual idea of RVFR method is shown in Figure 4.2 and Figure 4.3. In Figure 4.2, light gray areas represent ABT for voltage control and clear areas represent BT for users. Dark areas show stored energy in ABT. RVFR method controls ASOC to be close to 0% before charging. This is because it is necessary to charge active power to reduce voltage when voltage rapidly increases due to PV. On the other hand, in order to discharge ABT in case of sudden voltage drop due to PV, the proposed method controls ASOC to be close to 100% before the discharging. Accordingly, ASOC is controlled corresponding to rapid voltage fluctuation as shown in Figure 4.3.

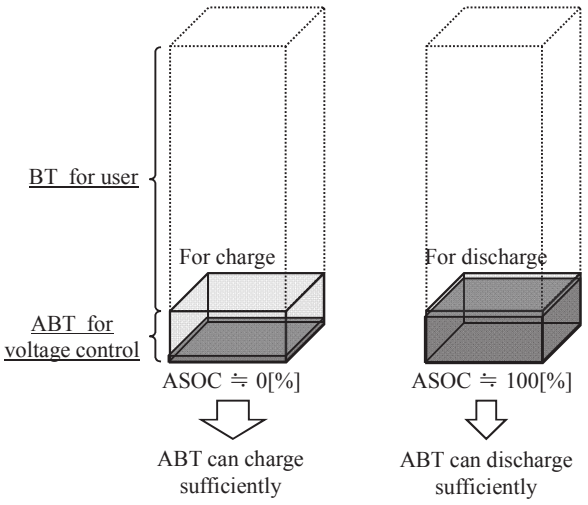

Figure 4.2 SOC of ABT.

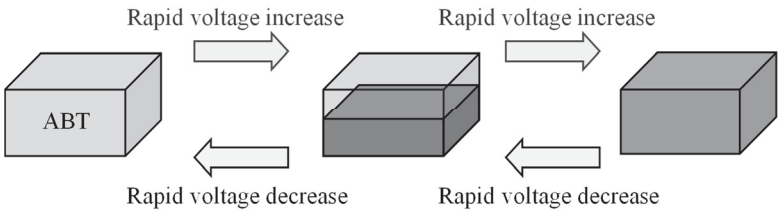

Figure 4.3 ASOC controlled by voltage deviation.

To implement this idea, the adjusting a dead band is proposed. The control with the dead band is easy to be implemented in BT controller due to its simple architecture. BT with this method monitors PCC voltage V_{PCC} as shown in Figure 4.4 and compares V_{PCC} with the upper or lower limit of dead band. BT charges or discharges active power so that V_{PCC} remains within the dead band. If V_{PCC} exceeds the upper limit of dead band, BT charges active power. On the other hand, BT discharges active power if V_{PCC} is below the lower limit of dead band. By changing a position of the dead band, ASOC can be controlled to satisfy the idea shown in Figure 4.2 and 4.3. The dead band is controlled within the control range. V_{MAX} and V_{MIN} represent the upper and lower limit of control range, respectively. These V_{MAX} and V_{MIN} are set as inside of the adequate range.

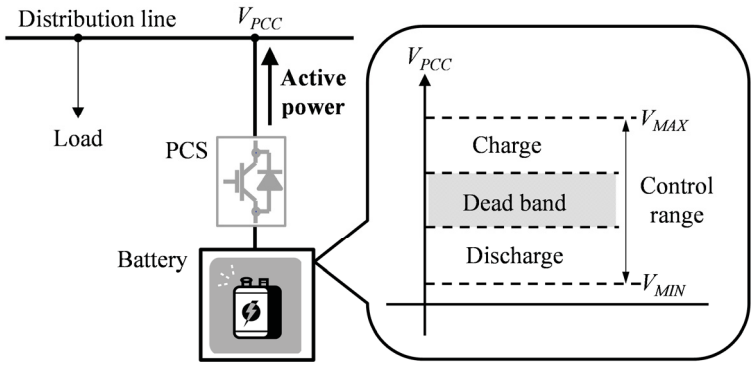

Figure 4.4 Control BT using the dead band.

An algorithm of the proposed method changing the position of dead band is shown in Figure 4.5 and 4.6 in detail.

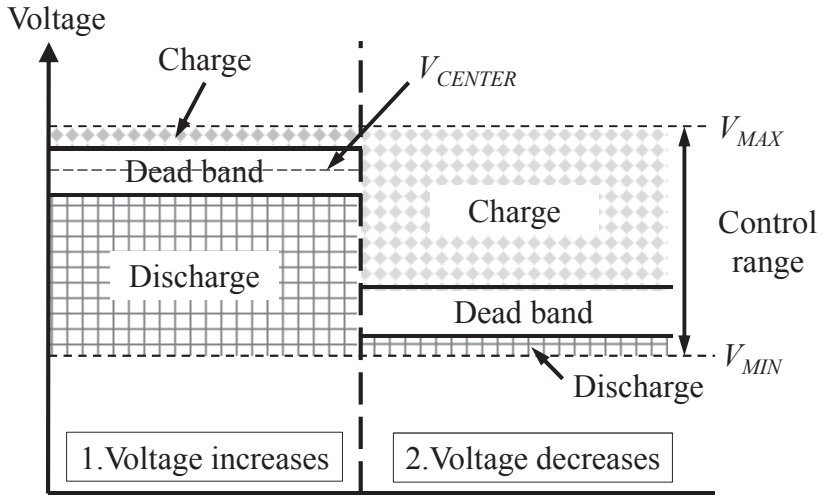

Figure 4.5 ABT control using dead band.

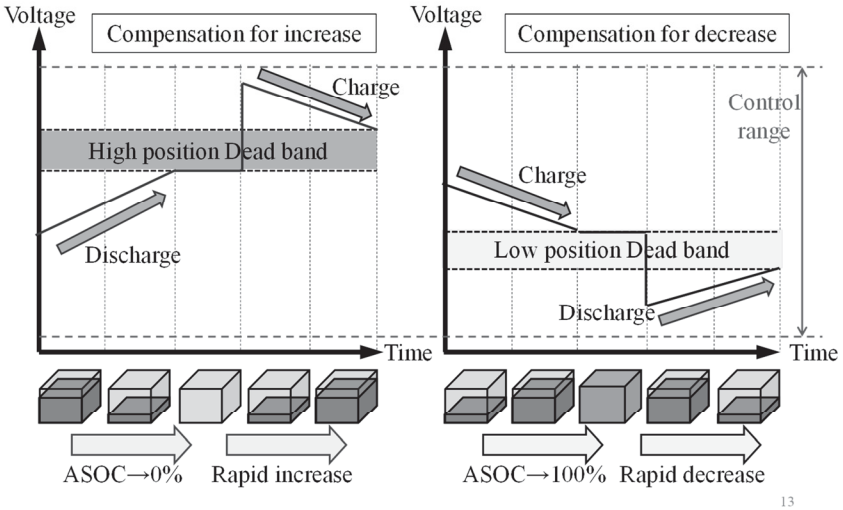

Figure 4.6 Voltage behavior controlled by ABT.

In the proposed approach, 1) before voltage rapidly increases by PV, the dead band of ABT is controlled to be close to V_{MAX} as shown in Figure 4.5. In this way, ABT discharges active power and controls ASOC close to 0% before voltage rapidly increases as shown in Figure 4.6. In case of rapid voltage rising due to PV, ABT with small ASOC charges active power and suppresses voltage violation from V_{MAX}. 2) Before voltage rapidly decreases due to PV, the dead band of ABT is controlled close to V_{MIN} as shown in Figure 4.5. ABT controls ASOC and prevent voltage violation from V_{MIN}. In the proposed method, the dead band position of ABT is determined based on a center voltage of dead band V_{CENTER} shown in Figure 4.5.

V_{CENTER} is controlled using solar radiation information. In this chapter, it is assumed that the output of PV at node #i in DS P^{i}_{PV} (i = 1,2,…,n) is in proportion to normalized solar radiation value S as shown in

Figure 4.7.

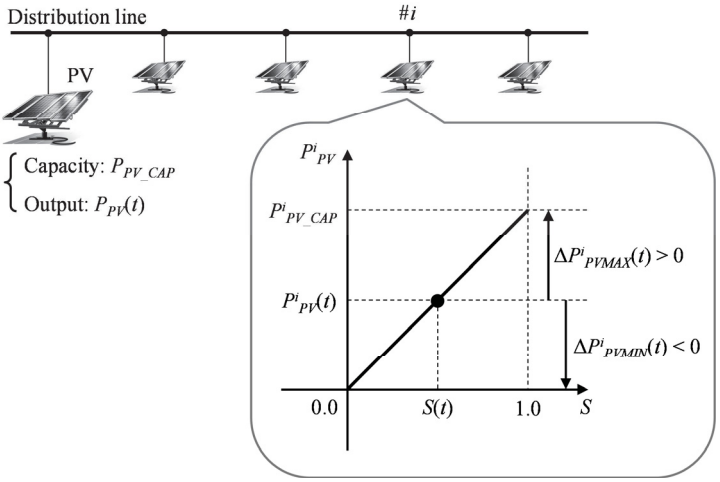

Figure 4.7 Estimation of PV's output using solar radiation.

The maximum amount of increment of P_{PV} $\Delta \boldsymbol{P}_{PVMAX}(t) = [\Delta P^1_{PVMAX}(t),\ldots,\Delta P^i_{PVMAX}(t),\ldots,\Delta P^n_{PVMAX}(t)]^{\mathrm{T}}$ and the maximum amount of decrement of P_{PV} $\Delta \boldsymbol{P}_{PVMIN}(t) = [\Delta P^1_{PVMIN}(t),\ldots,\Delta P^i_{PVMIN}(t),\ldots,\Delta P^n_{PVMIN}(t)]^{\mathrm{T}}$ are calculated using $S(t)$ at time t as follows:

$$\Delta \boldsymbol{P}_{PVMAX}(t) = \{1.0 - S(t)\}\boldsymbol{P}_{PV\_CAP} \tag{4.1}$$

$$\Delta \boldsymbol{P}_{PVMIN}(t) = \{0.0 - S(t)\}\boldsymbol{P}_{PV\_CAP} \tag{4.2}$$

where $\boldsymbol{P}_{PV\_CAP}=[P^1_{PV\_CAP}, \ldots, P^i_{PV\_CAP}, \ldots, P^n_{PV\_CAP}]^{\mathrm{T}}$

$P^i_{PV\_cap}$ is the sum of capacity of PVs connected to node #*i*. V^i_{PVMAX} and V^i_{PVMIN} that are the maximum voltage and the minimum voltage at node #*i* are obtained using $P^i_{PV\_cap}$ and Jacobean matrix $\boldsymbol{J}$ calculated utilizing voltage information from VS.

$$[\boldsymbol{V}_{PVMAX}(t), \boldsymbol{\theta}_{PVMAX}(t)]^T = [\boldsymbol{V}(t), \boldsymbol{\theta}(t)]^T + \boldsymbol{J}(t)^{-1}[\Delta \boldsymbol{P}_{PVMAX}(t), \boldsymbol{0}]^T \tag{4.3}$$

$$[\boldsymbol{V}_{PVMIN}(t), \boldsymbol{\theta}_{PVMIN}(t)]^T = [\boldsymbol{V}(t), \boldsymbol{\theta}(t)]^T + \boldsymbol{J}(t)^{-1}[\Delta \boldsymbol{P}_{PVMIN}(t), \boldsymbol{0}]^T \tag{4.4}$$

where

$\boldsymbol{V}_{PVMAX}(t)=[V^1_{PVMAX}(t),\ldots,V^i_{PVMAX}(t),\ldots,V^n_{PVMAX}(t)]^{\mathrm{T}}$,
$\boldsymbol{V}_{PVMIN}(t)=[V^1_{PVMIN}(t),\ldots,V^i_{PVMIN}(t),\ldots,V^n_{PVMIN}(t)]^{\mathrm{T}}$,
$\boldsymbol{V}(t) =[\ V^1(t), \ldots, V^i(t), \ldots, V^n(t)]^{\mathrm{T}}$,
$\boldsymbol{\theta}(t) =[\ \theta^1(t), \ldots, \theta^i(t), \ldots, \theta^n(t)]^{\mathrm{T}}$

$$\boldsymbol{J} = \begin{bmatrix} \dfrac{\partial \boldsymbol{P}}{\partial \boldsymbol{V}} & \dfrac{\partial \boldsymbol{P}}{\partial \boldsymbol{\theta}} \\ \dfrac{\partial \boldsymbol{Q}}{\partial \boldsymbol{V}} & \dfrac{\partial \boldsymbol{Q}}{\partial \boldsymbol{\theta}} \end{bmatrix}$$

$\boldsymbol{J}(t)$ is a Jacobian matrix at time t regarding active and reactive power. $V^i(t)$ and $\theta^i(t)$ represent the magnitude and phase angle of voltage at node #i, respectively. Assuming the output of PV is only active power, fluctuation of reactive power due to PV ΔQ_{PVMAX} and ΔQ_{PVMIN} on the second term in the right side of equation (4.3), (4.4) are set as 0. $\boldsymbol{J}(t)$ is calculated using voltage information from VS. See the Appendices A2 to know how to calculate Jacobian matrix.

Node #j is a point in which ABT observes V_{PCC} and controls V_{PCC} within the dead band. By predicting voltage magnitude fluctuated by PV, V_{CENTER} can be calculated as follows:

$$V_{CENTER}(t) = \begin{cases} V_{UPPER} & \left(V^{j}{}_{PVMIN}(t) \geq V_{MIN}\right) \\ V_{LOWER} & \left(V^{j}{}_{PVMAX}(t) \leq V_{MAX}\right) \end{cases} \tag{4.5}$$

If equation (4.5) is not satisfied, then

$$V_{CENTER}(t) = \begin{cases} V_{UPPER} & \left\{V^{j}{}_{PVMAX}(t) - V_{MAX} \leq V_{MIN} - V^{j}{}_{PVMIN}(t)\right\} \\ V_{LOWER} & \left\{V^{j}{}_{PVMAX}(t) - V_{MAX} \geq V_{MIN} - V^{j}{}_{PVMIN}(t)\right\} \end{cases} \tag{4.6}$$

V_{UPPER} is close to V_{MAX} and V_{LOWER} is close to V_{MIN} as shown in Figure 4.5. Figure 4.8 shows an overview of equation (4.5). In Figure 4.8, because V^j_{PVMIN} is not below V_{MIN}, it is not necessary to compensate for lower voltage violation. Hence, voltage violation from the upper limit of allowable range due to rapid voltage rising should be prevented by setting $V_{CENTER} = V_{UPPER}$. On the other hand, when V^j_{PVMAX} is below V_{MAX}, set $V_{CENTER} = V_{LOWER}$. Besides, if equation (4.5) is not held, equation (4.6) is used to calculate V_{CENTER}. This is because each capacity of ABTs is small and ABT cannot continually compensate for large voltage violation. ABT should compensate for small voltage violation, not large one. Therefore, the dead band position is determined to compensate smaller voltage deviation by predicting the magnitude of voltage violation due to PV. Figure 4.9 represents this case. In the proposed method, while ABT compensates for smaller voltage deviation, in case of large voltage deviation SVR is cooperatively controlled, which is explained in following section.

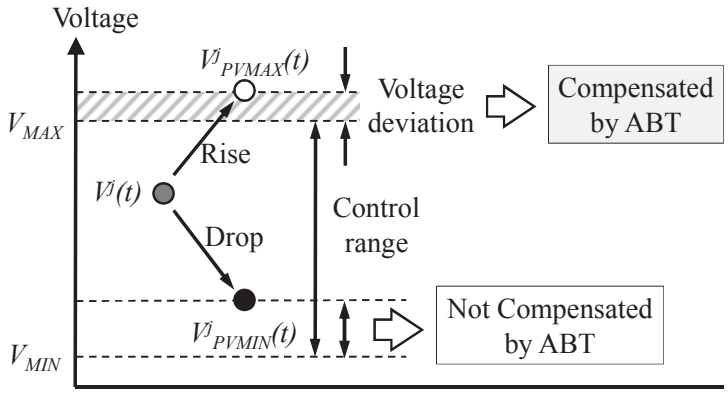

Figure 4.8 Predicting voltage fluctuation (1).

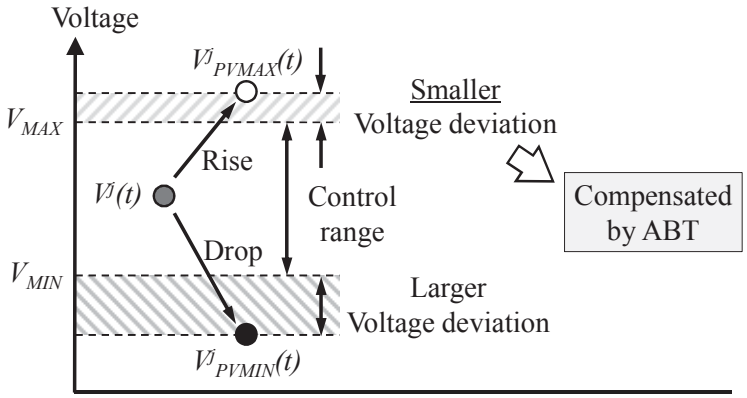

Figure 4.9 Predicting voltage fluctuation (2).

4.2.3 Synchronous control method of ABTs

Independent operation of each ABT cannot effectively compensate for voltage violation because each capacity of ABT is too small to regulate voltage. In order to manage voltage using small ABTs, it is effective to simultaneously operate all ABTs. Hence, as shown in Figure 4.10, all ABTs operate based on synchronous signal from AA (Administrator of ABT). AA is installed in a node (node #*j*) in which voltage tends to fluctuate and deviate from the allowable range. AA determines whether each ABT charges or discharges using V^j_{PVMAX} and V^j_{PVMIN}.

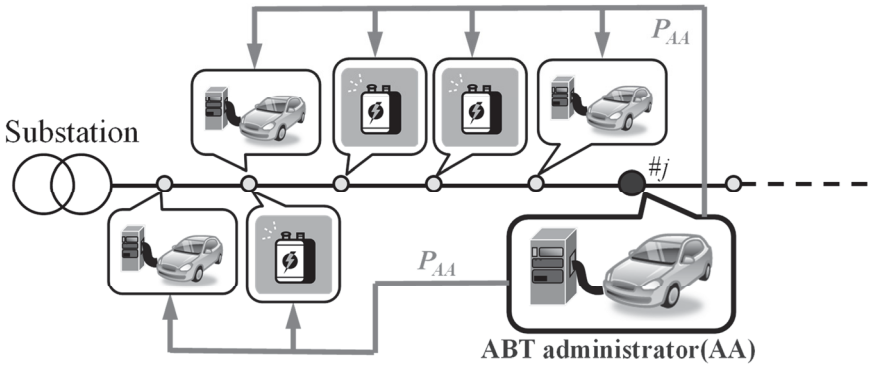

Figure 4.10 Synchronous control of many ABTs by AA.

PCS for connection of BT into DS operates based on a synchronous signal from AA. The proposed method assumes that users provide a part of PCS (Available PCS: APCS) for DSO to control voltage. The synchronous signal $P_{AA}(t)$ that is transferred from AA to ABT at time t is defined as a ratio of APCS's output $P^{j}_{APCS}(t)$ against the capacity of APCS $P^{j}_{APCS\_CAP}$ as shown in equation (4.7) and (4.8). Other APCSs ($i \neq j$) charge and discharge based on $P_{AA}(t)$ from AA.

$$P_{AA}(t) = \frac{P^{j}{}_{APCS}(t)}{P^{j}{}_{APCS\_CAP}} \tag{4.7}$$

$$P^{i}{}_{APCS}(t) = P_{AA}(t) P^{i}{}_{APCS\_CAP} \qquad (i \neq j) \tag{4.8}$$

Equations (4.7) and (4.8) can be held under the assumption that a ratio of each capacity of APCS against the capacity of ABT is same over entire DS. This is for simplification in this chapter.

4.2.4 Cooperative control with SVR

As mentioned in section 4.2.3, ABT can compensates for relatively small voltage violation according to capacity of all ABTs. Therefore, in this section, the cooperative control with SVR to reduce of ABT output is presented. SVR is controlled based on voltage data V_{VS} from VSs located on the distribution line as shown in Figure 4.11. It is assumed that real-time communication infrastructure can be realized in future when many BTs are connected into DS.

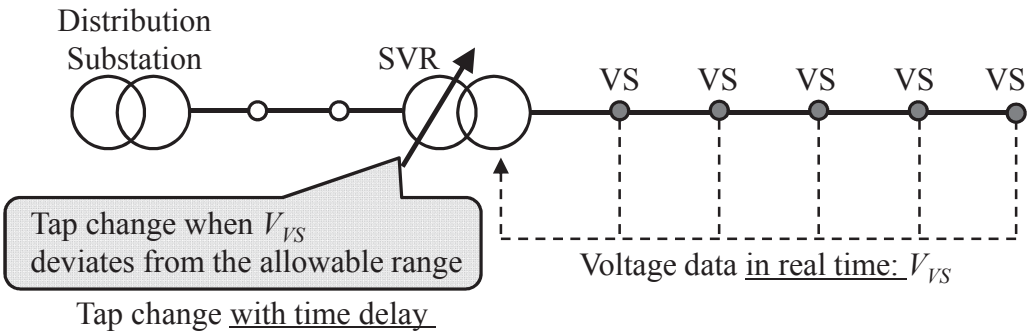

Figure 4.11 Cooperative control with SVR.

Using the proposed method, ABT can continue to charge and discharge in a short time, and rapid voltage fluctuation can be temporarily prevented. However, if ASOC becomes 0% or 100% after continued charging and discharging over a long period of time, voltage can deviate from the control range because the output of APCS rapidly reduces. In order to avoid this, AA sends an operating command T_{AA} to SVR before ASOC becomes 0% or 100%. Corresponding to the operating command from AA, SVR changes its tap position to avoid voltage violation as shown in Figure 4.12. Equation (4.9) represents a command of tap position N_{TAP_ref} from AA (+1: tap up, -1: tap down). In Equation (4.9), $P^j_{ABT\_CHARGE}$ represents charged power of AA (kWh) and P^j_{APCS} represents the output of APCS at AA (kW).

$$N_{TAP\_ref}(t)=\begin{cases} +1 \quad \text{if} \quad P^{j}{}_{ABT\_CHARGE}(t)-\dfrac{P^{j}{}_{APCS}(t)T_{AA}}{3600}\le 0 \\ -1 \quad \text{if} \quad P^{j}{}_{ABT\_CHARGE}(t)-\dfrac{P^{j}{}_{APCS}(t)T_{AA}}{3600}\ge P^{j}{}_{ABT\_CAP} \end{cases} \tag{4.9}$$

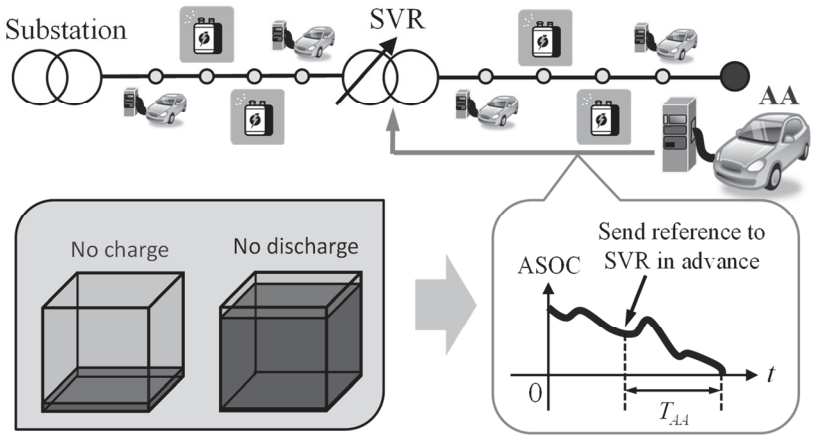

Figure 4.12 Reference signal to SVR from AA.

4.3 Model of ABT group

An amount of ABT provided from users to DSO is fluctuated according to the conditions of users. When there are users who do not want to provide ABT for DSO, the amount of ABT in DS reduces. In a similar way, the amount of ABT in DS reduces when EV or PHEV is not connected to DS. Thus, because the amount of ABTs is fluctuated, the uncertainty of ABT should be modeled. Considering the uncertainty of ABT interconnection, the amount of ABT at each node in DS is time varying.

4.3.1 Time varying model of the amount of ABT in DS

Assuming that average contract power of each user is P_{LOAD_AVE} and the total capacity of load connected to node #i is $P^i_{LOAD\_CAP}$, the total output of APCS $P^i_{APCS\_sum}$ connected to node #i at time t is calculated as shown in equation (4.10).

$$P^i{}_{APCS\_sum}(t) = \frac{P^i{}_{LOAD\_CAP}}{P_{LOAD\_AVE}} P^i{}_{APCS}(t) R_{BT} RAND^i(t) \tag{4.10}$$

$RAND^i(t)$ represents a rate of interconnection of ABT at node #i at time t, and has a random value from 0 to 1. The uncertainty of the amount of ABT connected to DS is simulated changing $RAND^i(t)$ at each node at random. Let R_{BT} denote a penetration rate of BT in DS. If R_{BT} is 1.0, all users provide their BT for DSO. In the numerical simulation, R_{BT} is set as 0.3 assuming that BT for EV, PHEV, and residences are introduced to DS in future. $RAND^i(t)$ is changed every 30min because the amount of ABT connected to DS is expected to be changed not in real-time but from tens of minutes to several hours. In this chapter, P_{LOAD_AVE} is 3.0kW and AA is always connected to DS to control other ABTs.

4.3.2 Communication of AA with ABT

Though all ABT synchronously operates in the proposed method, it might be difficult for AA to send $P_{AA}(t)$ to all ABTs in real-time. This is because many communications between ABTs can cause the congestion by traffic in communication line. Therefore, it is assumed that each ABT receives $P_{AA}(t)$ from AA every Δt=2s. Without real time communication, it is necessary for each ABT to control its output in real time based on intermittent signal from AA. Figure 4.13 shows the control mechanism of $P_{AA}(t)$. In Figure 4.13, AA gives the charge command to all ABTs after $V_i(t)$ exceeds the upper limit of dead band because voltage tends to exceed V_{MAX} when the dead band is in high position. At this time, the output of each APCS becomes the maximum value (P_{AA}=－1.0). Because all ABTs synchronously charge active power, rapid voltage rising due to PV can be prevented in this case. On the other hand, if $V_j(t)$ becomes less than the lower limit of dead band, P_{AA} increases by ΔP_{AA} at Δt and ASOC gradually approaches 0%. If the dead band is in the low position, AA and ABT operate in reverse way. In this chapter, ΔP_{AA} is less than 1.0

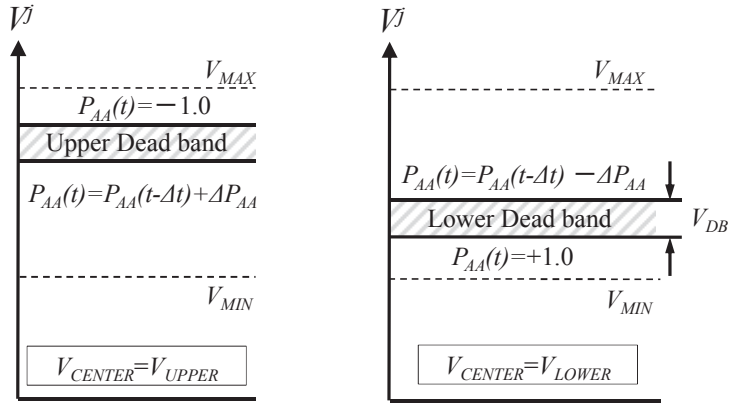

(a) High position. (b) Low position.

Figure 4.13 Control of P_{AA}.

(=0.01).

4.3.3 Charging and discharging model of ABT

This research assumes that ABT can charge and discharge active power based on command $P_{AA}(t)$ from AA without delay. Charging and discharging is modeled as time integral of P^i_{APCS}. P_{AA} has positive value to charge or negative value to discharge, respectively. Though the charging and discharging using BT and PCS lead to the loss of active power, for simplicity, this chapter assumes there is no conversion loss in ABT and APCS.

4.4 Case study

4.4.1 Distribution system model

The DS model in the numerical simulation is shown in Figure 4.14. Distribution system with a long line tends to cause several issues when a large amount of PVs are introduced. Hence, DS model with a SVR is employed for the numerical simulation. Parameters of the DS model are shown on Table 4.2. Line impedance in Table 4.2 is based on actual DS. Voltage drop in this model without PV is large, and hence SVR is indispensable to manage whole voltage within the allowable range. For simplicity, a simple network model without branches on the distribution line is employed in the numerical simulation. Assuming PVs are installed on roof of residence, PVs are connected to load nodes.

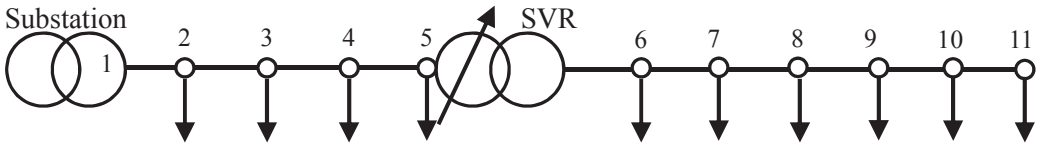

Figure 4.14 Distribution system model.

Table 4.1 Distribution system model parameters.

Primary node#	Secondary node#	R[Ω]	X[Ω]	Capacity of Load[kVA]
1	2	0.1	0.1	286
2	3	0.1	0.1	286
3	4	0.14	0.14	286
4	4	0.14	0.14	286
4	6	0.14	0.14	286
6	7	0.14	0.14	286
7	8	0.14	0.14	286
8	9	0.14	0.14	286
9	10	0.14	0.14	286
10	11	0.14	0.14	286
Total		1.32	1.32	2860

4.4.2 Load model

As a load pattern, a typical residence pattern is adopted. In order to simulate small fluctuation of load, each load is minutely varied at random corresponding to a basic pattern. Load pattern is shown in Figure 4.15. In Figure 4.15, time-varying model of total loads in DS, not each load and positive value of reactive power is lagging.

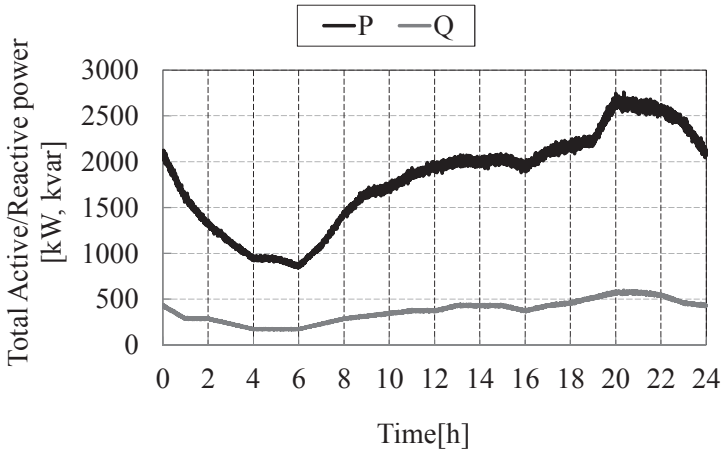

Figure 4.15 Load pattern.

4.4.3 PV system model

Using the maximum value of load at node #*i* $P^{i}_{LOAD\_CAP}$ and the capaciy of PV $P^{i}_{PV\_CAP}$, an interconection ratio of PV R^{i}_{PV} is

$$R^{i}_{PV} = \frac{P^{i}_{PV\_CAP}}{P^{i}_{LOAD\_CAP}} \tag{4.11}$$

Since the mass interconnection of PV is assumed in this research, all R^{i}_{PV} are set as

$$R^{i}_{PV} = 1.0 \quad (i = 2, \cdots, 11) \tag{4.12}$$

When the output of PV changes rapidly and frequently due to PV, functinal facilities such as BT that can flexibility control votlage may be important since voltage tends to exceed a limit of adequate range. Therefore, a pattern of the output of PV in cloudy day shown in Figure 4.16 is employed. The pattern shown in Figure 4.16 is built based on actual measured data in cloudy day. When all PVs in DS simultaniouely change their output, voltage fluctuation becomes large. It becomes difficult to manage voltage in that case. In order to verify whether voltage can be properly controlled under such the severe condition, the output pattern of PV is same value over entire PV.

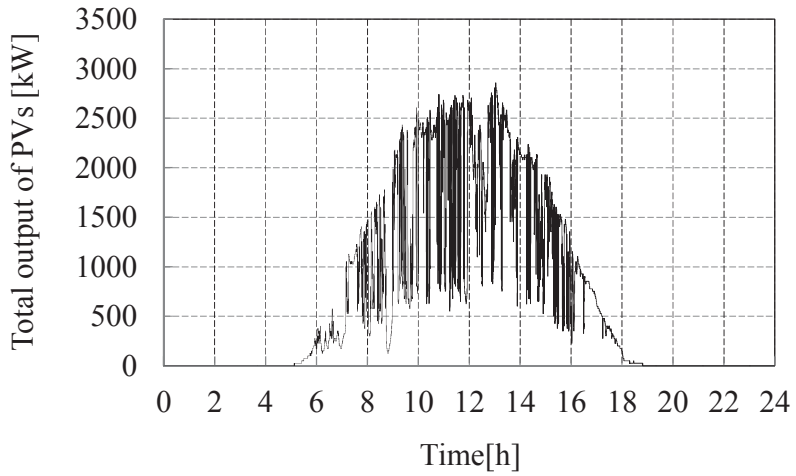

Figure 4.16 Output of PV.

4.4.4 Model parameters of ABT

Table 4.2 shows ABT parameters used in this chapter. Small APCS is employed to avoid the drawback for users. Current general capacity of BT in EV is about 10 ~ 30kWh and one for residence is only a few kWh. On the assumption of development of BT in future, the capacity of ABT P_{ABT_CAP} is set as 3.0kWh. In addition, current PCS of BT for EV has usually a few kW as the rated capacity, and the capacity of BT

for residence has only a few kW, hence the capacity of APCS P_{APCS_CAP} is set as 1.0kW. For simplicity, P_{ABT_CAP} and P_{APCS_CAP} of each user have same value over whole DS.

Table 4.2 Model parameters of ABT.

P_{LOAD_AVE}	3.0kW
R_{BT}	0.3
P_{ABT_CAP}	3.0kWh
P_{APCS_CAP}	1.0kW

4.4.5 Simulation conditions

Table 4.3 shows simulation conditions. High-side voltage (6.6kV) calculated by power flow calculation is transferred to low-side voltage (100V) using the turn ratio of pole transformers. The allowable range of low-side voltage (≠control range of ABT and SVR) is set as 101.0 ~ 106.5V considering voltage drop and rise in low voltage wire and lead-in wire (101.0 ~ 107.0 in case of no PVs in DS because voltage only decreases on lead-in wire). For simplicity, sending voltage in distribution substation is set as constant value 6660V. It has been confirmed that, in case of no PVs, voltage is kept within the allowable range even though the sending voltage is constant 6660V. Time delay of SVR $T_{operate}$ adopts a value used in actual SVR that employs a vacuum valve for arc interruption when the tap position is changed. Simulation is executed in 4 cases as shown in Table 4.4. First, in case 1, simulation with no PVs is executed. Next, with a large amount of PVs in case 2 ~ 4, the effectiveness of proposed method is verified through the numerical simulation. AA locates in node #11 (=#*j*) at the end of distribution line because the voltage at end of line tends to fluctuate in general and past researches of authors have revealed that it is difficult to control the end voltage within the adequate range.

Table 4.3 Simulation conditions.

Simulation interval			2.0s
Simulation time			24h
Allowable range (Low voltage)	Upper(V_{lim})	Case 1	107.0V
		Case 2～4	106.5V
	Lower		101.0V
Ratio of pole transformer (Low/High)			105/6600
Sending voltage at the substation			6660V
Control range in proposed method (Low voltage)		V_{MAX}	106.45V
		V_{MIN}	101.05V
SVR	Width of tap		150V
	Width of Dead Band	Conventional	189V(3[%])
		Proposed	Non
	T_{settle}	Conventional	60s
		Proposed	0.0s
	$T_{operate}$		5.0s
	Range of tap position		6450/6600 ～ 6900/6600
	Communication interval		0.0s
BT	AA position		#11
	Dead Band settings	V_{UPPER}	6681.7V
		V_{LOWER}	6361.1V
		V_{DB} (width)	6.3V
	ΔP_{AA}		0.01
	Δt		2.0s
	T_{AA}		6.0s

Table 4.4 Simulation cases.

Case	R_{PV}	BT	SVR
1	0.0	Non	Conventional
2	1.0	Non	Conventional
3	1.0	Non	Proposed
4	1.0	Proposed	Proposed

4.4.6 Evaluation method of simulation results

(1) Voltage violation

Simulation results are evaluated using voltage violation index *VD* that represents the amount of voltage exceeding the limit of allowable range as shown in equation (4.13).

$$VD = \sum_{t=0}^{T} \sum_{i=1}^{11} e_V(t,i)$$
$$e_V(t,i) = \begin{cases} V(t,i) - V_{\lim} & (V(t,i) > V_{\lim}) \\ 101.0 - V(t,i) & (V(t,i) < 101.0) \end{cases} \tag{4.13}$$

V_{lim} in equation (4.13) is upper voltage of the adequate range shown in Table 4.3. *VD* is the sum of value over all nodes (#1 ~ 11) that is the integral of voltage exceeding the limit of allowable range (101.0 ~ V_{lim}: low-side) over simulation periods. $V(t,i)$ is low-side voltage transformed from high-side voltage at time *t* at node #*i* using the turn ratio of pole transformers.

(2) Maximum/Minimum voltage

To evaluate the worst condition in the numerical simulation, the maximum voltage V_{MAX_sim} and the minimum voltage V_{MIN_sim} in the simulation, over all nodes are employed.

(3) Number of switching operation of SVR

Two indices described above show how voltage violation occurs. On the other hand, because the increase of switching operation of SVR causes degradation of SVR, the number of switching operation of SVR in a day N_{SVR} should be also evaluated.

4.4.7 Simulation results

(1) Case 1

Figure 4.17, 4.18, and 4.19 show simulation results in case 1. Figure 4.17 shows V_{SVR} and Figure 4.18 represents the tap position of SVR. Figure 4.19 shows that low-side voltage transformed from high-side voltage using the turn ratio of pole transformers. The tap position of SVR is 0 when primary/secondary voltage is 6600/6600. The tap position is changed +1 with a rise of tap, -1 with a down of tap. Figure 4.17 and 4.18 show that SVR raises voltage during heavy load periods. Figure 4.19 shows voltage profile at node #5, #6, and #11. In Figure 4.19, voltage at node #11 is close to the lower limit of allowable range near at 15:00. Hence, this DS model has heavy loads and it is indispensable to employ SVR for compensation of voltage drop on the distribution line. Because voltage is controlled within the adequate range in case 1, it can be seen that the install position of SVR, the parameters of SVR such as a position of dead band, and the settling time are properly set for voltage regulation.

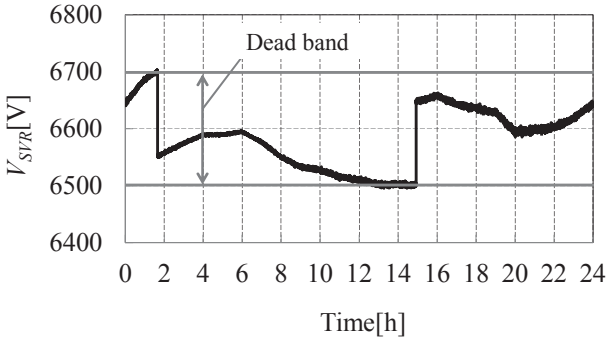

Figure 4.17 Secondary voltage of SVR (case 1).

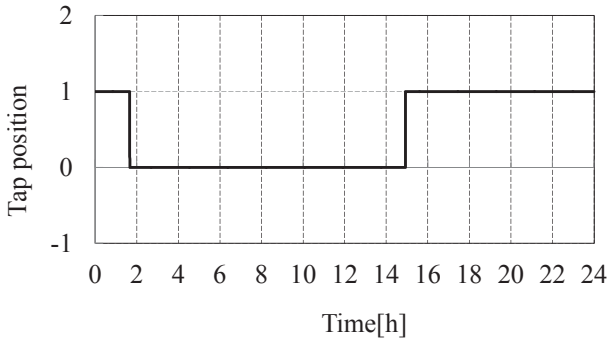

Figure 4.18 Tap position of SVR (case 1).

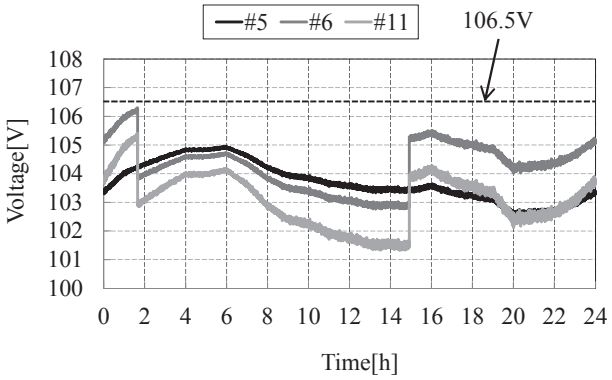

Figure 4.19 Voltage profile (case 1).

(2) Case 2

Figure 4.20, 4.21, and 4.22 show simulation results in case 2. In Figure 4.20, rapid and frequent voltage fluctuation occurs corresponding to the output of PV. On the other hand, N_{SVR} is small as shown in Figure 4.21 even though voltage in DS exceeds the upper limit of allowable range 106.5V as shown in Figure 4.20. This is because case 2 employs the conventional control method and parameters of SVR. Although the conventional control method is proper in case 1, that becomes improper in case of PV interconnection.

Like this, local control method of SVR using the dead band might not be able to properly manage voltage in DS with a large amount of PVs.

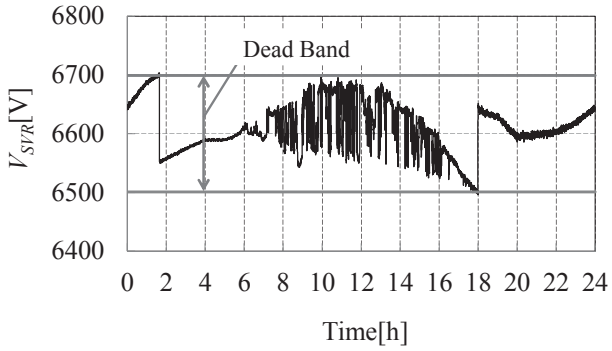

Figure 4.20 Secondary voltage of SVR (case 2).

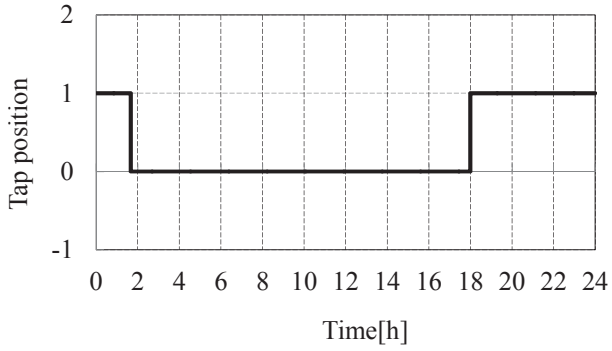

Figure 4.21 Tap position of SVR (case 2).

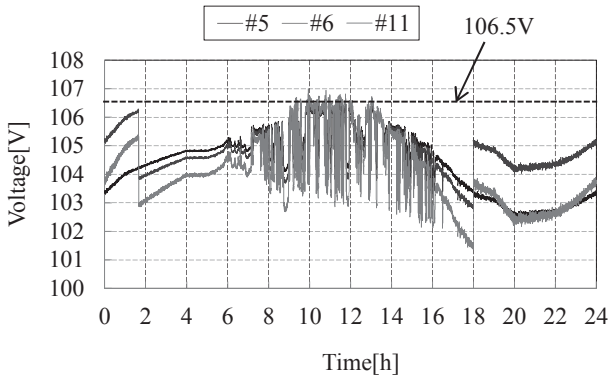

(a) Voltage in a day.

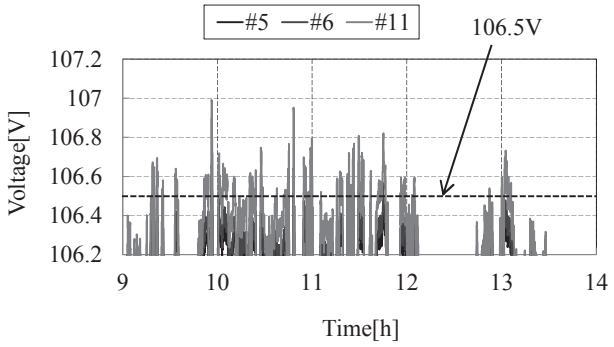

(b) Magnified voltage.

Figure 4.22 Voltage profile (case 2).

(3) Case 3

Figure 4.23 and 4.24 show simulation results in case 3. Comparing Figure 4.22 with 4.23, the control method of SVR using information from VSs with high-speed communication can reduce voltage violation. However, due to structural time delay of SVR, voltage violation may continue until SVR finishes its operation. It is necessary to compensate for this time delay. Besides, in Figure 4.24, SVR frequently operates over 9 ~ 14 h when PV frequently changes its output. This is because voltage on the distribution line frequently exceeds the limit of proper range. However, frequent switching of SVR deteriorates SVR and increases its maintenance cost, hence other facilities is necessary to suppress this rapid voltage fluctuation so that SVR does not frequently operate.

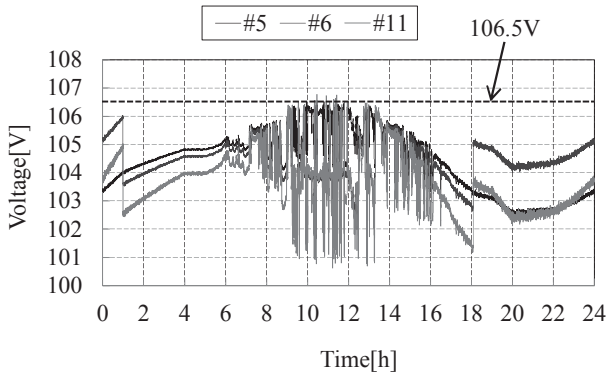

(a) Voltage in a day.

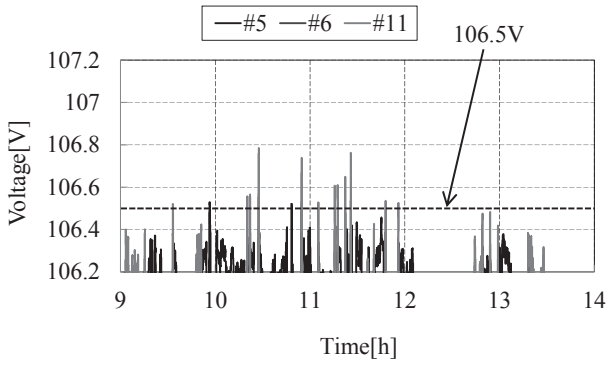

(b) Magnified voltage.

Figure 4.23 Voltage profile (case 3).

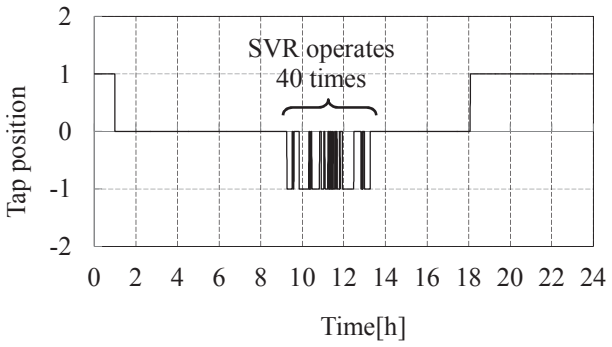

Figure 4.24 Tap position of SVR (case 3).

(4) Case 4

Figure 4.25 and 4.26 show simulation results in case 4. Voltage in Figure 4.25 is controlled almost within the allowable range. Though SVR changes its tap position at daytime when PV increases its output, N_{SVR} largely decreases compared to case 3. This is because that multiple ABTs can mitigate voltage fluctuation.

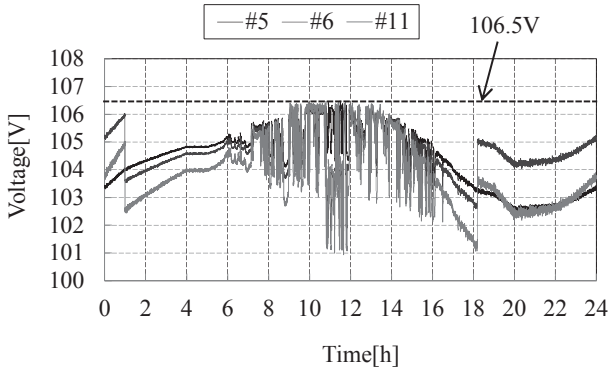

(a) Voltage in a day.

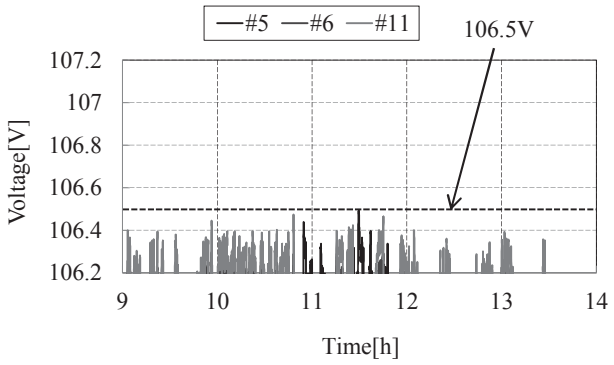

(b) Magnified voltage.

Figure 4.25 Voltage profile (case 4).

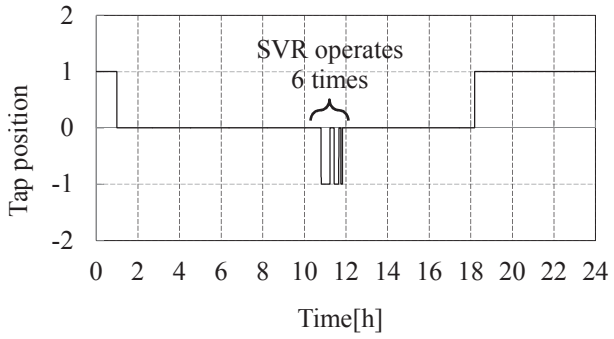

Figure 4.26 Tap position of SVR (case 4).

P_{APCS} of each ABT is shown in Figure 4.27. P_{APCS} has positive value when discharging, and negative value when charging. In addition, charged power of ABT P_{ABT_CHARGE}, total P_{APCS_CAP}, and P_{ABT_CAP} over whole DS are shown in Figure 4.28. Two vertical axes in Figure 4.27 are a one-to-one correspondence. For example, when the total ABT capacity provided from users is 180kWh, the total capacity of APCS becomes 60kW.

The amount of ABT and APCS in DS might fluctuate with time according to user's condition. Even

when the amount of available ABT and APCS is restricted, the proposed method can regulate voltage by avoiding non-charging and non-discharging state of ABT. Comparing Figure 4.23 with 4.25, voltage violation occurs due to rapid voltage rising in Figure 4.23, but in Figure 4.25 rapid voltage rising is prevented and voltage almost remains within the adequate range. In Figure 4.16, at 13h the output of PV becomes about 3MW in entire DS (3MW). Total P_{APCS_CAP} is about 40kW in Figure 4.28. Thus, even though the capacity of APCS is much smaller than one of PV, voltage can be properly managed in the proposed method. In addition, even though total P_{ABT_CAP} is about 7 ~ 20 times smaller than BT in EV, ASOC does not become 0 or 100% at daytime. From the simulation results, it can be seen that the proposed method needs small ABT and APCS, not large one.

In order to simultaneously operate all ABTs with real-time communication, it is important to evaluate a risk of communication between AA and ABT and to backup for communication troubles. Communication facilities include optical line and wireless communication for example. However, concrete means of communication in next generation DS is not yet clear at present. It is necessary to analyze factors of communication troubles (delay, disconnection, asynchronous, etc.) assuming concrete communication means. Accordingly, in this research, communication troubles are not considered and only constraint of communication speed is investigated.

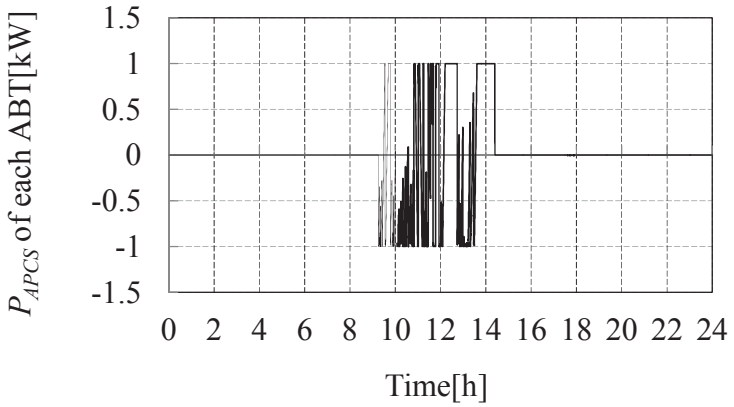

Figure 4.27 P_{APCS} of each ABT.

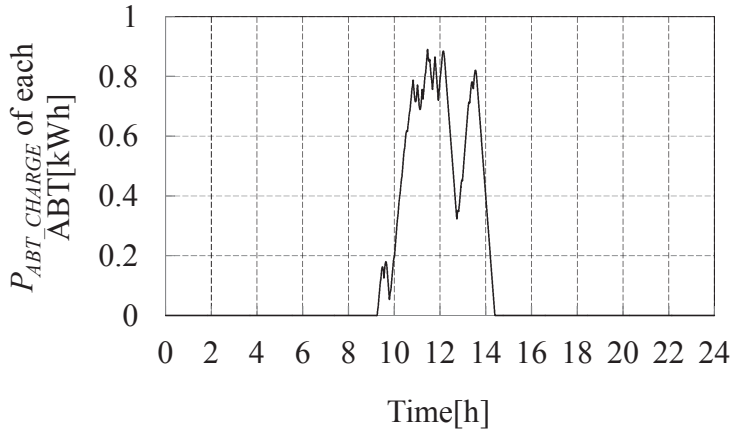

(a) Charge power of each ABT

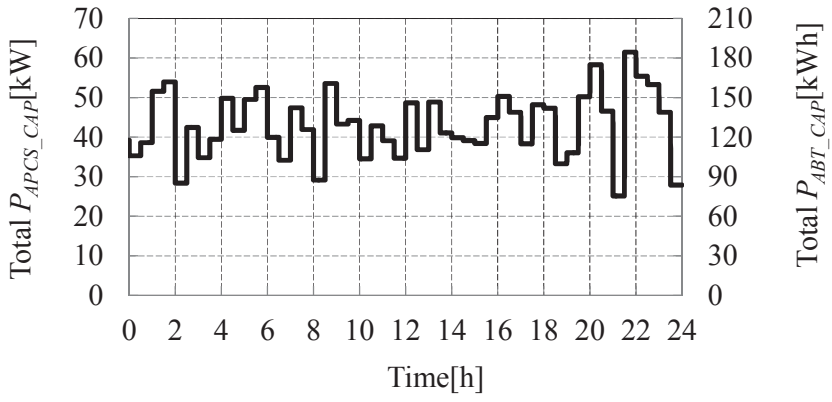

(b) Amount of ABTs and APCSs

Figure 4.28 Conditions of ABTs.

(5) Comparison of the results

Table 4.5 shows simulation results in case 1 ~ 4 evaluated using indices denoted in 4.4.6. Table 4.5 shows that *VD* in case 4 is greatly small and N_{SVR} is also small compared to other cases. Furthermore, in case 4, V_{MAX_sim} and V_{MIN_sim} do not largely deviate from the adequate range. Accordingly, it is confirmed that the proposed method can properly manage voltage as well as avoiding user's disadvantages using SVR with time delay and small ABTs provided by users.

Table 4.5 Comparison of results for 4 cases.

Case	1	2	3	4
VD	0.0Vs	669.2Vs	51.1Vs	0.8Vs
N_{SVR}	2	2	42	8
V_{MAX_sim}	106.3V	107.0V	106.8V	106.5V
V_{MIN_sim}	101.2V	101.3V	100.5V	100.9V

4.5 Discussion and summary

In this chapter, a novel method for voltage control using small BTs with SVR was developed. This is because it might be difficult to manage voltage using only SVR with low function when a large amount of PVs are introduced to DS in future. Through numerical simulation, it is confirmed that the proposed strategy can properly manage voltage controlling SVR with time delay and small BTs provided from users. In addition, because BTs controlled by the proposed method can suppress voltage fluctuation due to PV, the switching operation of SVR with deterioration and corresponding increase of maintenance cost can be restricted. Moreover, most part of BTs can be used by users since the proposed strategy uses only a part of use's BTs. The proposed method shows high user-friendliness. This is also the advantage of the proposed strategy.

This research assumes that sending voltage in distribution substation is constant. Hence, it is necessary to verify the feasibility and effectiveness of the proposed strategy considering fluctuation of sending voltage in substation. Furthermore, because a lot of voltage control methods using reactive power of PCS have been proposed in this field, it is important to compare these methods with the proposed strategy in order to confirm superiority of our work. Considering coordination of the proposed method with surplus power control using BT, above issues are scheduled to conduct a detailed study in future.

4.6 References

[1] Masaaki Takagi, Hiromi Yamamoto, Kenji Yamaji, Kunihiko Okano, Ryouji Hiwatari, and Tomohiko Ikeya, “Load Frequency Control Method by Charge Control for Plug-in Hybrid Electric Veicles with LFC Signal”, IEEJ Transactions on Power and Energy, Vol. 129, No. 11, pp. 1342-1348, 2009 (in Japanese)

[2] Koichiro Shimizu, Taisuke Masuta, Yutaka Ota, and Akihiko Yokoyama, “SOC Synchronization Control Method of Electric Vehicles Considering Customers’ Convenience for Suppression of System Frequency Fluctuation”, IEEJ Transactions on Power and Energy, Vol. 132, No. 1, pp. 57-64, 2012 (in Japanese)

[3] Takao Tsuji, Takuhei Hashiguchi, Tadahiro Goda, Takao Shinji, and Shinsuke Tsujita, “A Study of Autonomous Decentralized Voltage Profile Control Method considering Control Priority in Future Distribution Network”, IEEJ Transactions on Power and Energy, Vol. 129, No. 12 pp. 1533-1545, 2009 (in Japanese)

[4] Takao Tsuji, Tsutomu Oyama, Takuhei Hashiguchi, Tadahiro Goda, Takao Shinji, and Shinsuke Tsujita, “A Study of Autonomous Decentralized Voltage Profile Control Method considering Power Loss Reduction in Distribution Network”, IEEJ Transactions on Power and Energy, Vol. 130, No. 11 pp. 941-954, 2010 (in Japanese)

[5] Akira Koide, Takao Tsuji, Tsutomu Oyama, Takuhei Hashiguchi, Tadahiro Goda, Takao Shinji, and Shinsuke Tsujita, “A Study on Real-Time Pricing Method of Rective Power in Voltage Control Method of Future Distribution Network”, IEEJ Transactions on Power and Energy, Vol. 132, No. 4 pp. 359-370, 2012 (in Japanese)

[6] Shengnan Shao, Manisa Pipattanasomporn, and Saifur Rahman, “Demand Response as a Load Shaping Tool in an Intelligent Grid With Electric Vehicles”, IEEE Transactions on Smart Grid, Vol. 2, No. 4, pp. 624-631, 2011

[7] Hanne Saele, and Ove S. Grande, “Demand Response From Household Customers: Experiences From a Pilot Study in Norway”, IEEE Transactions on Smart Grid, Vol. 2, No. 1, pp. 102-109, 2011

[8] Johanna L. Mathieu, Phillip N. Price, Sila Kiliccote, and Mary Ann Piette, “Quantifying Changes in Building Electricity Use, With Application to Demand Response”, IEEE Transactions on Smart Grid, Vol. 2, No. 3, pp. 507-518, 2011

[9] Eric Sortomme, and Mohamed A. El-Sharkawi, “Optimal Charging Strategies for Unidirectional Vehicle-to-Grid”, IEEE Transactions on Smart Grid, Vol. 2, No. 1, pp. 131-138, 2011

[10] Eric Sortomme, and Mohamed A. El-Sharkawi, “Optimal Combined Bidding of Vehicle-to-Grid Ancillary Services”, IEEE Transactions on Smart Grid, Vol. 3, No. 1, pp. 70-79, 2012

Chapter 5
Reactive power management for voltage control considering transmission system

5.1 Introduction

In previous chapters, novel approaches for voltage regulation in DS have been presented. Though sending voltage in distribution substation V_{send} in previous chapters are set as constant value for simplicity, actual V_{send} is fluctuated due to an impact of Transmission System (TS). In a similar way, many researches for managing voltage fluctuated by PV have been done in literatures [1] ~ [8]. These literatures also assume that a primary node of distribution substation is an infinite bus. Voltage on TS is conventionally kept within the allowable range by the operation of transformers in upper substations and distributed phase modifying facilities in TS. Therefore, voltage fluctuation at primary nodes of distribution substations have been considered small, and transformers in distribution substations have been controlled based on local information and V_{send} have been properly managed.

However, introducing a large amount of PVs may change above situation, because power flow on the transmission lines becomes complex due to PV interconnection. In order to properly manage voltage on the power system in that case, it becomes necessary to control voltage considering the impact of PV on TS. Although several researches considering voltage behavior in TS have been done in literatures [8] [9], TS has been abbreviated to a node or modeled as simple line. For more detail investigation on the impact of PV in DS to TS, in this chapter, a power system including TS and DSs is proposed as a bench mark model using a part of a standard power system model provided by the Institute of Electrical Engineering of Japan (IEEJ). The model provided from IEEJ includes 66kV TS and 6.6kV distribution substations, which is for reliability analysis. The standard model is modified for analyzing the voltage behavior in TS assuming PV interconnection in DS. Based on the analysis using the model, a voltage control strategy suitable for PV interconnection is proposed. The effectiveness and feasibility of this approach are verified through numerical simulations.

This chapter organizes as follows. In section 5.2, the proposed 66kV model is represented in detail and analysis about voltage fluctuation caused by PV is done considering not only DS but also TS. In section 5.3, a control method for SVC to suppress voltage fluctuation in 66kV TS model is explained and the effectiveness of the proposed strategy is verified through the numerical simulation. In section 5.4, a summary of this chapter is made.

5.2 Modeling of 66kV system

5.2.1 Standard power system model of IEEJ

As an analytical model for reliability evaluation of TS (66kV ~ 77kV), IEEJ provides "Regional supply system model". The model consists of following three types.

I. "Overhead wire system including small hydro power plant"
II. "Underground line system assuming offices of city"
III. "Overhead lines and underground lines including industrial area"

In this chapter, a model of the third type "overhead lines and underground lines including industrial area" is employed. This model has been constructed based on actual data of 66kV system in an urban area, and transmission lines consists of overhead lines and underground lines as shown in Figure 5.1 (For more detail, see Appendices A5). There are five areas in this standard model and each area is separated from others through switching stations. One area with gray color in Figure 5.1 is extracted as "66kV system model" for analysis as shown in Figure 5.2. Figure 5.2 shows the extracted model assigned node number.

In Figure 5.2, black circle at node #1 represents an upper system (154kV) that is a slack node (voltage: 1.0pu) for power flow calculation. Node #2 ~ #11 shows the substation for transformation from 154kV to 66kV.. Thick gray lines in Figure 5.2 show principal buses. Symbols of transformers represent substations, and transformers at subsequent nodes of #18 are distribution transformers. Transformers at node #2, 4, 5, 8, and 10 are for connecting 66kV system with 154kV system. Loads at nodes except in distribution systems are special high voltage customers.

5.2.2 Distribution system model

In order to analyze 66kV system model including DS, it is necessary to embed the DS models into the secondary nodes of distribution substations. In general, a distribution substation has several DSs and hence a large model is required if many nodes are connected to 66kV system model. This increases a calculation load. Therefore, for simplicity, the feeders in a DS connected to a distribution substation are aggregated to one feeder connected to a secondary node of distribution substation. For example, nodes on a feeder connected to a distribution substation at node #19 are shown in Figure 5.3. A DS (node #211 ~ #220) whose capacity is 3.18MVA is connected to node #19 and other DSs connected to node #19 are aggregated to node #19. Model parameters of DS are shown on Table 5.1.

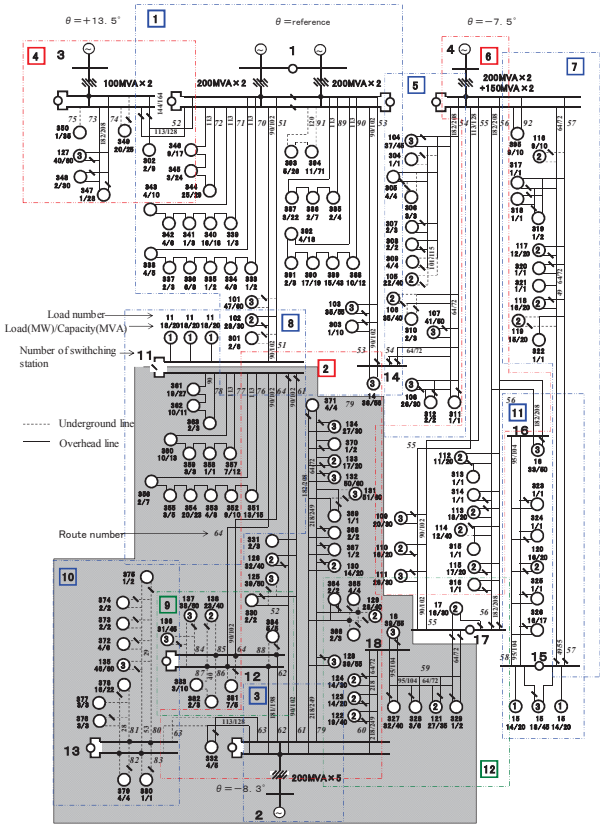

Figure 5.1 Basic model provided by IEEJ.

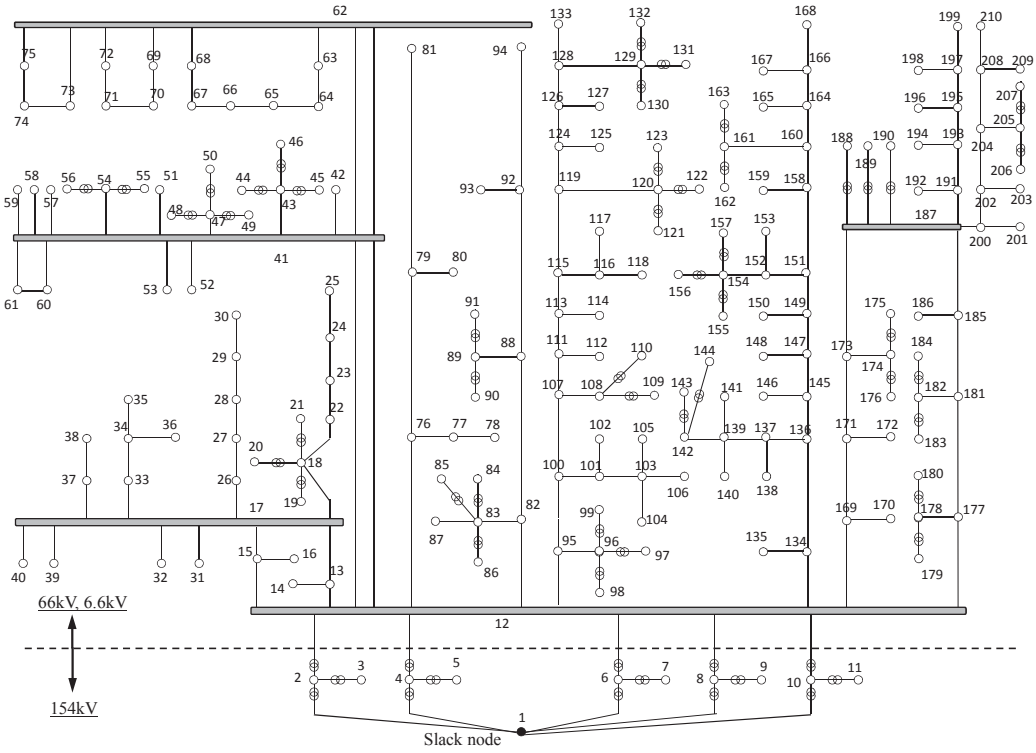

Figure 5.2 66kV system model including distribution systems.

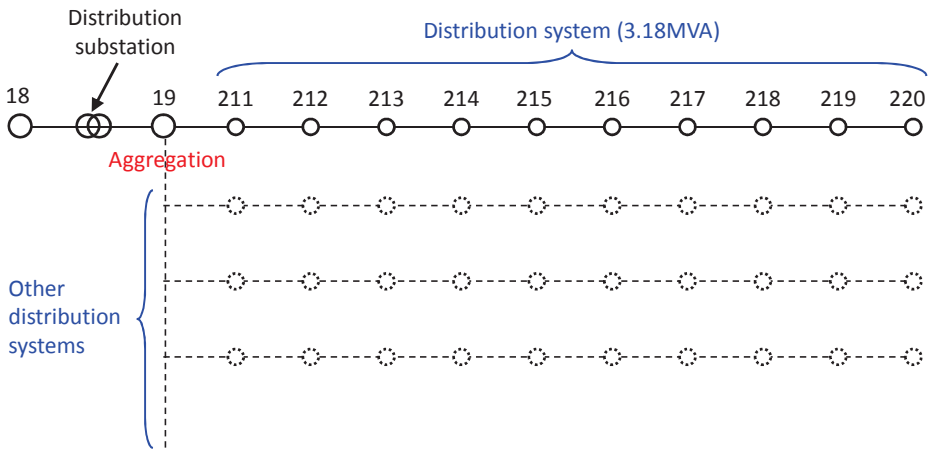

Figure 5.3 Distribution system model connected to node #19.

Table 5.1 Distribution system model parameters (Three-phase 10MVA base)

Node #(upper)	19	211	212	213	214	215	215	217	218	219	Total
Node #(lower)	211	212	213	214	215	215	217	218	219	220	
%R	0.443	0.805	0.921	1.012	1.201	1.384	1.507	1.749	2.098	3.740	14.95
%X	1.095	1.977	2.142	2.145	2.213	2.259	2.345	2.348	2.424	2.739	21.59
Load[pu] (at lower node)	0.007	0.022	0.031	0.040	0.037	0.040	0.040	0.040	0.037	0.025	0.318

Connecting DSs to distribution substations, the maximum node number increases to 660 (TS 210 + DS 10*45). Parameters in Table 5.1 are determined based on actual DS data in an urban area. It is assumed that all DSs in this 66kV system model have same parameters shown on Table 5.1. Since the base power in the standard power system model of IEEJ is 10MVA, parameters on Table 5.1 are also represented as per-unit (pu) value based on the base power. Figure 5.4 shows 66kV system and 6.6kV systems. In Figure 5.4, dotted lines represent distribution systems.

5.2.3 Parameter settings

(1) Setting of loads

Power factor of Loads in the standard model of IEEJ is set as lagging. However, the current power factor of load is improved due to power electronics technology, and Static Capacitor (SC) installed in a high voltage customer makes the power factor in DS close to 1.0 under both heavy and light load [11]. Since an investigation using an actual power factor is necessary for precise analysis, the power factor of loads connected to DSs are set as 1.0 assuming heavy load in this chapter. Special high voltage customers and phase modifying equipment are set as same as the standard model from IEEJ.

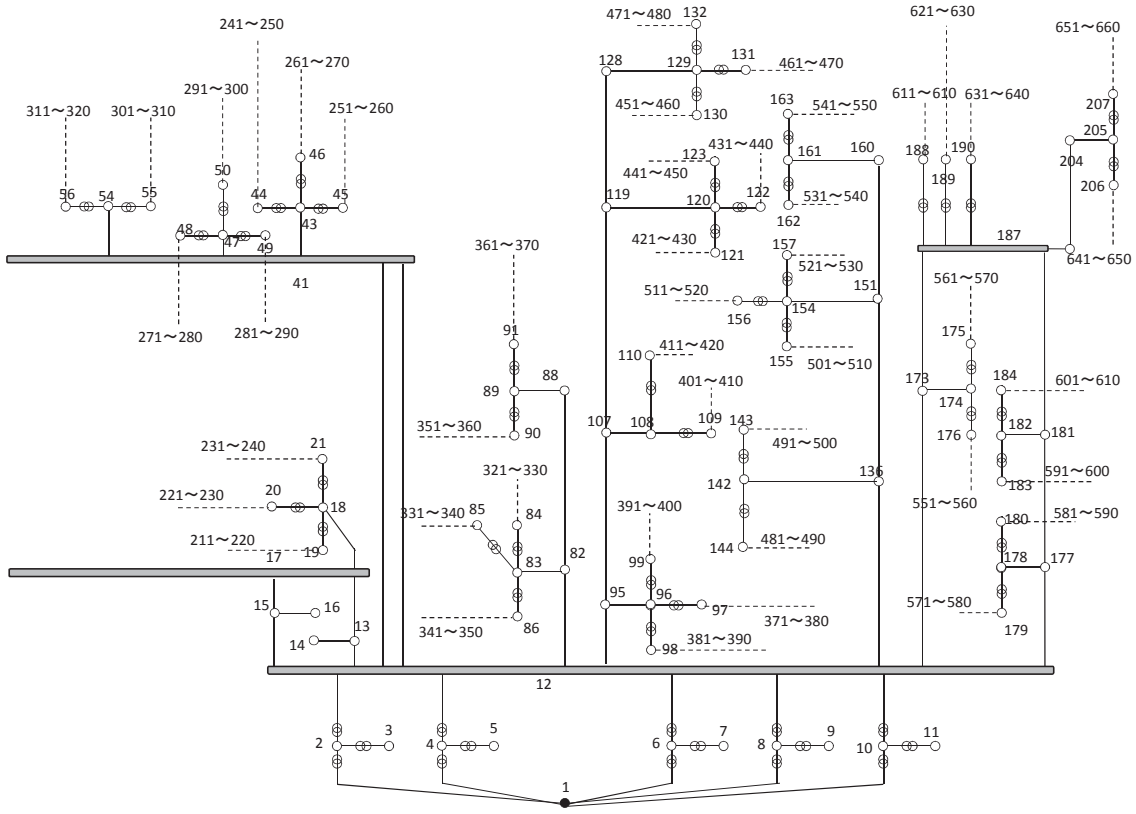

Figure 5.4 Distribution systems connected to distribution substations.

(2) Setting of transformers

The turn ratio of transformers in node #2 ~ #11 is set as 66000/154000 (secondary/primary). On the other hand, LRT in distribution substation can change its tap ratio from 6000/66000 ~ 7200/66000, and the number of taps is 17 based on standard model from IEEJ. Assuming LRT operates based on a dead band, the dead band is set as from 0.985pu to 1.015pu. LRT changes its tap position if the secondary voltage of LRT deviates from the dead band.

(3) Setting of phase modifying equipments

In order to regulate voltage on TS, Transmission System Operator (TSO) has usually installed phase modifying equipments such as SC and Shunt Reactor (SR) in TS. The model of IEEJ also has multiple SCs at node # 3, 5, 7, 9, 11, 120, 129, 161, 174, and 187. The number of SCs and those nodes in the model are set as same as the standard model of IEEJ. Parameters of the model used in this chapter are shown in Table 5.2.

Table 5.2 Model parameters.

Power factor of loads		
Special high voltage customers		Based on IEEJ model
Customers in DS		1.0
Transformers (secondary/primary)		
Turn ratio	Node #2 ~ #12	66000/154000 (constant)
	Distribution substations	6000/66000 ~ 7200/66000 (17taps)
Width of a tap	Distribution substations	0.107 pu
Phase modifying equipment		
SC		# 3, 5, 7, 9, 11, 120, 129, 161, 174, 187
SR		Non

5.3 Voltage violation in TS due to PV

In order to investigate an impact of PV on TS, a numerical simulation using 66kV system model shown in Figure 5.4 is executed. Voltage is calculated using a power flow calculation.

5.3.1 Voltage profile without PV

Figure 5.5 shows voltage profile of 66kV system model under heavy load condition and without PV. Vertical and horizontal axes in Figure 5.5 represent voltage and the node number, respectively. Since this model has different voltage levels (154kV, 66kV, 6.6kV), voltage is represented using pu representation. Nodes #1 ~ #210 are 66kV system and secondary nodes of distribution substation. Nodes #211 ~ #660 are DS. In Figure 5.5, V_{send} of distribution substation is controlled within 1.00±0.015 pu by the operation of LRT using the dead band.

5.3.2 Voltage profile with PV

(1) Simulation conditions

In this chapter, PVs are installed in DS not in TS. Each capacity of PV introduced into a node is set as 40% compared with the load capacity at a corresponding node. Each output of PV is in proportion to solar radiation and solar radiation is fluctuated in each area shown in Figure 5.6.

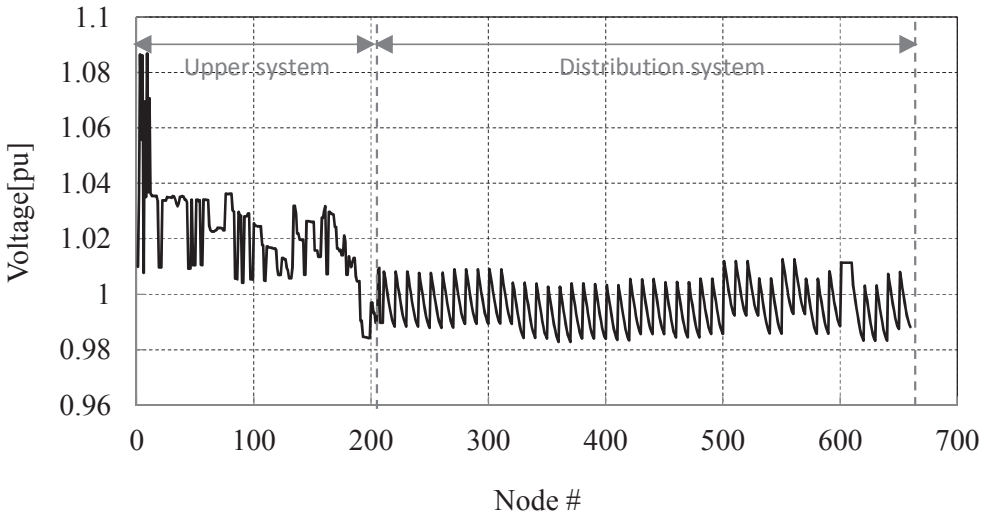

Figure 5.5 Voltage profile (Heavy load).

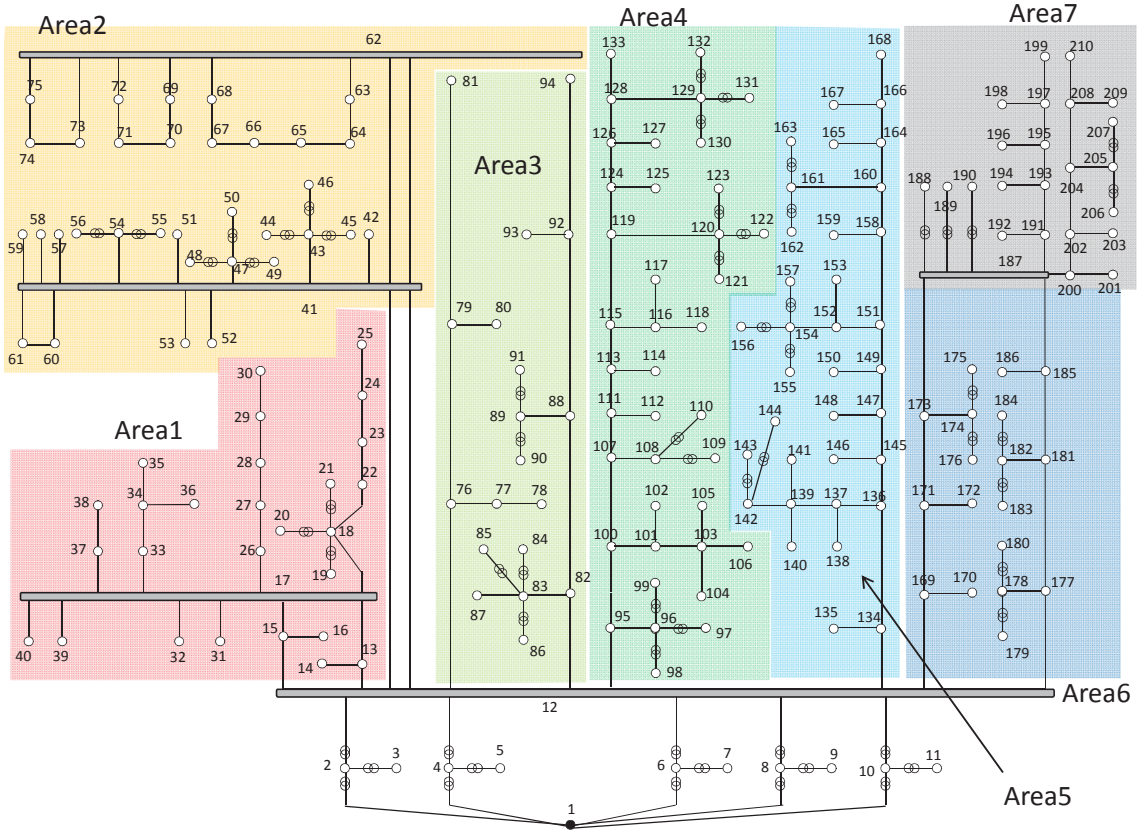

Figure 5.6 Division of power system.

PV generates 20% and 80% active power of each capacity under cloudy and sunny condition, respectively. Therefore, PVs at node #*i* generate 8% active power against the maximum load at node #*i* under cloudy condition. On the other hand, uner sunny condition, PVs at node #*i* generate 32% active

power against the maximum load at node #*i*. Solar radiation conditions are shown on Table 5.3. While all PVs generate 80% active power in case 1, all areas are gradually divided according to the conditions of sunny and cloud in case 2 ~ 8.

PCS is installed for interconnection of PV to a power system for each PV. PCS can output reactive power to reduce voltage rising due to PV. In this simulation, PCS output is controlled to maintain constant Power Factor (PF), which is set as the maximum value 1.0 in case 1 ~ 8, the minimum value 0.90 in case 9 ~ 15.

Table 5.3 Solar radiation conditions.

Case	Sunny	Cloudy	PCS
1 (Base case)	Area #1~7	—	PF: 1.0
2	Area #1~5	Area #7	
3	Area #1~5	Area #6,7	
4	Area #1~4	Area #5~7	
5	Area #1~3	Area #4~7	
5	Area #1,2	Area #3~7	
7	Area #1	Area #2~7	
8	—	Area #1~7	
9 (Base case)	Area #1~7	—	PF: 0.9
10	Area #1~5	Area #7	
11	Area #1~5	Area #6,7	
12	Area #1~4	Area #5~7	
13	Area #1~3	Area #4~7	
14	Area #1,2	Area #3~7	
15	Area #1	Area #2~7	
15	—	Area #1~7	

(2) PCS with PF 1.0

In order to investigate the amount of voltage violation due to PV, voltage behavior without LRT operation is simulated. Simulation results are shown in Figure 5.7. In Figure 5.7, (a) shows 154kV system, 66kV system, secondary nodes of distribution substations, and (b) shows 6.6kV systems. Vertical axes in Figure 5.7 represent voltage difference from case 1. The difference value represents the amount of voltage drop due to the decrease of solar radiation. In Figure 5.7, voltage gradually decreases with increasing cloudy area, and voltage in DS changes at most more than 0.025pu. On the other hand, V_{send} of distribution substations changes more than 2.0%. Since LRT generally changes its tap position based on V_{send}, the fluctuation of V_{send} causes the frequent switching operation of LRT.

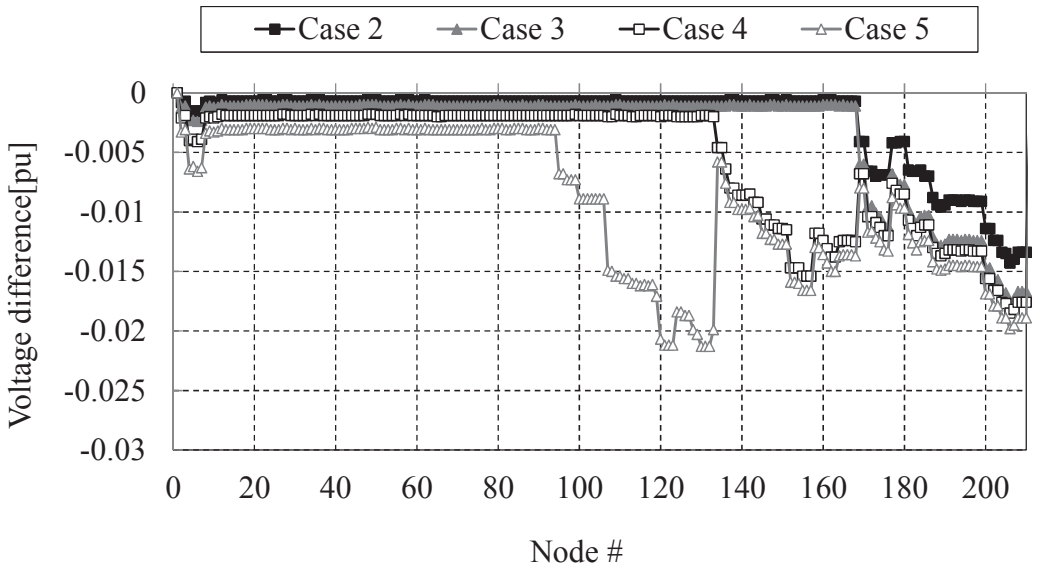

(a) Case 2 ~ 5

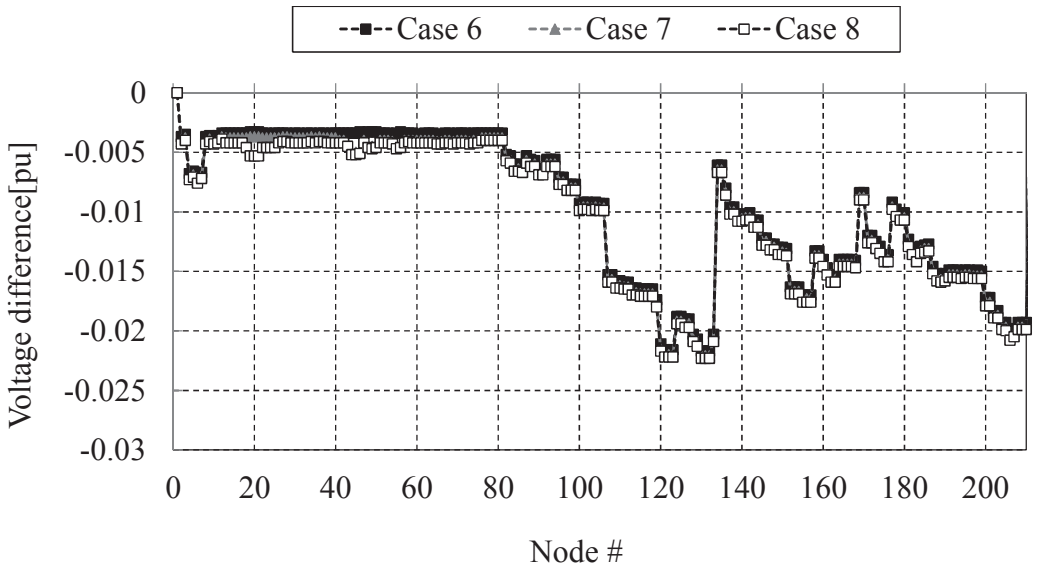

(b) Case 6 ~ 8

Figure 5.7 Voltage fluctuation by PV on upper system (PF=1.00).

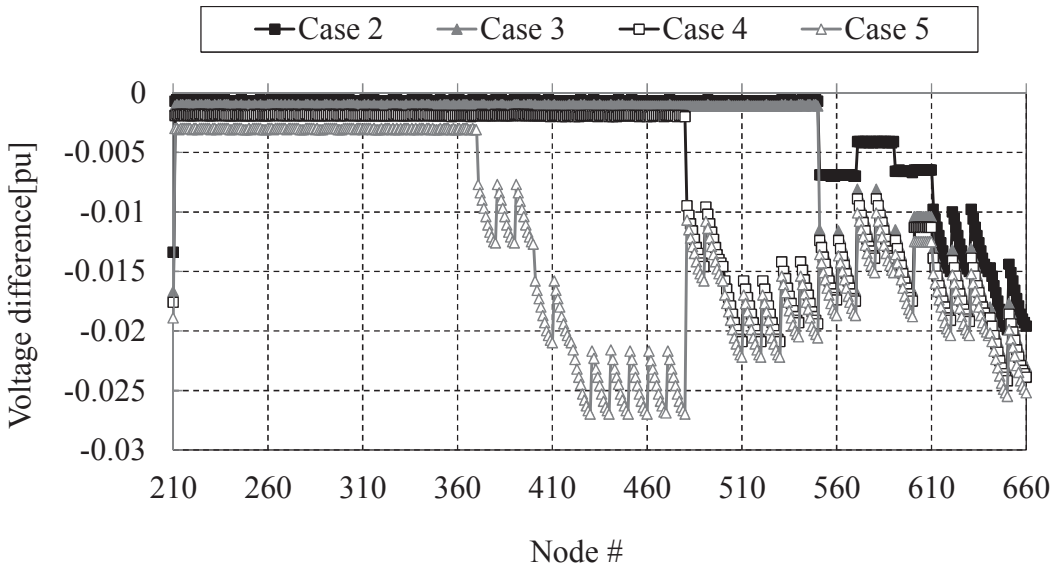

(a) Case 2 ~ 5

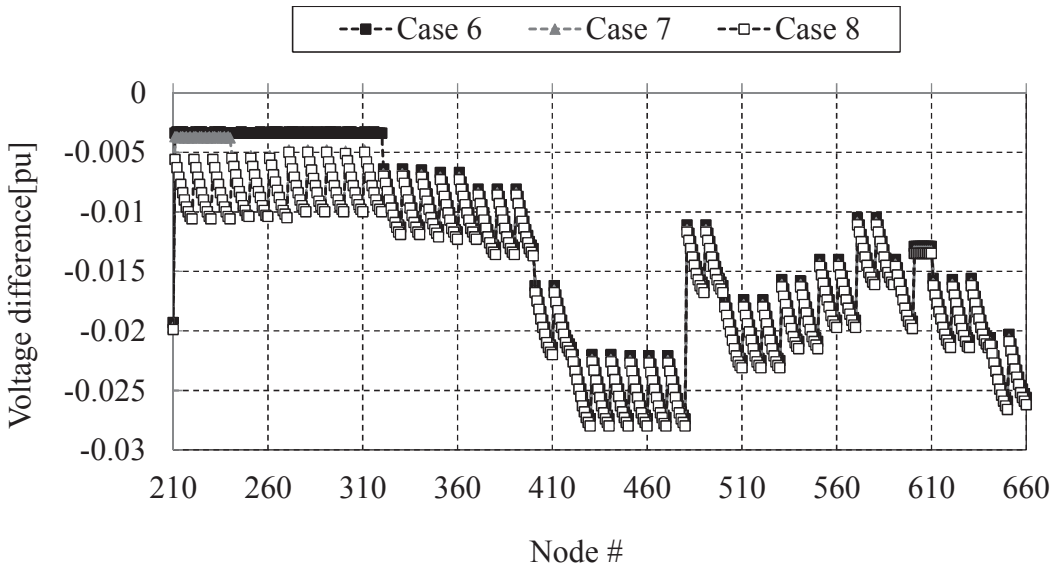

(b) Case 6 ~ 8

Figure 5.8 Voltage fluctuation by PV on distribution system (PF=1.00).

(3) PCS with PF 0.90

Figure 5.9 shows simulation results when PF of PCS is 0.90. Voltage fluctuation in Figure 5.9 and 5.10 are smaller than ones in Figure 5.7 and 5.8 due to leading PF of PCS. However, V_{send} (arrows points) in Figure 5.9 change at most 0.014pu. Although it is possible to reduce fluctuation of V_{send} as long as PF of PCS is properly set, implementing optimal PF into PCS is difficult since the optimal value is varied according to power system conditions.

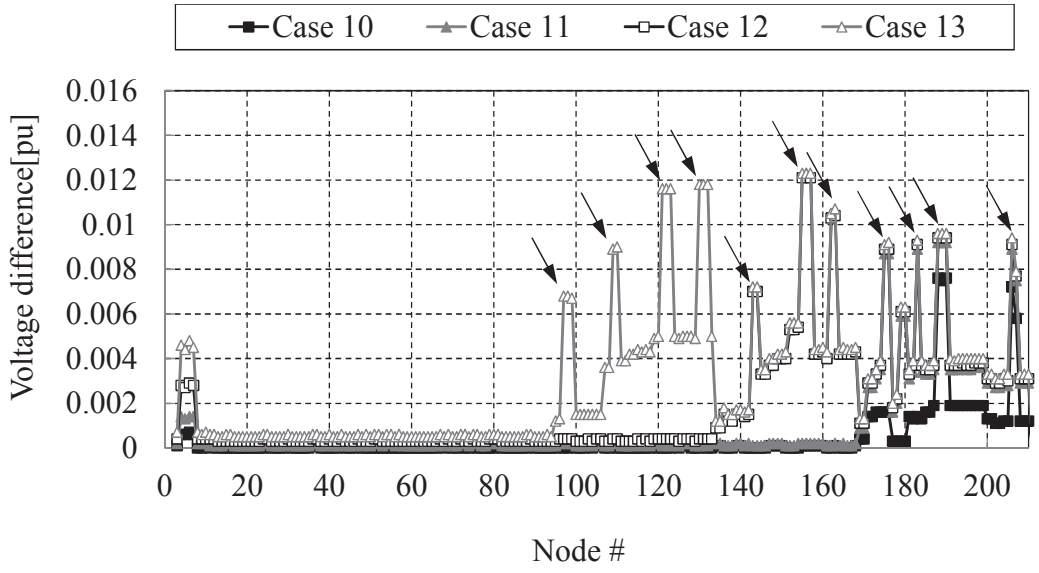

(a) Case 10 ~ 13

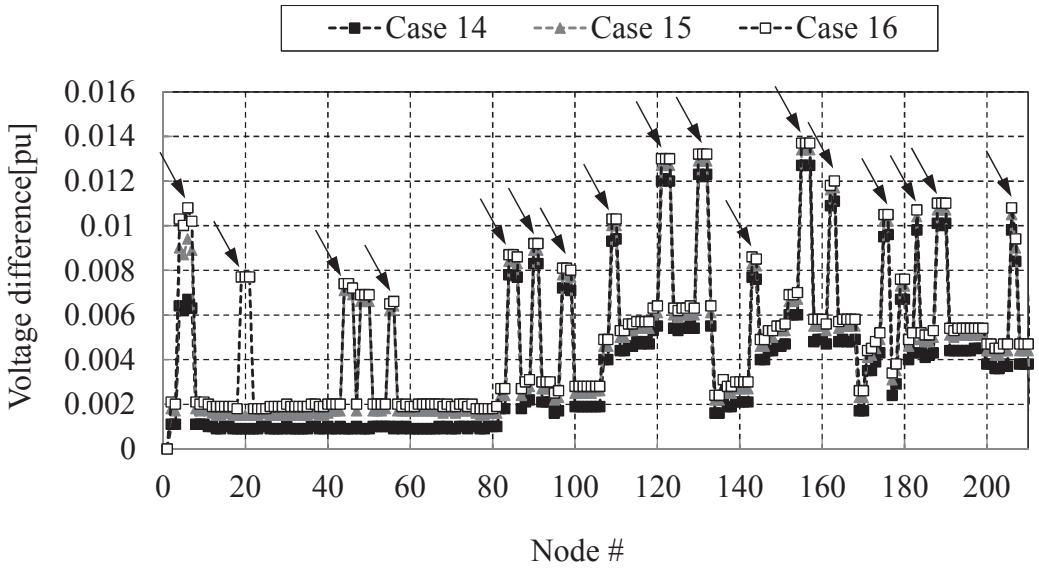

(b) Case 14 ~ 16

Figure 5.9 Voltage fluctuation by PV on the upper system (PF=0.90).

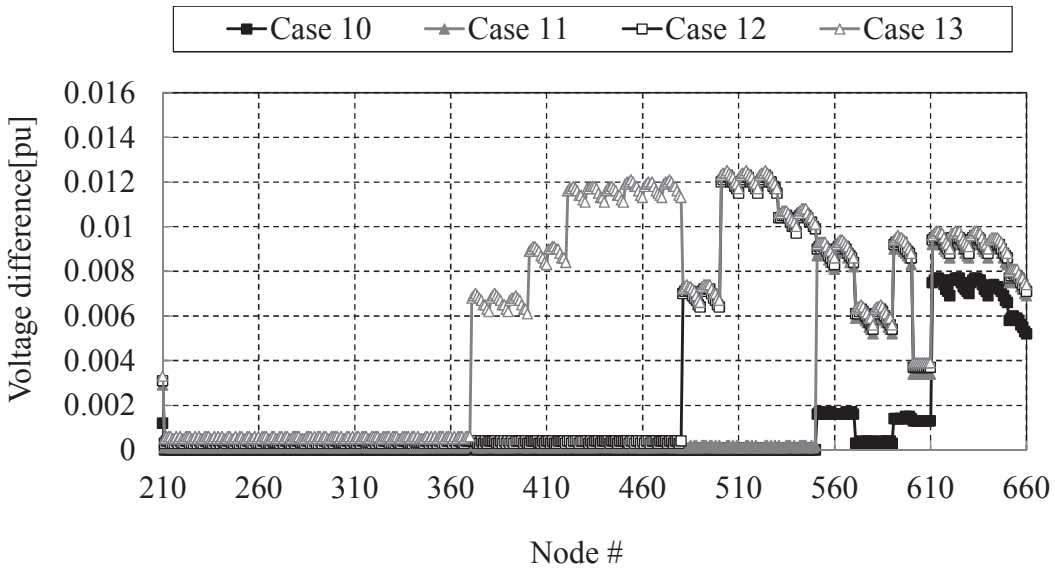

(a) Case 10 ~ 13

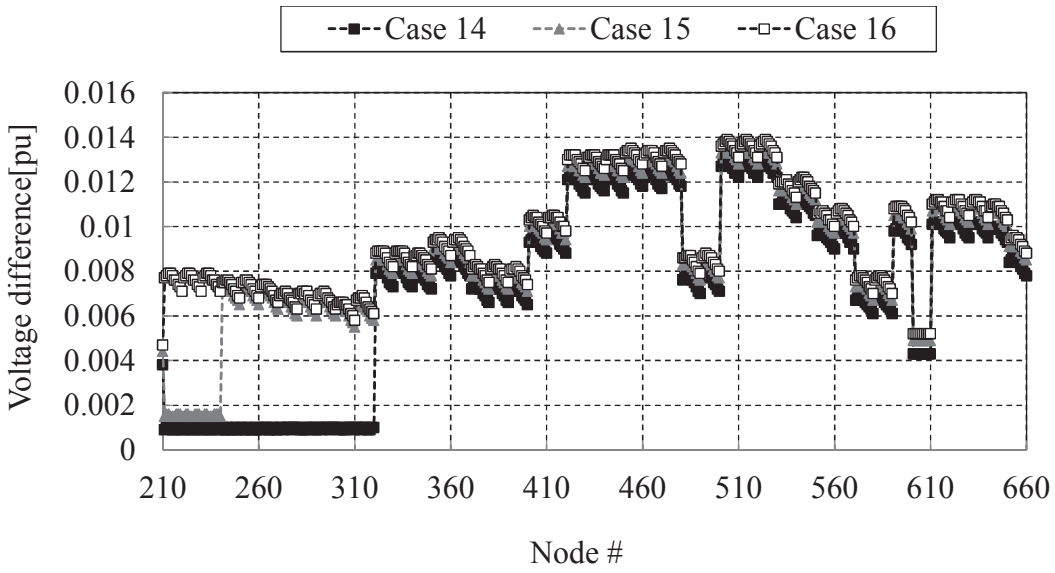

(b) Case 14 ~ 16

Figure 5.10 Voltage fluctuation by PV on the distribution systems (PF=0.90).

(4) Behavior of LRT in the distribution substations

In order to investigate the behavior of LRT corresponding to voltage fluctuation due to PV, LRT is controlled using the dead band and V_{send}. As an example, the switching operation of LRT controlled based on the dead band (1.00±0.015pu) is shown in Figure 5.11. The vertical axis in Figure 5.11 represents the tap ratio of LRT (secondary/primary) (pu), and the horizontal axis represents the case number. A Legend represents node numbers of LRTs (secondary nodes). In Figure 5.11, it can be seen that LRT operates corresponding to fluctuation of solar radiation. This result shows that fluctuation of solar radiation causes the frequent switching operation of LRT.

In Figure 5.11, it is also seen that LRT at node #207 (in area 7) changes its tap position in case 7 not in case 2. Since solar radiation in area 7 changes in case 2, voltage in area 7 largely changes and LRT tends to operate in that case. However, LRT at node #207 controls its tap position when solar radiation in distant area (in area 2) is changed. Voltage fluctuation due to solar radiation in an area leads to voltage fluctuation in other areas.

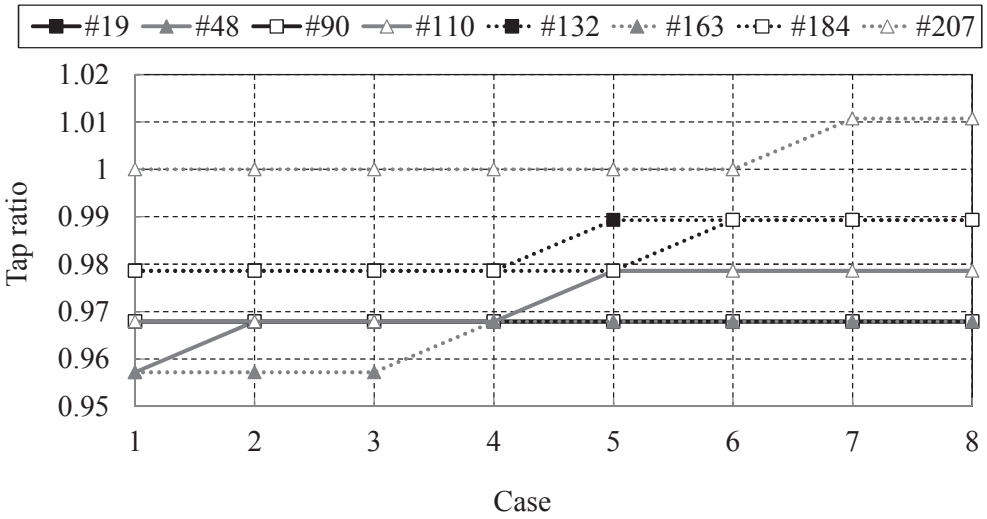

Figure 5.11 Switching operation of LRT due to PV (PF=1.00).

5.3.3 Coordinated operation in 66kV system

From above results, it can be seen that voltage in TS is largely changed corresponding to solar radiation. Fluctuation of solar radiation in each area causes voltage fluctuation not only in that area but also in distant other areas. Thus, PV makes power flow on transmission lines complex, and random voltage fluctuation is caused at each node. The random voltage fluctuation leads to the increase of operations for many LRTs. In that case, a conventional local control method for LRT is not suitable for proper voltage management. To prevent this problem, it is necessary to reduce voltage fluctuation due to PV on entire transmission lines. Considering power flows in the entire system, fluctuation of voltage on the transmission line can be suppressed, not locally at each point of transmission lines.

5.4 Coordinated control of SVC at 66kV system

5.4.1 Proposed strategy

To suppress voltage fluctuation due to PV on TS, a new control method of SVC is proposed. To do this, SVCs that can flexibility control reactive power are installed at primary nodes of distribution substations, and multiple SVCs are coordinately controlled to suppress voltage fluctuation on entire 66kV transmission lines. The proposed method is formulated as follows.

[Objective function]

$$F_i = \sum_{j=1}^{n} \omega_j \left| \Delta V_{ij} \right|^2 \rightarrow \min \tag{5.1}$$

Where

$$\Delta V_{ij} = \left(\frac{\partial V_j}{\partial P_i} \Delta P_i + \frac{\partial V_j}{\partial Q_i} \Delta Q_i \right) \tag{5.2}$$

i : Node number, n : Maximum number of nodes, ω : Weight coefficient

ΔV_{ij} : Voltage fluctuation at node #j due to power fluctuation at node #i

ΔP_i : Active power fluctuation at node #i

ΔQ_i : Reactive power fluctuation at node #i

Objective function F_i represents a goal to minimize voltage fluctuation at any nodes due to power fluctuation at node #i. Therefore, F_i aims to suppress voltage fluctuation on the entire system. Differentiating equation (5.1) with respect to ΔQ_i, following equations can be calculated.

$$\begin{aligned} \frac{\partial F_i}{\partial \Delta Q_i} &= 2 \sum_{j=1}^{n} \omega_j \left(\frac{\partial V_j}{\partial P_i} \Delta P_i + \frac{\partial V_j}{\partial Q_i} \Delta Q_i \right) \left(\frac{\partial V_j}{\partial Q_i} \right) \\ &= 0 \end{aligned} \tag{5.3}$$

$$\frac{\Delta Q_i}{\Delta P_i} = - \frac{\sum_{j=1}^{n} \omega_j \left(\frac{\partial V_j}{\partial P_i} \frac{\partial V_j}{\partial Q_i} \right)}{\sum_{j=1}^{n} \omega_j \left(\frac{\partial V_j}{\partial Q_i} \right)^2} \tag{5.4}$$

Equation (5.4) represents the optimal ratio between ΔQ_i and ΔP_i for minimizing voltage fluctuation on 66kV transmission lines due to ΔP_i. In the proposed strategy, controlling the output of SVC based on equation (5.4), it is possible to effectively reduce voltage fluctuation on TS.

5.4.2 Controller of SVC

A controller of SVC to realize the proposed algorithm is shown in Figure 5.12.

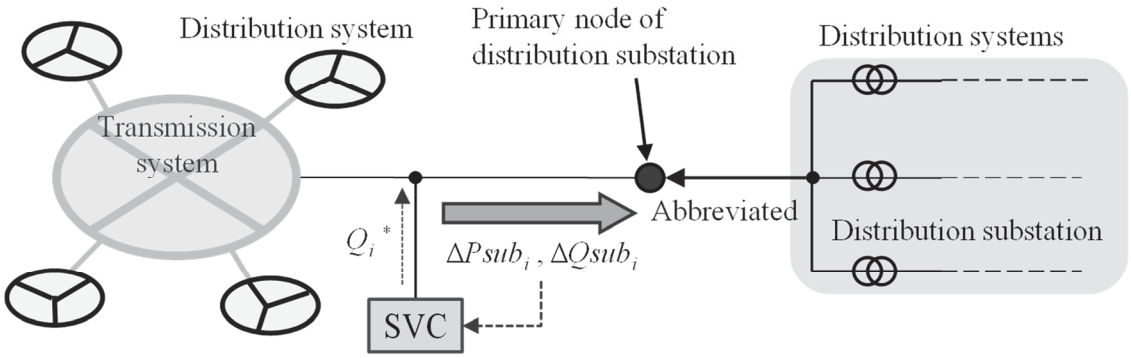

(a) Install point.

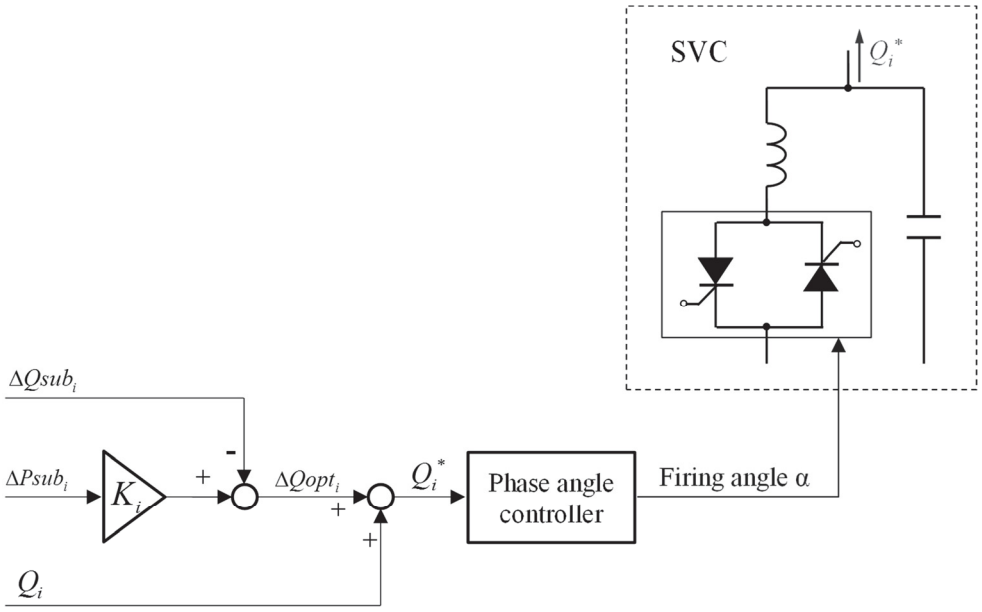

(b) Controller.

Figure 5.12 Control structure of SVC.

As shown in Figure 5.12 (a), a SVC installed at node #*i* has a sensor to monitor active and reactive power flowing through a distribution substation $Psub_i$ and $Qsub_i$. SVC observes fluctuation of these power $\Delta Psub_i$ and $\Delta Qsub_i$ in real time. Optimal fluctuation of its output $\Delta Qopt_i$ is calculated using following equation (Active power: consumption has positive value, generation has negative value. Reactive power:

lag has positive value, lead has negative value.).

$$\Delta Qopt_i = \frac{\Delta Q_i}{\Delta P_i} \Delta Pline_i - \Delta Qline_i \tag{5.5}$$

Second term of the right side in equation (5.5) is compensating for fluctuation of reactive power in DSs. Using equation (5.5), SVC can control the ratio of fluctuation between active and reactive power flowing to 66kV transmission system. Generally, though SVC determines a fire angle of thyristors based on a characteristic of slope reactance and voltage at PCC, the proposed method controls the output of SVC based on reference reactive power not voltage at PCC. Hence, as shown in Figure 5.11 (b), the fire angle is calculated based on reference reactive power using a phase angle controller. In this chapter, SVC can output reactive power corresponding to reference signal without time delay.

5.5 Case study

Under same conditions in section 5.3, a numerical simulation is executed to verify the effectiveness of the proposed method. SVCs are installed in primary nodes of all distribution substations and $\Delta Q_i/\Delta P_i$ is calculated using equation (5.4) when the output of PV is 80% against its capacity. All weight coefficient ω_i are set as 1.0 over whole 66kV system model.

5.5.1 PCS with PF 1.0

Figure 5.13 shows simulation results using PCS with PF 1.0. From Figure 5.13, it can be seen that voltage fluctuation on 66kV transmission system except for upper substation (Node #1 ~ #11) is suppressed up to ±0.002pu. The magnitude of voltage fluctuation on TS and DSs become about one-ten as much as in Figure 5.7 and 5.8.

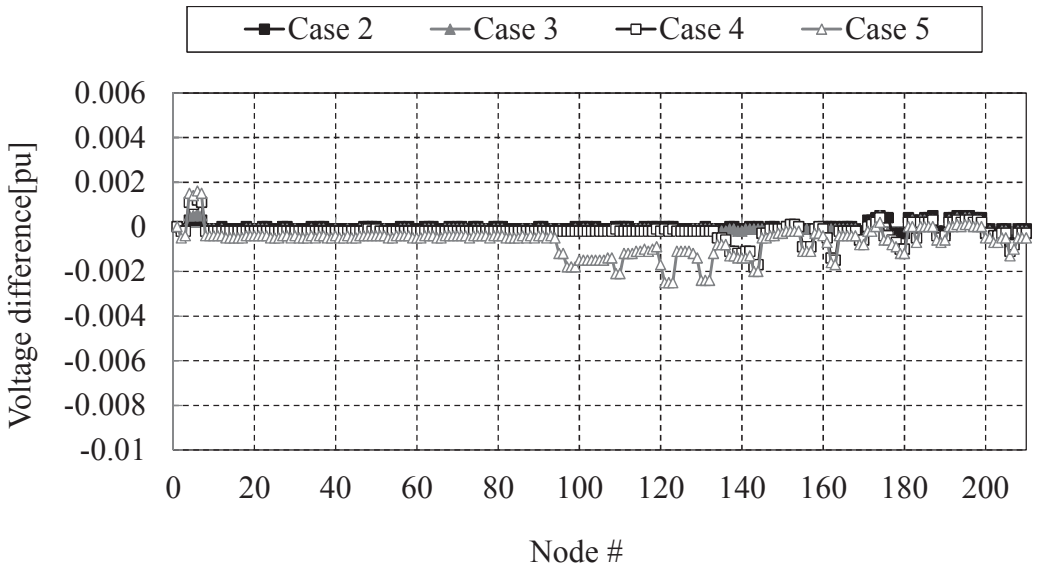

(a) Case 2 ~ 5

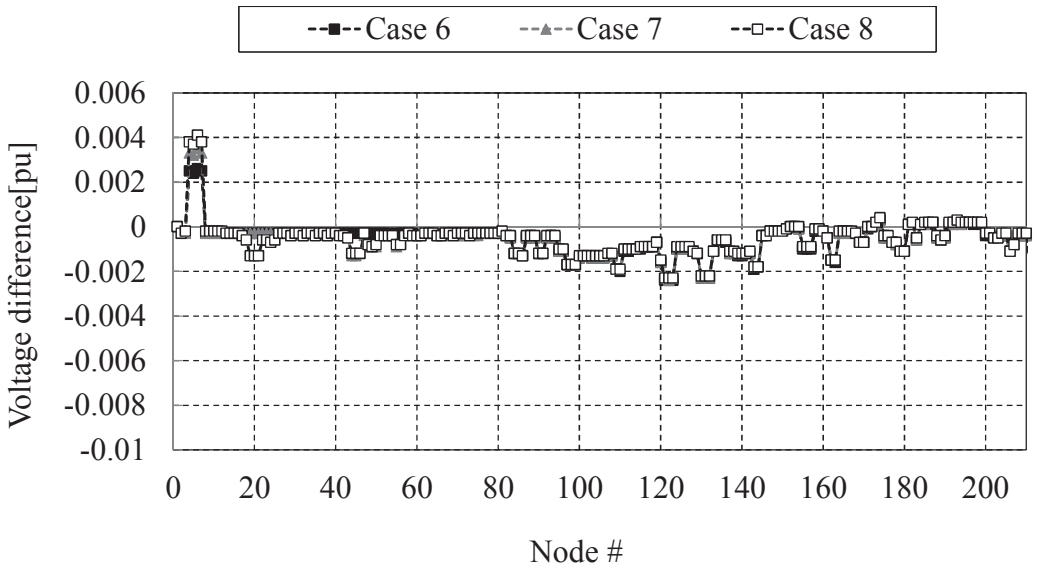

(b) Case 6 ~ 8

Figure 5.13 Voltage fluctuation by PV on upper system using the proposed method (PF=1.00).

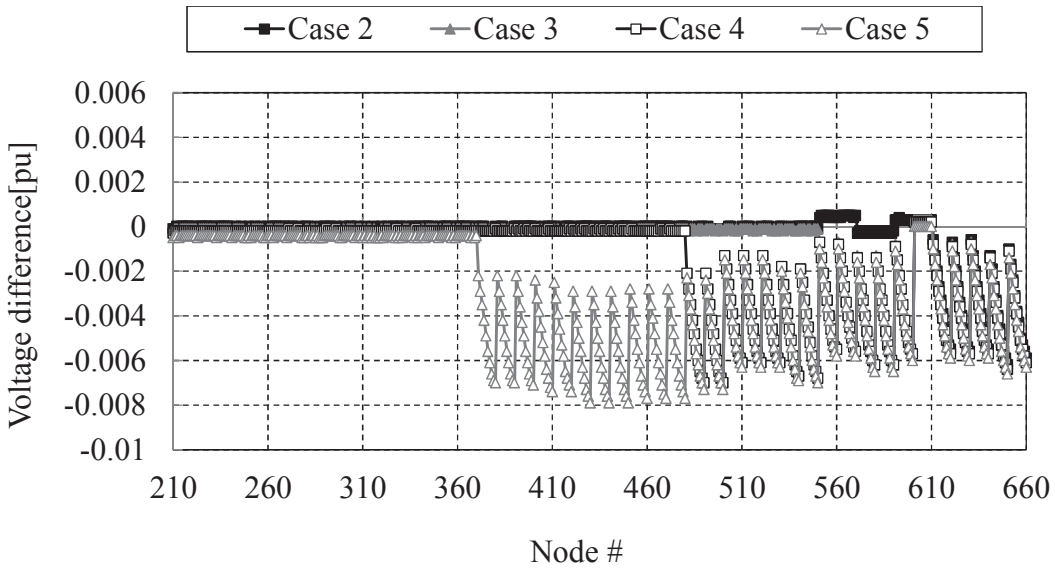

(a) Case 2 ~ 5

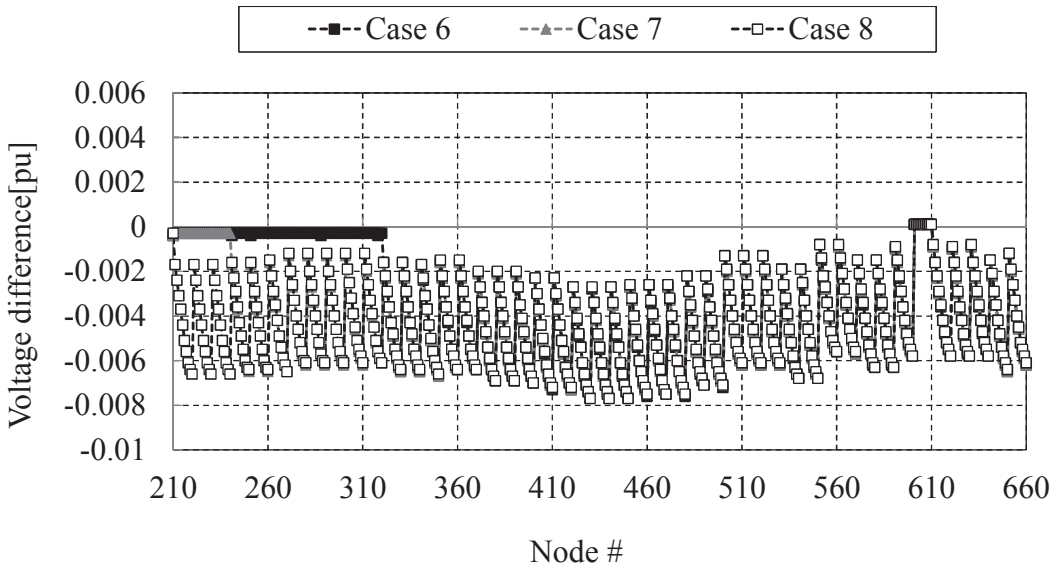

(b) Case 6 ~ 8

Figure 5.14 Voltage fluctuation by PV on DS using the proposed method (PF=1.00).

5.5.2 PCS with PF 0.90

As shown in Figure 5.15, voltage fluctuation due to PV is suppressed and is up to about ±0.002pu at 66kV transmission line. It is necessary to compensate for voltage fluctuation due to a distribution transformer and a distribution line using both LRT and SVR, because the proposed method cannot control power flow by a distribution transformer.

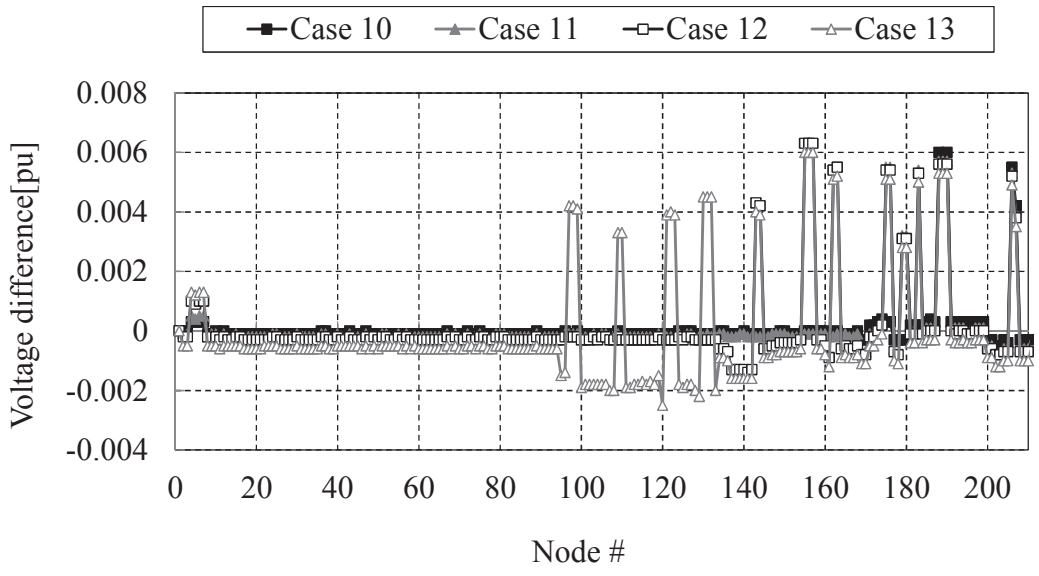

(a) Case 10 ~ 13

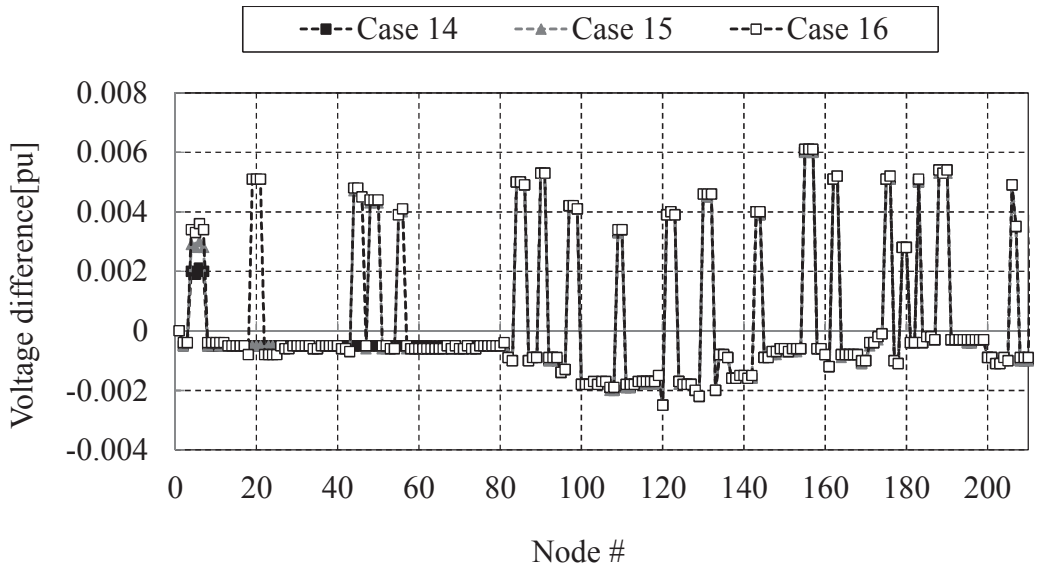

(b) Case 14 ~ 16

Figure 5.15 Voltage fluctuation by PV on upper system using the proposed method (PF=0.90).

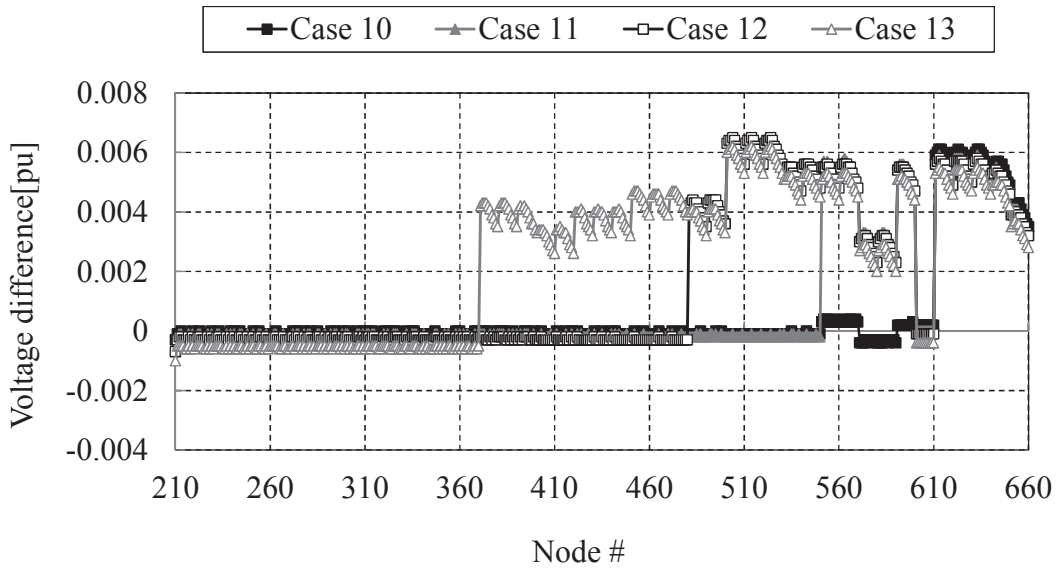

(a) Case 10 ~ 13

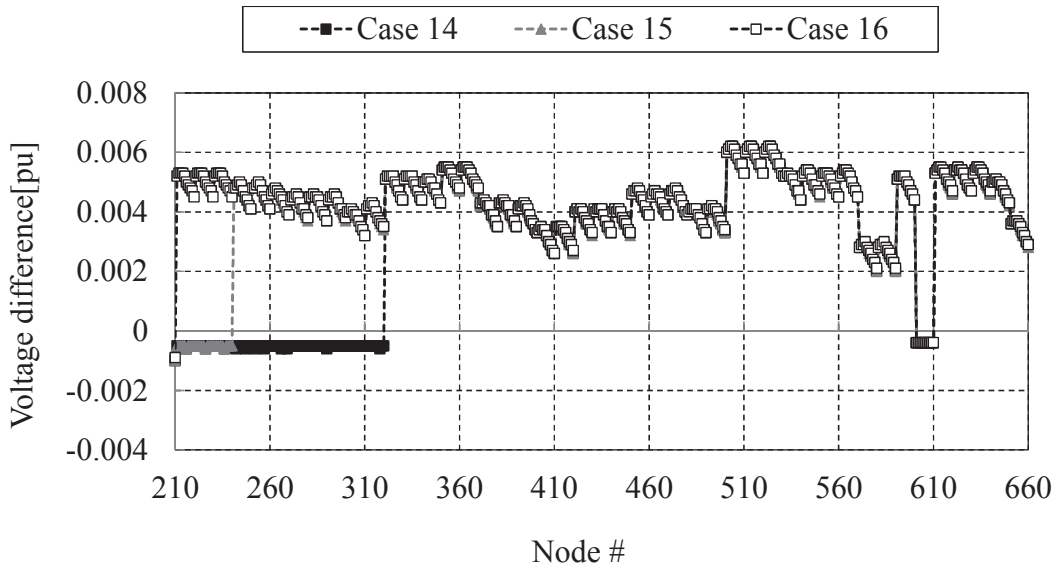

(b) Case 14 ~ 16

Figure 5.16 Voltage fluctuation by PV on DS using the proposed method (PF=0.90).

5.5.3 Behavior of LRT with the proposed method

In the same manner as section 5.3, the behavior of LRTs corresponding to the fluctuation of PV's output using the proposed approach is shown in Figure 5.17. In Figure 5.17, LRT does not change its tap position, and LRT is almost never affected by PV in other areas. From this result, it can be seen that the proposed method suppresses voltage fluctuation in entire 66kV transmission lines in a coordinated manner.

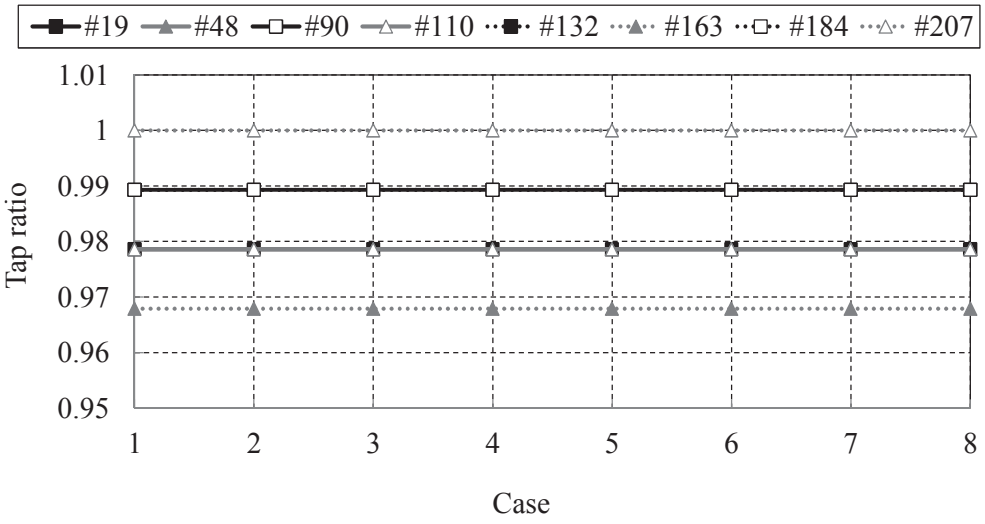

Figure 5.17 Switching operation of LRT due to PV using the proposed method (PF=1.00).

5.5.4 Advantages of the proposed method

(1) Communication cycle

The optimal output of SVC can be obtained using voltage sensitivity $\partial V/\partial P$ and $\partial V/\partial Q$ that are calculated by Jacobian matrix. Voltage magnitude and phase angle data from sensors in a power system are necessary to calculate Jacobian matrix. Considering that SVCs are installed at primary nodes of distribution substations, vital information for calculating Jacobian matrix are just voltage magnitude and phase angle on an upper system and secondary nodes of distribution substations (Node #2 ~ #210). Though time synchronization sensor such as PMU (Phasor Measurement Unit) is assumed to be used, SVC does not need real-time communication since SVC operates based on the local information $\Delta Psub_i$ and $\Delta Qsub_i$ until next communication.

(2) Superiority against active power control

Figure 5.18 shows $\Delta Q_i/\Delta P_i$ against PV output in heavy load. In Figure 5.18, vertical axis represents $\Delta Q_i/\Delta P_i$ at primary sides of distribution substations, and horizontal axis represents node number. From Figure 5.18, it can be seen that small reactive power is required comparing with active power since the amount of $\Delta Q_i/\Delta P_i$ is smaller than 1.0. Hence, it is effective to control reactive power than active power to suppress voltage fluctuation on 66kV transmission lines. The capacity of SVC required to control reactive

power is determined based on the capacity of PV and $\Delta Q_i/\Delta P_i$ at each node. In order to appropriately manage voltage, SVCs with the sufficient capacity should be installed in TS considering loads, PV, LRT, and other factors. In this chapter, for simplicity, the restriction of output by its capacity is not considered.

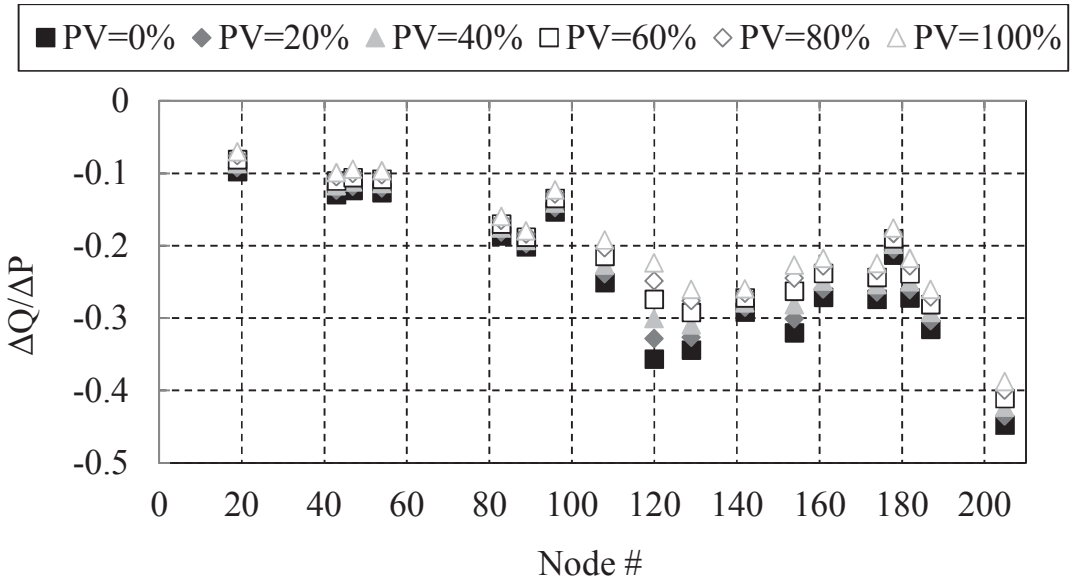

Figure 5.18 Optimal $\Delta Q/\Delta P$ at distribution substations.

(3) Small impact on power system

The output of SVC in the proposed approach does not rely on voltage magnitude but active/reactive power flow in distribution substation. Hence, SVC with the proposed method makes low impact on any other devices for voltage control. For example, SVC operated based on voltage changes its reactive power output corresponding to voltage fluctuation on the upper system (more than 154kV). As shown in Figure 5.11, fluctuation of power at each node makes adverse impact on any other nodes in 66kV system and this disturbance should be avoided for proper voltage management. Each SVC controlled using voltage arbitrarily responds to voltage fluctuation at each point and makes the adverse disturbance on the power system. On the other hand, SVC with the proposed method is not affected by voltage violation, and SVCs are operated in a coordinated manner to suppress voltage fluctuation due to PV. However, it might be necessary to compensate for load fluctuation using LRT to reduce the capacity of SVC because the proposed method suppresses voltage fluctuation due to not only PV but also load fluctuation.

(4) Reducing cost

To date, many researches for voltage control in DS using power electronics technologies have been presented in literatures [2] [4] [5] [6] [7] [8]. These literatures insist to introduce power electronics devices such as SVC into DS to avoid voltage violation due to DG. Introducing these facilities is difficult because

of cost. It is necessary to reduce introducing these high cost devices.

From results in this chapter, it was revealed that large voltage fluctuation due to PV is occurred in not DS but TS. Hence, it is not suitable to introduce high cost devices mentioned above into DS for voltage regulation. To more effectively control voltage, introducing above facilities to TS is better choice. If SVC is introduced to TS not DS, the number of SVC can be reduced compared with in DS because the number of distribution substations are smaller than DSs. Furthermore, SVC has better performance for voltage regulation if X/R of line is large. For reducing cost, a better install point for SVC is TS.

5.6 Discussion and summary

In this chapter, voltage fluctuation issue on 66kV transmission line that is expected to occur when a large amount of PVs are connected to DS has been focused and analyzed. From the analysis using 66kV transmission system model based on "Overhead lines and underground lines including industrial area" provided by IEEJ, it can be seen that it is necessary to coordinately suppress voltage fluctuation on entire transmission lines since voltage profile on 66kV transmission lines becomes complex and fluctuates randomly and largely due to PV. Hence, a novel control strategy using SVCs that are installed at primary nodes of distribution substations has been presented for coordinated control of voltage on 66kV transmission line. By executing numerical simulations, it can be seen that the proposed strategy shows good performance for reducing voltage fluctuation at 66kV transmission line. Though the proposed method requires system information obtained through periodic communication, SVC can operate based on local information (active/reactive power flowing through distribution substation) until next communication and real-time communication is not required. Also, since SVC operation in the proposed strategy does not depend on voltage magnitude in the power system, it is possible to reduce disturbance on voltage, and the proposed strategy is suitable for combination operation with other voltage control devices.

As a primary voltage of distribution substation can be controlled close to constant using the proposed method, voltage control methods in DS proposed in previous chapters and in [1] ~ [8] can be easily adopted. Although this chapter employs SVC, the proposed method can also apply for PCS control if information in DS can be monitored and power factor of each PCS can be controlled by remote. Results of this research show that the proposed strategy is useful for voltage regulation when a large amount of PVs are connected to DS.

5.7 References

[1] Yasuhiro Hayashi, “Trend and Future View of Voltage Control for Distribution System with Distributed Generators”, IEEJ Transactions on Power and Energy, Vol. 129, No. 4, pp. 491-494, 2009 (in Japanese)

[2] Taro Kondo, Jumpei Baba, Akihiko Yokoyama, “Voltage Control of Distribution Network with a Large Penetration of Photovoltaic Generations using FACTS Devices”, IEEJ Transactions on Power and Energy, Vol. 126, No. 3, pp. 347-358, 2006 (in Japanese)

[3] Junji Kondo, “Evaluation on Reduction of Output Suppression Loss by Cooperative Control of Voltage Profile in a Distribution System with a Large Amount of Photovoltaic Power Generation”, IEEJ Transactions on Power and Energy, Vol. 130, No. 11, pp. 981-988, 2010 (in Japanese)

[4] Takao Tsuji, Takuhei Hashiguchi, Tadahiro Goda, Takao Shinji, and Shinsuke Tsujita, “A Study of Autonomous Decentralized Voltage Profile Control Method considering Control Priority in Future Distribution Network”, IEEJ Transactions on Power and Energy, Vol. 129, No. 12 pp. 1533-1545, 2009 (in Japanese)

[5] Takao Tsuji, Tsutomu Oyama, Takuhei Hashiguchi, Tadahiro Goda, Takao Shinji, and Shinsuke Tsujita, “A Study of Autonomous Decentralized Voltage Profile Control Method considering Power Loss Reduction in Distribution Network”, IEEJ Transactions on Power and Energy, Vol. 130, No. 11 pp. 941-954, 2010 (in Japanese)

[6] Akira Koide, Takao Tsuji, Tsutomu Oyama, Takuhei Hashiguchi, Tadahiro Goda, Takao Shinji, and Shinsuke Tsujita, “A Study on Real-Time Pricing Method of Reactive Power in Voltage Control Method of Future Distribution Network”, IEEJ Transactions on Power and Energy, Vol. 132, No. 4 pp. 359-370, 2012 (in Japanese)

[7] Yasuhiro Hayashi, Junya Matsuki, Ryoji Suzuki, and Eiji Muto, “Determination Method for Optimal Sending Voltage Profile in Distribution System with Distributed Generators”, IEEJ Transactions on Power and Energy, Vol. 125, No. 9, pp.846-854, 2005 (in Japanese)

[8] Naoto Yorino, Takahiro Miki, Yuuki Yamato, Yoshifumi Zoka, and Hiroshi Sasaki, “A Time Scale Separation Method for the Coordination of Voltage Controls for SVC and SVR”, IEEJ Transactions on Power and Energy, Vol. 124, No. 7, pp. 913-919, 2004 (in Japanese)

[9]Masa-aki Ishimaru, Hideki Tamachi, and Shintaroh Komami, “Positive Effect of PV’s Constant Leading Power Factor Operation in Power System”, IEEJ Transactions on Power and Energy, Vol. 132, No. 7, pp. 615-622, 2012 (in Japanese)

[10] “Japanese Power System model”, IEEJ, HP: http://www2.iee.or.jp/ver2/pes/23-st_model/english/ 2013

[11] Technical committee for power factor problems in distribution network, “Power Factor Problems and Measures in Distribution Network”, Report of Electric Technology Research Association, Vol. 66, No. 1, Electric Technology Research Association, 2011 (in Japanese)

Chapter 6

Summary, conclusions and future research

6.1 Summary

This thesis has presented several techniques for improving voltage profile in DS complicated by a large amount of PVs interconnection. This research is initiated from a critical phase the Japanese power system faces. The number of PVs connecting into DS is increasing in Japan due to a policy of the Japanese government. However, current DS in Japan is not designed considering interconnection of DG, and DSO does not have sufficient ability to control voltage within an adequate range in this situation. Therefore, it is urgent that DSO takes the effect measures against the problem.

Multiple measures against above issues have been proposed to date using power electronics devises such as SVC. These devices are effective for controlling voltage. On the other hand, these devices are very costly and installing these devises into many DSs leads to huge additional cost. Hence, it is very important to properly manage voltage in DS without the additional costly devices. In this thesis, from the viewpoint of cost, voltage control strategies suitable for PV penetration have been proposed.

In chapter 2, a novel control method using existing SVR with low additional cost has been presented. Voltage fluctuation due to PV tends to be large in a DS with a long distribution line or heavy loads. This type of DS needs SVR to compensate voltage drop on the distribution line. Hence, in order to investigate voltage issues caused by PV in detail under the severe condition, an analysis using an actual DS model with multiple SVRs has been done. From the numerical simulation results using the actual scale DS model, voltage issues occurred in DS with SVR have been revealed. 1) One issue is voltage violation due to time delay of SVR. Since classical SVR with time delay is not designed for PV interconnection, rapid voltage fluctuation due to PV cannot be compensated by conventional SVR. 2) The other issue is deterioration of SVR caused by frequent switching operation of SVR. As conventional SVR attempts to regulate voltage within the dead band, the frequent switching operation corresponding to frequent voltage fluctuation due to PV is occurred. To solve these issues, a novel control method using solar radiation sensors has been proposed in chapter 2. The proposed method controls the tap position of SVR to increases voltage margin which is defined as an index of difficulty of voltage violation from the allowable range. If voltage margin is sufficiently large, voltage can be kept within the allowable range without the operation of SVR. Hence, using the proposed method for SVR with time delay, it is possible to prevent voltage violation as well as avoiding the deterioration of SVR. From the numerical simulation, the effectiveness of the proposed strategy has been verified.

In chapter 3, a more effective control approach for voltage regulation has been proposed. DSO has

installed multiple sensors in DS in section switches to monitor voltage information on distribution line. Using these sensors, it can be possible to more effectively control voltage with existing SVR. However, since current these sensors cannot communicate with DSO in real-time, a local control of SVR is necessary. Moreover, in chapter 3, a serious problem caused by SVR has been revealed. A DS with multiple SVRs in series leads to ROS resulting in both voltage violation and deterioration of SVR in case of PV interconnection. To avoid ROS, it is necessary to control SVR only when needed using precise voltage information on the distribution line. However, voltage information from sensors is not constantly obtained due to low speed communication. Therefore, an online parameter tuning method for SVR using low speed communication has been presented. In the proposed strategy, SVR periodically gets voltage information on the distribution line from voltage sensors and calculates relationship between sending active power of SVR and voltage drop on the distribution line. SVR monitors sending active power in real-time and operates its tap position based on the estimated value of voltage at the sensor node. As SVR can know voltage profile through communication, SVR can change its tap position only when needed. From the numerical simulation, the effectiveness of the proposed strategy has been verified.

In chapters 2 and 3, existing devices which DSO has been installed in DS are used for voltage regulation. Utilizing low-performance existing facilities has an advantage in terms of cost; however, these devices are insufficient to properly control voltage fluctuated by PV. This is because that SVR has mechanical time delay which cannot be avoided. Even if voltage data in DS can be obtained through real time communication, the voltage violation caused by this delay cannot be prevented in the conventional way. Moreover, frequent voltage fluctuation causes the frequent switching operation of SVR resulting in degradation. Though this transient voltage fluctuation can be prevented using additional power electronics devices, introducing these high cost devices should be avoided. Therefore, in chapter 4, user's interface which will be introduced in future is used for voltage regulation. BT in residences for HEMS and EV is increasing under the condition in which there are shortage of electric power and energy saving. Even though without additional equipment, it can be possible to manage voltage using these users' interfaces. In the proposed strategy, BT is used to suppress rapid voltage fluctuation that cannot be compensated by SVR. The proposed strategy has an advantage in which users can use most part of their BTs because DSO uses not only BTs but also SVR. From simulation results, it can be seen that the proposed approach using users' interfaces can reduce both voltage violation and deterioration of SVR.

Chapter 5 focused on voltage fluctuation in not only DS but also TS to manage voltage in DS. In chapters 2, 3, and 4, several approaches have been presented to control voltage in DS under the assumption that sending voltage in distribution substation can be kept close to constant. Since TS has multiple facilities for voltage regulation, current voltage at distribution substations can be properly managed. However, it is necessary to investigate voltage behavior in TS in detail in case of PV interconnection because PV may change voltage at distribution substations. Thus, 66kV system model including TS and DSs have been built and voltage fluctuation due to PV has been analyzed. From numerical simulations, it can be seen that PV

can make a large impact on voltage in TS. Since voltage fluctuation in TS affects sending voltage in DS, it is indispensable to manage voltage in TS. Many DSs are connected to each other through transmission lines; hence power flow and voltage profile on TS can be complex due to PV in DS. This means that PVs in each DS take mutual influences each other. Local voltage control cannot regulate voltage complicated by PV in that case. Therefore, coordinated voltage control is necessary. In the proposed strategy, SVCs are installed at primary nodes of distribution substations and controlled coordinately. The effectiveness of the proposed strategy is verified through numerical simulations. Using the proposed method in chapter 5, secondary voltage at distribution substations can be controlled close to constant, and hence the proposed methods in chapter 2, 3, and 4 can be easily realized.

6.2 Concluding remarks and view of future research

Current power system is changing its structure and components such as generators, transmission network, and loads corresponding to the penetration of DGs. In order to maintain power quality level and continue to introduce the DG using RES, a framework of voltage control strategy should be flexibly modified according to the circumstances of the power system. From this point of view, the thesis has researched various voltage control methods suitable for PV penetration.

In this thesis, with little additional costs, the effective approaches for voltage management in case of PV interconnection were presented. As the results, it was found that existing facilities owned by DSO have an ability to efficiently manage voltage if they are controlled in a smart manner. Besides, the demand response using user's facilities with the proposed algorithm also showed good performance for voltage control. Thus, in smart grid with ICT, proper data utilization can considerably improve the ability of existing devices. Introducing a lot of high-cost devices for voltage management is NOT absolutely necessary even if PV is introduced in the power system. The thesis contributed to avoid useless investment and to show fully maintain power quality by low cost power apparatus. Furthermore, the amount of PV interconnection without voltage violation can be increased using the proposed method. With few additional investments, a large amount of PVs can be connected to the power system. This means the research is useful to realize a sustainable society.

The thesis enhanced voltage control strategy considering TS. Current power system basically has layered structure which is composed of many subsystems with different voltage level. These subsystems influence each other and they are independently controlled to properly keep voltage at each level. However, with many DGs, each subsystem could not appropriately control voltage in independent way. It is necessary to cooperatively control whole system voltage. The thesis focused on upper TS not only DS with PV to develop the voltage management method as a first step of an optimal global control. As a result, the thesis revealed the influence of PV on voltage in complex subsystems and developed a novel voltage control method suitable for PV interconnection. These results contributed to develop the next generation

power system, particularly in Japan.

Though this thesis assumed that DSO manages voltage in DS, recent circumstances of power system are changing the conventional control framework. In future, it is expected that electricity market in Japan will expand and the structure of electric power industry will change by the policy concerning to the separation of power generation and transmission. However, power quality can be deteriorated due to the participation of Independent Power Producer (IPP) into the electricity market. Thus, it is important to construct an appropriate framework of electricity market which fulfills needs of consumers for power quality. Meanwhile, a lower electricity rate under the market competition leads to suppress the capital investment for maintaining power quality level. Next generation power system should be designed for optimizing both the electricity rate and power quality under the market competition. Because the result of this research is useful to reduce the additional cost as well as maintaining power quality, it is expected that the proposed method can contribute to build the framework of next generation power system.

The components in the power system including generators, transformers, and loads are operated in a simple manner because current power system structure and characteristics of its components are relatively simple. In this research, each component is simply controlled in the proposed control method. However, with technological innovation and penetration of DG, above components are expected to be diversified in future. For example, those are from central power plant to distributed power generators, and from passive loads (constant impedance) to active loads (power electronics device). Furthermore, with development of ICT, a variety of information in the power system can be obtained, in which bidirectional communication between components can be realized. In that situation, the control method for above diversified components using various data on power system will be complicated, and an appropriate decision-making of system control will be critically important. For the decision making of multiple components, a Multi-Agent System (MAS) is known as an effective measure. In MAS, there is no overall system goal, simply the local goals of each separate agent. MAS is composed of multiple intelligent agents, and individual agents may play different roles. Each agent can autonomously work, independently make decisions, and interact with each agent to achieve global goals. Hence, MAS is suitable for controlling complicated power system in future. In future research, applying MAS to power system control, appropriate control strategy for complicated power system will be developed.

As electrical energy situation in Japan are changing so rapidly, power system are forced to be reorganized to maintain power quality with few additional and maintenance cost. To achieve this purpose, coordination of Power System Operator (PSO) with consumers is necessary. For example, though current power system has a leading power factor problem due to many SCs, this problem can be solved by disconnecting the SCs. Thus, in future, a role of consumer is expected to be important. Conventional consumers were just consumers of electric power without contribution of power system. On the other hand, conventional PSO was just a generator of electric power. If consumers cooperate with PSO to maintain power quality, more efficient and flexible control can be realized. Actually, the effectiveness of demand

response was verified in the thesis. However, due to participation of users in control system, reliability of power system which is maintained by PSO is deteriorated. Current power system is managed by PSO such as electric power company because it is effective, reliability and flexible. To improve the reliability, it is indispensable to prescribe the role of PSO and consumers. In particular, because electricity market will be opened to ordinal consumers in future Japan, cooperative consensus building between PSO and consumers is critically important to maintain power quality as high level. Furthermore, not only cooperative control but also cooperative planning of power system in future is important. PSO and consumers should be cooperated at a planning stage, and power system which is easy to be controlled should be built. Accordingly, in order to build more efficient power system structure and control framework, modifying the role of PSO and consumers should be required. I wish to build the next generation power system satisfying above requirements.

Appendices

A1 Mechanism of SVR

A1.1 Aim of SVR

SVR is a transformer installed on 6.6kV high-voltage distribution line. Since LRT at a distribution substation cannot compensate for voltage drop (or rising) on high-voltage distribution line, voltage drop (or rising) due to load current is compensated by SVR. As shown in Figure A1.1, voltages at receiving point of consumers are kept within an allowable range by appropriate control of LRT and SVR.

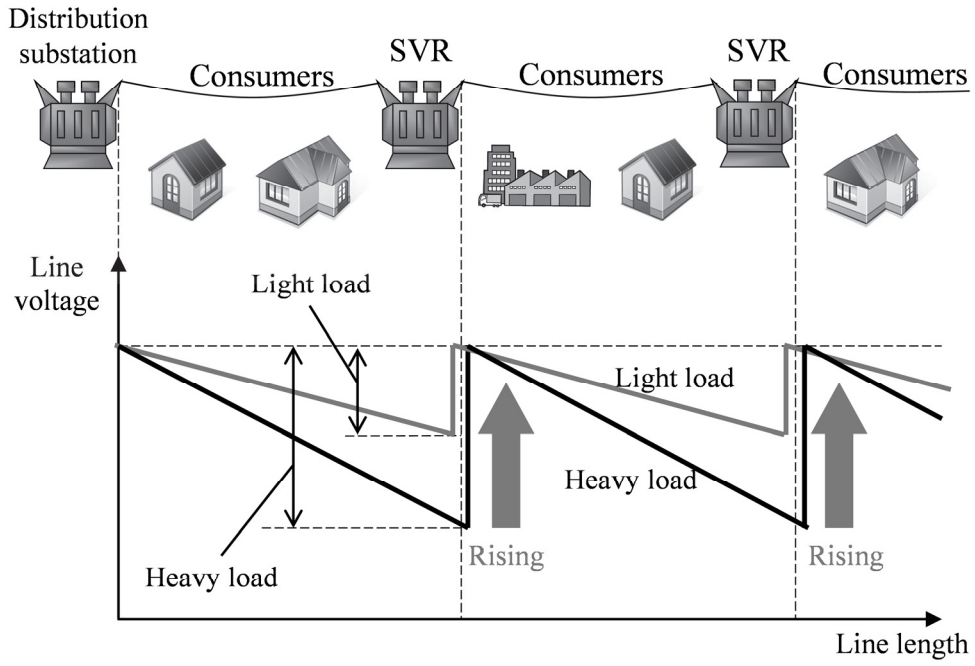

Figure A1.1 Compensation of voltage drop by SVR.

In Figure A1.1, voltage drop are compensated in case of both heavy and light load. This is because that SVR can automatically control voltage fluctuation according to voltage condition. Though Figure A1.1 shows voltage drop compensated by SVR, SVR can also compensate for voltage rising due to Ferranti effect and a generation of DG.

A1.2 Structure of SVR

SVR is an autotransformer which can control the secondary voltage by regulating its tap position. Figure A1.2 shows the structure of SVR.

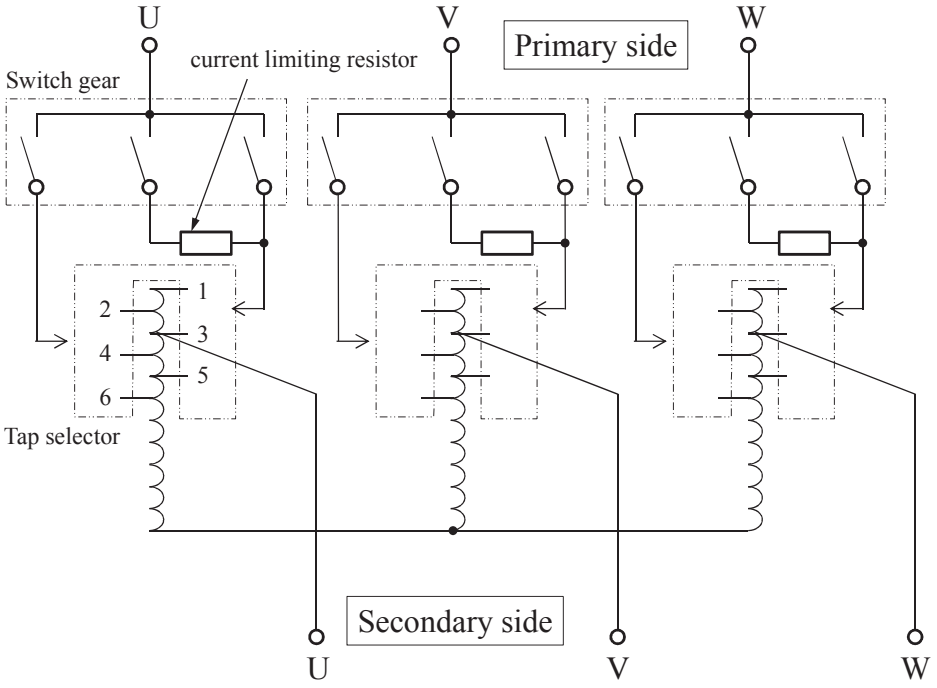

Figure A1.2 Structure of SVR.

SVR mainly consists of switch gears, tap selectors, a transformer, and current limiting resistors. As an autotransformer uses low-voltage winding as a part of high-voltage winding, the autotransformer becomes smaller than two-winding transformer and has highly efficiency compared to the two-winding transformer. A primary and a secondary side of SVR are connected to switch gears and tap selectors in each phase, respectively. In order to continue the power supply from the primary side to the secondary side even when tap is being changed, the switch gear and the current limiting resistor are used.

A1.3 Switch gear

SVR controls its secondary voltage by operating the switch gear shown in Figure A1.2. When the switch gear turns off load current, surge current flows in the switch gear. This surge current causes deterioration of SVR. Hence, SVR has the maximum allowable switching number over a day.

A1.4 Classical control method of SVR

SVR can control the secondary voltage V_{SVR} by changing its tap position as shown in Figure A1.3.

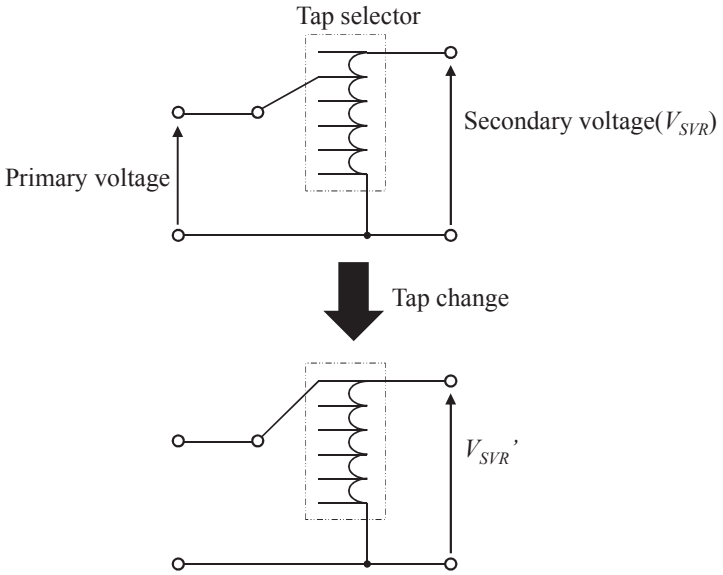

Figure A1.3 Tap change of SVR.

The classical control methods of SVR are classified into several types regarding to the tap operation. Voltage violation time, amount of voltage violation, LDC method are used for the tap operation. This thesis assumes that a controller of SVR using the dead band and settling time is a "classical control method". The classical controller is shown in Figure A1.4.

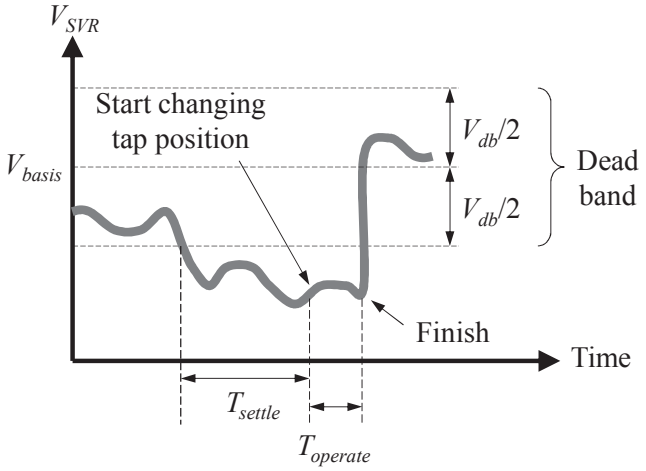

Figure A1.4 Conventional control method of SVR.

In Figure A1.4, V_{basis} is basis voltage in DS and V_{db} is the width of dead band. SVR observes V_{SVR} and starts time counting after V_{SVR} deviates from the dead band. Since the tap change of SVR leads to the deterioration of SVR, the dead band and settling time (T_{settle}) are necessary to prevent the deterioration.

SVR changes its tap position to keep V_{SVR} within the dead band if the count reaches T_{settle}. SVR has count time T_{up} and T_{down} for determining whether the tap position is changed or not. Assuming sampling time of controller in SVR is set as dt, T_{up} and T_{down} are calculated as follows.

$$\begin{aligned} &V_{SVR} > V_{basis} + V_{db}/2 \quad \rightarrow \quad T_{up} = T_{up} + dt \\ &V_{SVR} < V_{basis} + V_{db}/2 \quad \rightarrow \quad T_{up} = T_{up} - dt \\ &T_{up} < 0 \quad \rightarrow \quad T_{up} = 0 \end{aligned} \tag{A1.1}$$

$$\begin{aligned} &V_{SVR} < V_{basis} - V_{db}/2 \quad \rightarrow \quad T_{down} = T_{down} + dt \\ &V_{SVR} > V_{basis} - V_{db}/2 \quad \rightarrow \quad T_{down} = T_{down} - dt \\ &T_{down} < 0 \quad \rightarrow \quad T_{down} = 0 \end{aligned} \tag{A1.2}$$

If T_{up} or T_{down} reaches T_{settle}, the tap position of SVR N_{tap} is changed as dN_{tap}.

$$\begin{aligned} &T_{down} \geq T_{settle} \quad \rightarrow \quad N_{tap} = N_{tap} + dN_{tap} \\ &T_{up} \geq T_{settle} \quad \rightarrow \quad N_{tap} = N_{tap} - dN_{tap} \end{aligned} \tag{A1.3}$$

After the switching operation, T_{up} and T_{down} are reset to 0. SVR changes its tap position when V_{SVR} continually deviates from the dead band. Therefore, equations (A1.1) and (A1.2) are used. When V_{SVR} continually deviates from the dead band, T_{up} or T_{down} increases. On the other hand, V_{SVR} transiently deviates from the dead band, T_{up} or T_{down} do not increase.

SVR is installed on a distribution line in series and hence there is an issue called as “hunting” that increases of the switching operation of SVR. Hunting is occurred when several SVRs are installed on the distribution line in series. In this case, the operation of upper SVR causes step voltage change on the downstream distribution line, and hence that may lead to the tap operation of lower SVR. In particular, when multiple SVRs are installed in the distribution line in series, the operation of upper SVRs causes frequent step voltage fluctuation on the distribution line. This causes many operations of lower SVRs. In order to reduce the switching operation of lower SVRs, the upper SVR should operate prior to the lower SVRs. In general, T_{settle} of upper SVR tends to be set as smaller than those of lower SVR so that the upper SVR operates earlier than lower one. SVR needs few seconds ($T_{operate}$) to finish the switching operation which is structural time delay against voltage fluctuation.

A2 Power flow calculation

A2.1 Introduction

An analysis tool for power network is *power flow calculation* which is often employed in this field. The power flow calculation is applied to the system-planning researches and also the starting point for transient and dynamic stability studies. This section presents a formulation of power flow calculation. Power flow calculation assumes following things.

(1) Three-phase and balanced circuit

Assuming three-phase and balanced circuit, circuit can be considered as single-phase circuit that is good for reducing calculation burden.

(2) Constant frequency

Since power flow calculation is executed under steady-state, impedance can be considered as constant.

Because the supply/demand at a node is generally specified in terms of active and reactive power, the problem becomes nonlinear. Hence, the power flow analysis is a set of simultaneous nonlinear algebraic equations.

A2.2 Formulation

Following notations for the power flow model are used.

P_{ij}: Active power flow from node i to j
Q_{ij}: Reactive power flow from node i to j
P_j: Active power injection for a node i
Q_j: Reactive power injection for a node i
V_i: Voltage magnitude of node i
θ_i: Phase angle of voltage at node i
I_i: Current magnitude injected into node i
$Y_{ij}=G_{ij}+jB_{ij}$: Admittance of series branch between node i and j
$Y_{ii}=G_{ii}+jB_{ii}$: Admittance of shunt branch at node i

(1) Line model

Lines used in power system include transmission line and distribution line. These lines have resistance *r*, reactance *x*, and capacitance *b* as shown in Figure A2.1.

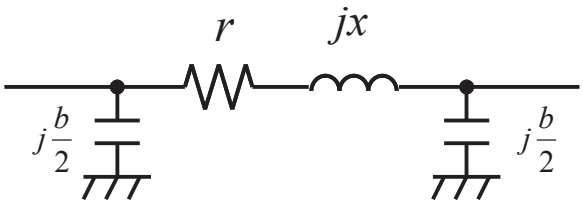

Figure A2.1 Line model.

The line is represented by its equivalent π network. In power flow calculation, active/reactive power flowing through a line is modeled using above model.

(2) Power injected in nodes

Current flowing through a line between node #*m* and #*n* are shown in Figure A2.2. In Figure A2.2, I_{mn} represents current from node #*m* to #*n*, and vice versa. b_{Cm} and b_{Cn} represent shunt capacitance at node #*m* and #*n*, respectively. r_{mn} and x_{mn} show *r* and *x* of the line between node #*m* and #*n*, respectively. b_{mn} is a capacitance of line between node #*m* and #*n*.

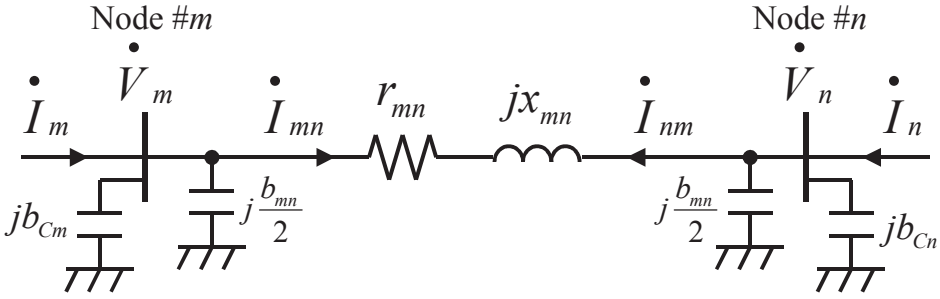

Figure A2.2 Current flowing through a line.

Using above line model, following equations can be obtained. Following equations must satisfy Kirchhoff's current and voltage laws.

$$\dot{I}_m = j\left(b_{Cm} + \frac{b_{mn}}{2}\right)\dot{V}_m + \dot{I}_{mn} \tag{A2.1}$$

$$\dot{I}_{mn} = \frac{\dot{V}_m - \dot{V}_n}{r_{mn} + jx_{mn}} \tag{A2.2}$$

$$\dot{I}_m = j\left(b_{Cm} + \frac{b_{mn}}{2}\right)\dot{V}_m + \frac{\dot{V}_m - \dot{V}_n}{r_{mn} + jx_{mn}} \tag{A2.3}$$

If the total node number is #*k*, the equation (A2.3) can be described as follows.

$$\begin{aligned}\dot{I}_m &= \left[\sum_{\substack{n=1 \\ m\neq n}}^{k}\left(\frac{1}{r_{mn} + jx_{mn}} + j\frac{b_{mn}}{2}\right) + jb_{Cm}\right]\dot{V}_m - \sum_{\substack{n=1 \\ m\neq n}}^{k}\frac{\dot{V}_n}{r_{mn} + jx_{mn}} \\ &= \sum_{n=1}^{k}\dot{Y}_{mn}\dot{V}_{nm}\end{aligned} \tag{A2.4}$$

$$\begin{cases}\dfrac{b_{mn}}{2} = 0 \\ \dfrac{1}{r_{mn} + jx_{mn}} = 0\end{cases} \qquad (\text{if node } \#m \text{ and } \#n \text{ are not connected}) \tag{A2.5}$$

$$\dot{Y}_{mn} = \begin{cases}\displaystyle\sum_{\substack{n=1 \\ m\neq n}}^{k}\left(\frac{1}{r_{mn} + jx_{mn}} + j\frac{b_{mn}}{2}\right) + jb_{Cm} & (m = n) \\ -\dfrac{1}{r_{mn} + jx_{mn}} & (m \neq n)\end{cases} \tag{A2.6}$$

Active and reactive power injections at node #*m* are calculated.

$$\begin{aligned}P_m + jQ_m &= \dot{V}_m\overline{\dot{I}_m} \\ &= \dot{V}_m\sum_{n=1}^{k}\overline{\dot{Y}_{mn}}\,\overline{\dot{V}_{nm}}\end{aligned} \tag{A2.7}$$

Hence, the equations for active and reactive power injections at node #*i* are obtained as follows.

$$P_i = V_i \sum_{i=1}^{n} V_j \left\{ G_{ij} \cos\left(\theta_i - \theta_j\right) - B_{ij} \sin\left(\theta_i - \theta_j\right) \right\} \tag{A2.8}$$

$$Q_i = V_i \sum_{i=1}^{n} V_j \left\{ B_{ij} \cos\left(\theta_i - \theta_j\right) + G_{ij} \sin\left(\theta_i - \theta_j\right) \right\} \tag{A2.9}$$

Since line impedance is constant, the active and reactive power are represented as a function of voltage at each node.

$$\dot{\boldsymbol{S}} = \dot{\boldsymbol{P}} + j\dot{\boldsymbol{Q}} = f\left(\dot{\boldsymbol{V}}\right) \tag{A2.10}$$

$$\dot{\boldsymbol{P}} + j\dot{\boldsymbol{Q}} = \begin{bmatrix} \dot{P}_1 + j\dot{Q}_1 \\ \dot{P}_2 + j\dot{Q}_2 \\ \vdots \\ \dot{P}_k + j\dot{Q}_k \end{bmatrix} \tag{A2.11}$$

(3) Types of nodes

Each node introduces two equations. To obtain solutions for a set of these equations, it is necessary to have the same number of equations as unknowns. Two variables associated with each node must be specified. The conventional method of specifying node type is classified as follows:

(i) PQ node

At PQ node, active and reactive power injections are specified. The active and reactive power injecting into a node is the power supplied to the grid from the generating sources minus the power consumed by loads.

(ii) PV node

At PV node, active power injections and voltage magnitude are specified. The reactive power injecting to a node is unknown that is calculated based on power flow analysis. This type of node is used to stand for a node with generators (active and reactive power source). Generators at this node specified the magnitude of output voltage.

(iii) Slack node

At slack node, voltage magnitude and phase angle are specified. Generally, the angle is set to zero as an infinite bus. Unlike the other two node types, this node type is indispensable for a mathematical requirement. Slack node is needed to absorb any active and reactive power across the network. It is impossible to specify the active and reactive power at all nodes in the network, because transmission losses

on lines are unknown until the power flow calculation is completed. Normally, there can only be a slack node in the network.

A2.3 Power flow solution

Though there are multiple methods to solve power flow calculations, this thesis employs Newton-Raphson method that is suitable for solving nonlinear problems with efficiency. As an error function, function *g* is defined.

$$\begin{aligned} g\left(\widetilde{\boldsymbol{V}}\right) &= f\left(\boldsymbol{V}^{*}\right) - f\left(\widetilde{\boldsymbol{V}}\right) \\ &= 0 \end{aligned} \tag{A2.12}$$

In equation (A2.12), $\boldsymbol{V}^{*}$ represents the real value of voltage and $\tilde{\boldsymbol{V}}$ represents the estimation value of voltage. The purpose of Newton-Raphson method is fitting $\tilde{\boldsymbol{V}}$ and $\boldsymbol{V}^{*}$. If voltage vector $\boldsymbol{V}$ is incremented by $\boldsymbol{dV}$, *g* can become as follows.

$$g\left(\boldsymbol{V}_{0} + \boldsymbol{dV}\right) = f\left(\boldsymbol{V}^{*}\right) - f\left(\boldsymbol{V}_{0} + \boldsymbol{dV}\right) \tag{A2.13}$$

$$\widetilde{\boldsymbol{V}} = \boldsymbol{V}_{0} + \boldsymbol{dV} \tag{A2.14}$$

Taking Taylors series expansion about an operating point $\boldsymbol{V}_{0}$ of (A2.13) and considering only the first derivatives, following equation can be obtained.

$$\begin{aligned} g\left(\boldsymbol{V}_{0} + \boldsymbol{dV}\right) &= g\left(\boldsymbol{V}_{0}\right) + \frac{1}{1!} g'\left(\boldsymbol{V}_{0}\right)\boldsymbol{dV} + \frac{1}{2!} g'\left(\boldsymbol{V}_{0}\right)\left(\boldsymbol{dV}\right)^{2} + \cdots \\ &\approx g\left(\boldsymbol{V}_{0}\right) + g'\left(\boldsymbol{V}_{0}\right)\boldsymbol{dV} \approx \boldsymbol{0} \end{aligned} \tag{A2.15}$$

The equation (A2.15) gives

$$g'\left(\boldsymbol{V}_{0}\right)\boldsymbol{dV} \approx -g\left(\boldsymbol{V}_{0}\right) \tag{A2.16}$$

$$\begin{aligned} \boldsymbol{dV} &\approx -g'\left(\boldsymbol{V}_{0}\right)^{-1} g\left(\boldsymbol{V}_{0}\right) \\ &= -\boldsymbol{J}\left(\boldsymbol{V}_{0}\right) g\left(\boldsymbol{V}_{0}\right) \end{aligned} \tag{A2.17}$$

In equation (A 2.17), $\boldsymbol{J}$ is called as Jacobian matrix. $\boldsymbol{J}$ represents voltage sensitivity against active and

reactive power ($\Delta \boldsymbol{V}/\Delta \boldsymbol{P}$, $\Delta \boldsymbol{V}/\Delta \boldsymbol{Q}$) when the state of voltage in the power system is $\boldsymbol{V_0}$. $\boldsymbol{J}$ can be calculated using the voltage magnitude and phase angle at each node in a power system model.

In Newton-Raphson method, the estimation value of voltage $\tilde{\boldsymbol{V}}_{\boldsymbol{OLD}}$ is updated to the improved value using equation (A2.18) as shown in equation (A2.18) and Figure A2.3.

$$\tilde{\boldsymbol{V}}_{\boldsymbol{NEW}} = \tilde{\boldsymbol{V}}_{\boldsymbol{OLD}} + \boldsymbol{dV} \tag{A2.18}$$

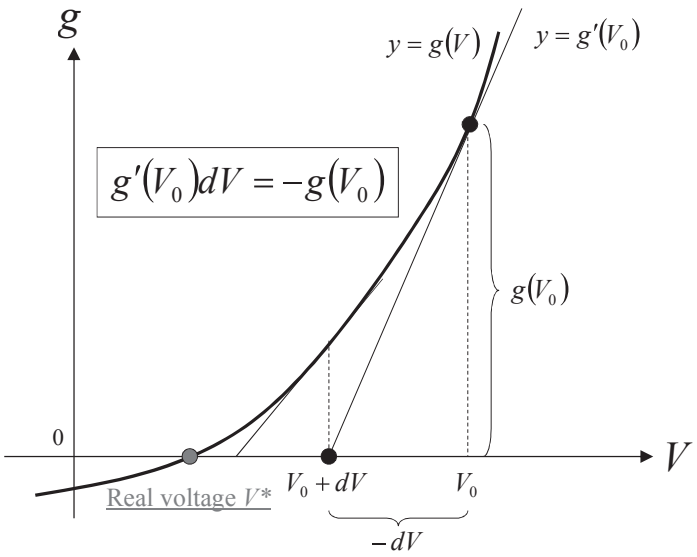

Figure A2.3 Newton-Raphson method.

Newton-Raphson method continues to update $\tilde{\boldsymbol{V}}$ until g becomes close to **0**. When g is equal to **0**, $\tilde{\boldsymbol{V}}$ is equal to $\boldsymbol{V}^*$.

A2.4 SVR model in power flow calculation

In order to simulate the behavior of SVR in power flow calculation, it is necessary to implement SVR into admittance matrix. As SVR is a transformer, the model is represented using resistance and reactance. In this thesis, SVR is modeled as an ideal transformer without internal resistance and reactance. SVR is modeled as shown in Figure A2.4. In Figure A2.4, node #*i* is a primary node and node #*j* is a secondary node. The tap ratio of SVR (secondary/primary) is represented as n. Z is line impedance between the secondary node of SVR and node #*j*. From transformer laws, following equations can be obtained.

$$\begin{cases} \dot{I}_i + n\dot{I}_j = 0 \\ \dot{V}_j - \dot{Z} \cdot \dot{I}_j = n\dot{V}_i \end{cases} \tag{A2.19}$$

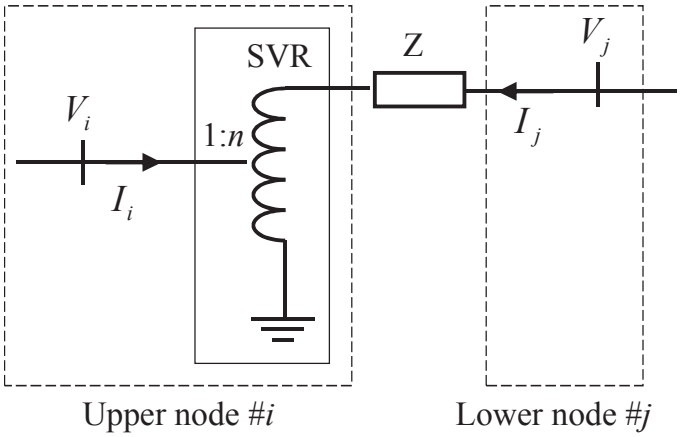

Figure A2.4 SVR in power flow calculation.

These equations can be transformed to

$$\begin{cases} \dot{I}_i = n(n-1)\dot{Y}\cdot\dot{V}_i + n\dot{Y}\left(\dot{V}_i - \dot{V}_j\right) \\ \dot{I}_j = n\dot{Y}\left(\dot{V}_j - \dot{V}_i\right) + (1-n)\dot{Y}\cdot\dot{V}_j \end{cases} \qquad \text{(A2.20)}$$
$$\dot{Y} = 1/\dot{Z}$$

From equation (A2.20), the model of SVR shown in Figure A2.4 can be transformed into π model as shown in Figure A2.5.

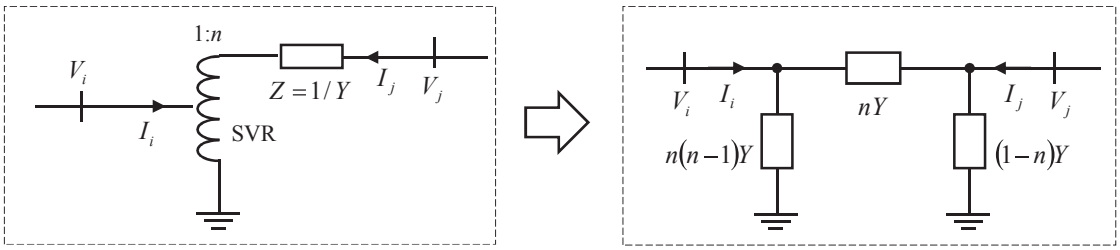

Figure A2.5 Transform of SVR to π model.

The operation of SVR in power flow calculation can be simulated my changing admittance matrix whenever the tap position of SVR is changed.

A2.5 Power flow calculation with time varying

To calculate the behavior of voltage with time varying, it is necessary to repeatedly execute the power flow calculation at each time step. In this procedure, load is varied and SVR determines its operation based on V_{SVR}. Simulation step is described as follows.

STEP 1: Reading parameters

In step 1, parameters of DS are read. These parameters include following data.

- Impedance of line
- Voltage magnitude and phase angle at slack node with time varying
- Active/reactive power of load data at PQ node with time varying
- Active power of load data and voltage magnitude at PV node with time varying
- Parameters regarding to SVR
- Simulation time T
- Sampling time of simulation dt

STEP 2: Calculating data for power flow calculation

In order to execute power flow calculation at time t, it is necessary to get admittance matrix and load at t. Admittance matrix at time t can be calculated using the tap position of SVR. Load data at time t is also calculated.

STEP 3: Execute Newton-Raphson method

From results using Newton-Raphson method, voltage profile at time t can be obtained.

STEP 4: Determination of the operation of SVR

SVR counts up or down T_{up} and T_{down} based on V_{SVR}. When T_{up} or T_{down} reaches T_{settle}, SVR changes its tap position. If the tap position is restricted by its limit (maximum or minimum tap position), SVR cannot change its tap position.

STEP 5: Update of time t

Time t is updated as sampling time dt, hence $t = t + dt$. If t reaches simulation time T, simulation is end, otherwise, simulation step returns to step 2.

Above simulation procedure is shown in Figure A2.6.

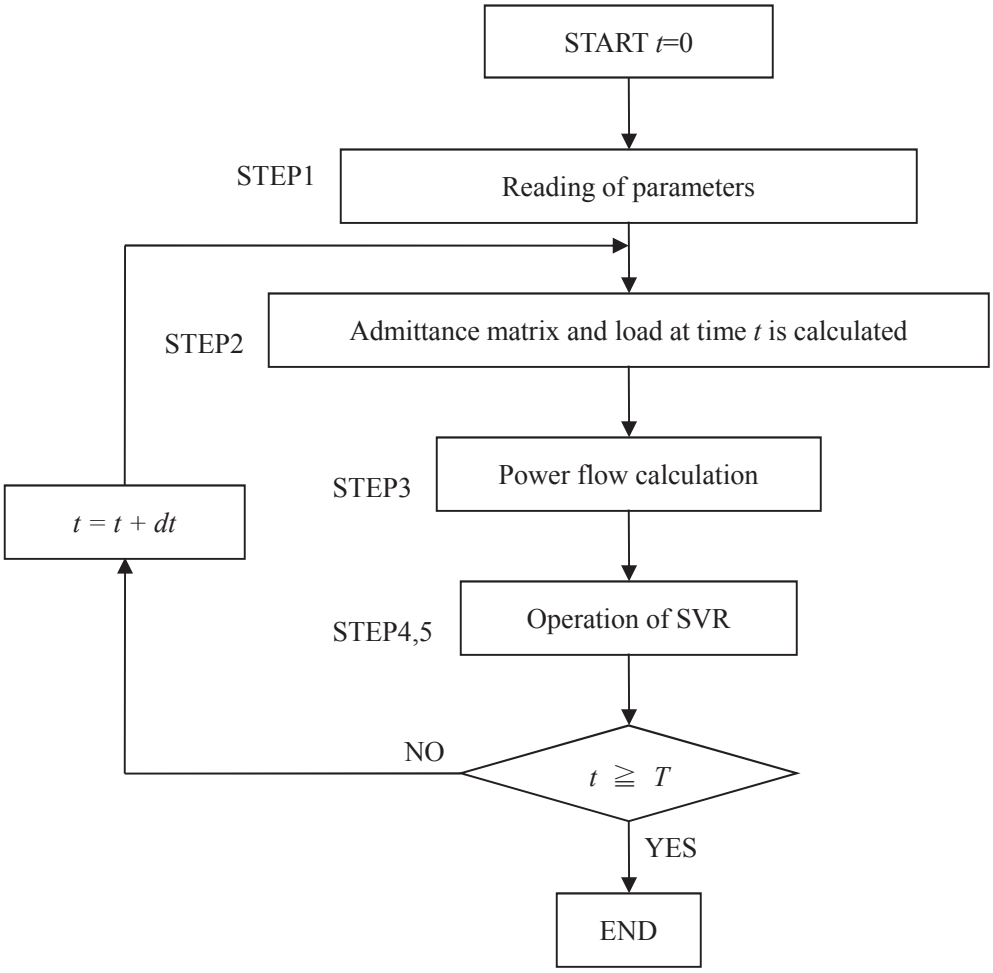

Figure A2.6 Simulation procedure.

A3 Actual scale distribution system model

Parameters of actual scale DS model used in chapter 2 is shown in Table A3.1.

Table A3.1 Parameters of actual scale DS model

Node #		$R[\Omega]$	$X[\Omega]$	I_{max} [A]		Node #		R [Ω]	X[[Ω]	I_{max} [A]
Upper	Lower					Upper	Lower			
1	2	0.006	0.014	0		59	60	0.04	0.103	0
2	3	0.012	0.0305	3		60	61	0.071	0.106	0
3	4	0.012	0.0305	0		60	62	0.038	0.099	0
4	5	0.006	0.015	0		62	63	0.0285	0.0725	1
5	6	0.046	0.118	0		63	64	0.0285	0.0725	0
6	8	0.004	0.011	0		64	65	0.006	0.008	0
6	7	0.001	0.004	0		64	72	0.009	0.023	1
6	43	0.006	0.015	0		72	73	0.009	0.023	0
8	9	0.016	0.042	0		65	68	0.0835	0.0925	17
9	10	0.004	0.011	0		68	69	0.0835	0.0925	0
9	11	0.046	0.083	0		65	66	0.073	0.0465	17
11	12	0.094	0.123	0		66	67	0.073	0.0465	0
12	13	0.016	0.025	0		69	70	0.273	0.137	6
13	14	0.11	0.143	0		70	71	0.273	0.137	0
14	15	0.0385	0.0635	1		73	74	0.0265	0.0685	5
15	16	0.0385	0.0635	0		74	75	0.0265	0.0685	0
16	17	0.012	0.0305	11		73	76	0.0065	0.0175	5
17	18	0.012	0.0305	0		76	77	0.0065	0.0175	0
18	19	0.0785	0.061	11		77	78	0.003	0.008	0
19	20	0.0785	0.061	0		78	81	0.012	0.0305	1
18	21	0.013	0.02	0		81	82	0.012	0.0305	0
21	26	0.058	0.106	3		78	106	0.004	0.011	0
26	27	0.058	0.106	0		78	79	0.008	0.0135	24
21	22	0.0485	0.0655	16		79	80	0.008	0.0135	0
22	23	0.0485	0.0655	0		82	83	0.02	0.053	0
27	28	0.028	0.037	0		82	85	0.014	0.027	0

28	29	0.022	0.029	0		82	84	0.017	0.024	0
29	30	0.083	0.1085	22		82	99	0.007	0.012	0
30	31	0.083	0.1085	0		85	86	0.047	0.0615	2
31	32	0.0295	0.039	1		86	87	0.047	0.0615	0
32	33	0.0295	0.039	0		87	88	0.043	0.039	8
33	34	0.0675	0.088	2		88	89	0.043	0.039	0
34	35	0.0675	0.088	0		87	90	0.072	0.0575	8
35	38	0.039	0.051	1		90	91	0.072	0.0575	0
38	39	0.039	0.051	0		87	92	0.032	0.042	8
35	36	0.0095	0.0045	19		92	93	0.032	0.042	0
36	37	0.0095	0.0045	0		87	94	0.0545	0.0705	8
39	40	0.097	0.127	0		94	95	0.0545	0.0705	0
40	41	0.2655	0.1315	24		87	96	0.1345	0.175	8
41	42	0.2655	0.1315	0		96	97	0.1345	0.175	0
23	24	0.536	0.296	22		97	98	0.022	0.04	0
24	25	0.536	0.296	0		99	100	0.0825	0.1065	4
43	44	0.0415	0.107	5		100	101	0.0825	0.1065	0
44	45	0.0415	0.107	0		101	102	0.0445	0.056	4
45	46	0.027	0.0685	2		102	103	0.0445	0.056	0
46	47	0.027	0.0685	0		103	104	0.055	0.0715	5
47	48	0.0345	0.0895	7		104	105	0.055	0.0715	0
48	49	0.0345	0.0895	0		106	107	0.0455	0.059	3
49	50	0.004	0.011	0		107	108	0.0455	0.059	0
50	53	0.02	0.0515	1		108	109	0.0365	0.0465	2
53	54	0.02	0.0515	0		109	110	0.0365	0.0465	0
50	51	0.028	0.0365	15		110	111	0.0515	0.0675	29
51	52	0.028	0.0365	41		111	112	0.0515	0.0675	0
54	55	0.074	0.19	0		112	113	0.1015	0.1335	8
55	56	0.3355	0.1655	14		113	114	0.1015	0.1335	0
56	57	0.3355	0.1655	0		114	115	0.0425	0.055	6
55	58	0.006	0.015	0		115	116	0.0425	0.055	0
58	59	0.04	0.103	2						

A4 Principle component analysis

Principal Components Analysis (PCA) is a useful statistical technique that has found application in fields such as face reconfiguration and image compression. It is a way of identifying patterns in data, and expressing the data in such a way to highlight their similarities and differences.

A4.1 Basic idea of PCA

PCA is one method to reduce the number of features that represent data. Figure A4.1 shows a data set of x_1 and x_2 and projection of the 2 dimension data set.

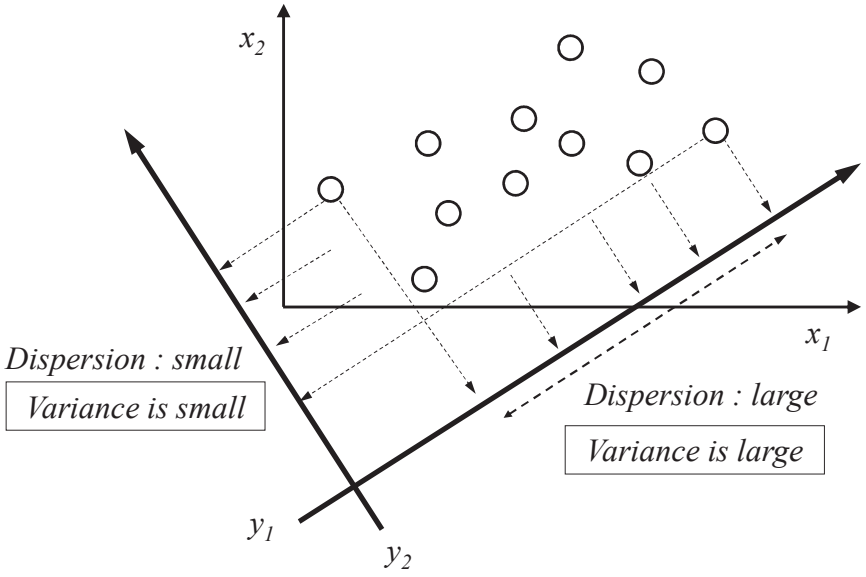

Figure A4.1 projections of 2 dimension data set.

In Figure A4.1, a data set of x_1 and x_2 is projected to following axis.

$$y_1 = w_{11}x_1 + w_{12}x_2 \tag{A4.1}$$

$$y_2 = w_{21}x_1 + w_{22}x_2 \tag{A4.2}$$

From Figure A4.1, dispersion of y_1 is larger than dispersion of y_2. PCA is a technique to find the axis that maximizes dispersion of data set. In PCA, the axis that maximizes dispersion of data set is called as first principal component, and the axis which maximizes dispersion of data set orthogonal to first principal component is called second principal component.

Assume a data set of 2 dimensions is

$$\boldsymbol{x}_i = \begin{pmatrix} x_{i1} \\ x_{i2} \end{pmatrix} \tag{A4.3}$$

$$\boldsymbol{w} = \begin{pmatrix} w_1 \\ w_2 \end{pmatrix} \tag{A4.4}$$

$$\begin{aligned} y_i &= w_1 x_{i1} + w_2 x_{i2} \\ &= \boldsymbol{w}^{\boldsymbol{T}} \boldsymbol{x}_{\boldsymbol{i}} \qquad (i = 1,2,\cdots,n) \end{aligned} \tag{A4.5}$$

An average of y is

$$\begin{aligned} \bar{y} &= \frac{1}{n}\sum_{i=1}^{n} y_i \\ &= \frac{1}{n}\sum_{i=1}^{n}\left(w_1 x_{i1} + w_2 x_{i2}\right) \\ &= w_1 \overline{x_1} + w_2 \overline{x_2} \\ &= \boldsymbol{w}^{\boldsymbol{T}} \overline{\boldsymbol{x}} \end{aligned} \tag{A4.6}$$

Covariance of $y_1 \sim y_n$ is

$$\begin{aligned} s_y^2 &= \frac{1}{n}\sum_{i=1}^{n}\left(y_i - \bar{y}\right)^2 \\ &= \frac{1}{n}\sum_{i=1}^{n}\left\{w_1\left(x_{i1} - \overline{x_1}\right) + w_2\left(x_{i2} - \overline{x_2}\right)\right\}^2 \\ &= w_1^2 \frac{1}{n}\sum_{i=1}^{n}\left(x_{i1} - \overline{x_1}\right)^2 + 2w_1 w_2 \frac{1}{n}\sum_{i=1}^{n}\left(x_{i1} - \overline{x_1}\right)\left(x_{i2} - \overline{x_2}\right) + w_2^2 \frac{1}{n}\sum_{i=1}^{n}\left(x_{i2} - \overline{x_2}\right)^2 \\ &= w_1^2 s_{11} + 2w_1 w_2 s_{12} + w_2^2 s_{22} \\ &= \boldsymbol{w}^{\boldsymbol{T}} \boldsymbol{S}\boldsymbol{w} \end{aligned} \tag{A4.7}$$

In equation (A4.7), $\boldsymbol{S}$ is covariance matrix that is defined as

$$S = \begin{pmatrix} s_{11} & s_{12} \\ s_{21} & s_{22} \end{pmatrix} \tag{A4.8}$$

where

$$s_{jk} = \frac{1}{n}\sum_{i=1}^{n}\left(x_{ij} - \overline{x_j}\right)\left(x_{ik} - \overline{x_k}\right), \quad j,k=1,2 \tag{A4.9}$$

In order to calculate $w=(w_1,w_2)^{\mathrm{T}}$ that maximize covariance of data set, it is necessary to maximize $s_y^2 = w^T S w$ under the condition that $w^T w = 1$. This problem can be solved using Lagrange multiplier. Assume that Lagrange multiplier is λ, Lagrange function can be calculated as follows.

$$L(\boldsymbol{w},\lambda) = \boldsymbol{w}^{\boldsymbol{T}} S\boldsymbol{w} + \lambda\left(1 - \boldsymbol{w}^{\boldsymbol{T}}\boldsymbol{w}\right) \tag{A4.10}$$

From Lagrange function, following equation is obtained

$$S\boldsymbol{w} = \lambda\boldsymbol{w} \tag{A4.11}$$

A solution of this equation is an eigenvector $\boldsymbol{w_1}=(w_{11},w_{12})^{\mathrm{T}}$ corresponding to λ_1 that is the maximum eigenvalue of $\boldsymbol{S}$. Hence, first principal component is

$$\begin{aligned} y_1 &= w_{11}x_1 + w_{12}x_2 \\ &= \boldsymbol{w_1^T x} \end{aligned} \tag{A4.12}$$

Similarly, second principal component can be obtained as

$$\begin{aligned} y_2 &= w_{21}x_1 + w_{22}x_2 \\ &= \boldsymbol{w_2^T x} \end{aligned} \tag{A4.13}$$

where the eigenvector $\boldsymbol{w_2}=(w_{21},w_{22})^{\mathrm{T}}$ corresponding to λ_2 is the second largest eigenvalue of $\boldsymbol{S}$.

A5 66kV transmission system model provided by IEEJ

A detail 66kV transmission system model provided by IEEJ is shown in Figure A5.1.

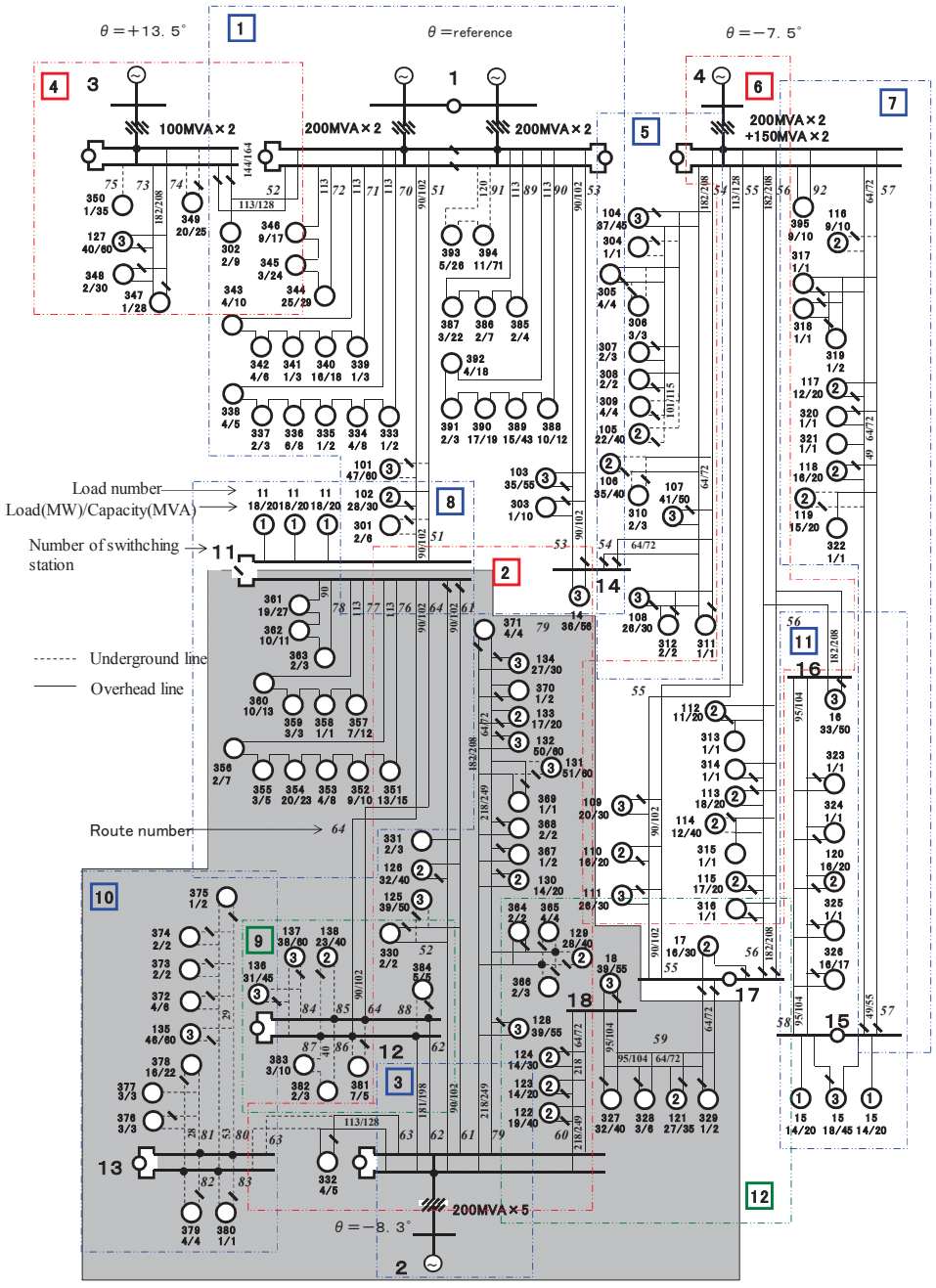

Figure A5.1 66kV transmission system model.

In Figure A5.1, symbols of voltage generator represent 154kV substations. Circles connected to transmission line show consumers or distribution systems.

List of Publications

Journals

Chapter 2

[1] Shinya Sekizaki, Mutsumi Aoki, Hiruyuki Ukai, Takuma Sakaguchi, and Takaya Shigetou, "Voltage Control using Solar Radiation Information in Distribution System with Large Amount of Photovoltaic Generators", Journal of IEIEJ, Vol. 32, No. 3, pp. 226-235, 2012 (in Japanese)

Chapter 3

[2] Shinya Sekizaki, Mutsumi Aoki, Hiruyuki Ukai, Shunsuke Sasaki, and Takaya Shigetou, "Control of Multistage SVRs using Voltage Sensor in Distribution System with Large Amount of Photovoltaic Generations", IEEJ Transactions on Power and Energy, Vol. 133, No. 1, pp. 45-55 2013 (in Japanese)

Chapter 4

[3] Shinya Sekizaki, Mutsumi Aoki, Hiruyuki Ukai, Shunsuke Sasaki, and Takaya Shigetou, "Voltage Control using Small Batteries in Distribution System with Large Amount of PVs", IEEJ Transactions on Power and Energy, Vol. 133, No. 5, pp. 439-448, 2013 (in Japanese)

Chapter 5

[4] Shinya Sekizaki, Mutsumi Aoki, Hiruyuki Ukai, "Reactive Power Control in Distribution Substation for Reducing Voltage Fluctuation on Upper System", IEEJ Transactions on Power and Energy (in Japanese) (submitted)

International conferences

Chapter 2

[1] Shinya Sekizaki, Mutsumi Aoki, Hiroyuki Ukai, Takaya Shigetou, and Shunsuke Maru, "VOLTAGE CONTROL IN DISTRIBUTION SYSTEM WITH LARGE AMOUNT OF PHOTOVOLTAIC GENERATIONS", Proceedings of the IASTED Technology and Management Conferences 2010, Power and Energy Systems, AsiaPES 2010, 701-098, pp. 21-27, Phuket, Thailand (2010)

[2] Shinya Sekizaki, Mutsumi Aoki, Hiroyuki Ukai, Takuma Sakaguchi, and Takaya Shigetou, "Cooperative Voltage Control of SVR and SVC using Solar Radiation Information", Proceedings of the International Conference on Electrical Engineering 2011, ICEE-A216, 2011

Chapter 3

[3] Katsuma WATANABE, Mutsumi AOKI, Hiroyuki UKAI, Shinya SEKIZAKI, Shunsuke SASAKI, and Takaya SHIGETOU, "Determination Method of Optimal Sending Voltage for Voltage Regulation by LRT Control in Distribution System with a Large amount of PVs", Proceedings of the International Conference on Electrical Engineering 2012, pp.20-25, No.PO1-4, 2012

Chapter 4

[4] Shinya Sekizaki, Mustumi Aoki, and Hiroyuki Ukai: "Voltage Control using Electrical Storage and Advanced SVR for Smart Community", ISETS '11 International Symposium on EcoTopia Science 2011, 10G05-15(7270), 2011

Others

[5] Shinya Sekizaki, Mutsumi Aoki, Hiroyuki Ukai, Shunsuke Sasaki, Takaya Shigetou, Weihua WANG, and Jean BÉLANGER, "Effective Voltage Control by SVR to Reduce the Capacity of SVC using Solar Radiation Information with Real Time Simulator", Proceedings of the International Conference on Electrical Engineering 2012, pp. 14-19, No. PO1-3, 2012

[6] Mutsumi Aoki, Shinya Sekizaki, Tsukasa Honda, and Hiroyuki Ukai, "The Influence to the Harmonics Voltages in the branch distribution system by the Static Capacitors in HV Consumers", Proceedings of Asia-Pacific Conference on Electrical Installation(APEI) (The 10th International Workshop) , APEI-1, pp. 551-554, 2012

National/Regional conferences

Chapter 2

[1] Shinya Sekizaki, Mutsumi Aoki, Hiroyuki Ukai, Shunsuke Maru, Masatoshi Nakamura, and Komichi Hiroya, "Fundamental Investigation of Voltage at Distribution System With Many Photovoltaic Generations Using Actual Scale Distribution System Model", Proceedings of Twenty-Eighth Annual Conference of IEIEJ, C-20, pp.141-142, 2010 (in Japanese)

[2] Shinya Sekizaki, Mutsumi Aoki, Hiroyuki Ukai, Takaya Shigetou, and Takuma Sakaguchi, "Voltage Control using SVR in Distribution System with Large Amount of Photovoltaic Generators", Proceedings of the Twenty-Second Annual Conference of Power & Energy Society. IEEJ, 171, pp. 14-1－14-2, 2011 (in Japanese)

Chapter 3

[3] Shinya Sekizaki, Mutsumi Aoki, Hiroyuki Ukai, and Takaya Shigetou, "Decreasing Voltage Deviation by Optimizing Dead Band of SVR in Distribution System with A Large Amount of Photovoltaic Generators", Proceedings of Tokai Section Joint Conference on Electrical and related Engineering 2011, L2-1, 2011 (in Japanese)

[4] Katuma Watanabe, Shinya Sekizaki, Mutsumi Aoki, Hiroyuki Ukai, Takaya Shigetou, and Shunsuke Sasaki, "A Control Method for Distribution Substation using Voltage Information from Voltage Regulator on Distribution Line", Society of Signal Processing Applications and Technology of Japan 2012, 2012 (in Japanese)

[5] Katuma Watanabe, Shinya Sekizaki, Mutsumi Aoki, Hiroyuki Ukai, Takaya Shigetou, and Shunsuke Sasaki, "Inquest into Introduction Amount of PVs when SVR and LRT are Controlled in a Coordinated way", Proceedings of Annual Conference 2012 on IEIEJ, E-12, pp. 253-254, 2012 (in Japanese)

[6] Shinya Sekizaki, Mutsumi Aoki, Hiruyuki Ukai, Shunsuke Sasaki, and Takaya Shigetou, "Control of Multistage SVRs using Voltage Sensor in Distribution System with Large Amount of Photovoltaic Generations", Proceedings of The 2012 Annual Conference of Power & Energy Society, IEEJ, No.4, pp.03-1-03-10, 2012 (in Japanese)

[7] Katuma Watanabe, Mutsumi Aoki, Hiroyuki Ukai, Shinya Sekizaki, LIM MENG THOUNG, Takaya Shigetou, and Shunsuke Sasaki, "Cooperative Control of SVRs in Distribution System with a Large amount of PVs", Proceedings of The 2012 Annual Conference of Power & Energy Society, IEEJ, No.252, pp. 27-15－27-16, 2012 (in Japanese)

Chapter 4

[8] Shinya Sekizaki, Mutsumi Aoki, Hiroyuki Ukai, Takaya Shigetou, and Shunsuke Sasaki, "Suitable Control Method of SVR and Small Battery in Distribution System with A Large Amount of PVs", Proceedings of 2012 Annual meeting record IEEJ, A-1, pp.1-2, 2012 (in Japanese)

[9] Shinya Sekizaki, Mutsumi Aoki, Hiruyuki Ukai, Shunsuke Sasaki, and Takaya Shigetou, "Voltage Control using Small Batteries in Distribution System with Large Amount of PVs", Proceedings of The 2012 Annual Conference of Power & Energy Society, IEEJ, 6-160, pp. 286-287, 2012 (in Japanese)

[10] Shinya Sekizaki, Mutsumi Aoki, Hiruyuki Ukai, Shunsuke Sasaki, and Takaya Shigetou, "Effect of Active and Reactive Power Control using Battery in Distribution system (1)", Proceedings of 2013 Annual Meeting Record, IEEJ, 6-113, pp. 202-203, 2013 (in Japanese)

[11] Shinya Sekizaki, Mutsumi Aoki, Hiruyuki Ukai, Shunsuke Sasaki, and Takaya Shigetou, "Effect of Active and Reactive Power Control using Battery in Distribution system (2)", Proceedings of 2013 Annual Meeting Record, IEEJ, 6-114, pp. 204-205, 2013 (in Japanese)

Others

[12] Shinya Sekizaki, Mutsumi Aoki, and Hiroyuki Ukai, "A Study of Modeling the Inverter for Analyzing Power Quality", Proceedings of Annual Conference 2009 on IEIEJ, F-17, pp. 355-356, 2009 (in Japanese)

[13] Shinya Sekizaki, Mutsumi Aoki, Hiroyuki Ukai, and Takaya Shigetou, "A Study of Voltage Management using TVR in Distribution System with A Large Amount of Photovoltaic Generators", Proceedings of Joint Technical Meeting on Power Engineering and Power Systems Engineering, IEEJ 2011, PE-11-96, PSE-11-113, pp. 43-48, 2011 (in Japanese)

[14] Shinya Sekizaki, Mutsumi Aoki, Hiroyuki Ukai, Takuma Sakaguchi, and Takaya Shigetou, "A Study of Optimal Location of SC with L to Reduce the Harmonic Voltage at Distribution System of Actual Scale using Mode Analysis Method", Proceedings of Annual Conference 2011 on IEIEJ, H-22, pp. 435-436, 2011 (in Japanese)

[15] Shinya Sekizaki, Mutsumi Aoki, Hiroyuki Ukai, Takaya Shigetou, and Shunsuke Sasaki, “A Study of SC with L in Distribution Systems Connected to Same Substation Transformer”, Proceedings of Annual Conference 2012 on IEIEJ, A-1, pp.1-2, 2012 (in Japanese)

[16] Shinya Sekizaki, Mutsumi Aoki, Hiroyuki Ukai, Takaya Shigetou, and Shunsuke Sasaki, “A Study about the Influence of PCS on Operation of SVR in Distribution System”, Proceedings of Joint Technical Meeting on Power Engineering and Power Systems Engineering, IEEJ 2012, PE-12-123, PSE-12-139, pp. 1-6, 2012 (in Japanese)

[17] Shinya Sekizaki, Mutsumi Aoki, Hiroyuki Ukai, Takaya Shigetou, and Shunsuke Sasaki, “Control of SVR using solar radiation and communication”, Proceedings of Tokai Section Joint Conference on Electrical and related Engineering 2012, F3-7, 2012 (in Japanese)